Emergency Energy Power System Composed of Multiple Multi-ports Energy Routers in Microgrid

Yu Nie

PhD

University of York

School of Physics, Engineering and Technology

July 2024

Abstract

The current emergency power supply measures are not perfect and standardized in response to large-scale power failures, such as city-wide ones. This thesis focuses on reasonably using the emergency electric power source to supply power in case of an abnormal urban power grid, to ensure the regular operation of urban electrical equipment and the daily life of the people.

The purpose of this study is to investigate potential emergency electric power sources and identify the most effective future emergency power distribution approaches, given their critical applications during power outages. Initially, a literature review is conducted to evaluate three common emergency electric power sources and two emergency distribution methods. Additionally, the feasibility of utilizing electric vehicle (EV) batteries for emergency energy supply (EES) and the energy router (ER) as an efficient distribution method is proposed. Building on this foundation, the study then delves into the relevant theories and techniques to ensure practical application. Specifically, the study introduces an ER composed of two power electronic converters: a bidirectional AC/DC converter and a partial power processing (PPP) based triple active bridge (TAB) converter. These components are detailed to demonstrate their reliability. Furthermore, an automatic power direction control strategy is proposed to facilitate efficient and consistent power transfer within the system, eliminating the need for manual adjustments, particularly during emergencies. Finally, by integrating multiple energy routers into an emergency power system within microgrids, the automatic power direction control method can be extended to manage power transfer not only between ports within a single energy router but also between different energy routers, enabling peer-to-peer (P2P) trading.

Key words: Energy router; bidirectional AC/DC converter; partial power processing based triple active bridge converter; automatic power direction control method

Table of Contents

Abbreviations

EES	Emergency energy supply
EV	Electric vehicle
ER	Energy router
PPP	Partial power processing
TAB	Triple active bridge
P2P	Peer to peer
MER	Multi-port energy router
PWM	Pulse width modulation
DAB	Dual active bridge
EEPS	Emergency energy power system
UPS	Uninterrupted power supply
EPS	Emergency power supply
AC	Alternating current
DC	Direct current
SPWM	AC pulse band modulation
V2G	Vehicle-to-grid
SST	Solid state transformer
MPPT	Maximum power tracking
ICBB	Integrated circuit building block
CPM	Current programmed mode
SenseFET	Sense Field Effect Transistor
FPIC	Four-port isolated DC/DC converter
ESC	Energy storage converter
IVC	Improved virtual capacitor
CCM	Continuous conduction mode

ERSU	Energy router storage unit
PLL	Phase-locked loop
PD	Phase angle detector
LF	Loop filter
VCO	Voltage-controlled oscillator
SOGI	Second-order generalized integrator
FPG	Frequency/phase angle generator
QSG	Quadrature signal generator
SOC	State of charge
ZVS	Zero-voltage switching
SPS	Single-phase shift

List of Tables

List of Figures

Acknowledgements

First and foremost, I would like to express my deepest gratitude to my main supervisors, Dr. Yihua Hu and Dr. Mohammad Nasr Esfahani, for granting me the precious opportunity to further myself at the highest level. They have encouraged and helped me to progress academically from a fresh graduate to a professional researcher and a mature individual. I have learned so much from them both academically and personally. Thank them for the invaluable comments and advice on my research as well as my life and career. It is a great honour for me to be their PhD student, and I hope I have fulfilled their high expectations and faith through my achievements.

I would also like to take this opportunity and thank my parents. They have always been greatly supportive of me. Their continuous help and understanding have made my life full of love, and I am grateful for everything they have done. I feel very sorrowful that my father passed away on Dec. 31, 2023. Although he cannot witness my graduation, I believe he must be proud of me. I have to thank my father again and I miss him very much. Additionally, I would like to express my appreciation to Dr. Yixuan Zhang and Dr. Haocheng Shi who gave his help on my experiment verifications. I have to say without their help, I would not have made it this far. I am very grateful to Dr. Xinian Li (Shangdong Technology and Business University), Dr. Xing Zhao and Dr. Asim Mumtaz, who have given me many useful suggestions for my research. Special thanks are also paid to my brilliant and lovely colleagues and friends, in particular to Dr. Xiaotian Zhang, Dr. Hongzuo Liu, Mr. Shangming Mei, Mr. Mengyu Cheng and Mr. Chengdong Xu for many fruitful discussions and enjoyable moments.

Last but not least, the support from the Department of Electronic Engineering at the University of York is gratefully acknowledged. Especially, I am grateful to Ms. Camilla Danese who is really elegant, patient and kind.

Declaration

I declare that this thesis is a presentation of original work, and I am the sole author. This work has not previously been presented for an award at this, or any other, University. All sources are acknowledged as References.

Main contents in Chapter 2 have been published in *Power Electronics and Drives*. Title is "Energy Router for Emergency Energy Supply in Urban Cities: A Review".

Main contents in Chapter 3 have been published in *Energies*. Title is "Multi-port Energy Router in Mobile Energy Storage for Emergency Power Outage in Urban Cities".

Main contents in Chapter 4 have been published in *Sustainability*. Title is "Automatic Power Direction Control of DAB/TAB Converter in Emergency Energy Supply".

Yu Nie

July. 2024

List of Publications

[1] **Y. Nie,** H. Xu, Y. Hu and X. Ye, “Energy Router for Emergency Energy Supply in Urban Cities: A Review.,” *Power Electronics and Drives,* vol. 7, no. 1, pp. 246-266, 2022.

[2] **Y. Nie,** Y. Zhang and Y. Hu, "Integrated Power/Signal Transmission in Triple Active Bridge Converters Based on Partial Power Processing for Energy Routers," *2022 IEEE Transportation Electrification Conference and Expo, Asia-Pacific (ITEC Asia-Pacific)*, Haining, China, 2022, pp. 1-6, doi: 10.1109/ITECAsia-Pacific56316.2022.9942161.

[3] **Y. Nie,** Y. Zhang, Y. Hu, M. Alkahtani, M. Alquraish and H. Xu, "Energy Router for Peer-to-Peer Trading under Emergency with Energy Traceable Functionality," in *IEEE Access*, doi: 10.1109/ACCESS.2023.3285198。

[4] **Y. Nie**, X. Zhang, M. N. Esfahani and M. S. Alkahtani, "Automatic Power Direction Control of DAB Converter in Emergency Energy Supply," *2024 IEEE 4th International Conference on Power, Electronics and Computer Applications.*

[5] X. Zhang, Y. Liu, C. Gong, **Y. Nie** and J. Rodriguez, "Electric Motor Bearing Fault Noise Detection with Mel-Transformer Model and Multi-Timescale Feature Extraction," *2023 IEEE 4th China International Youth Conference On Electrical Engineering (CIYCEE)*, Chengdu, China, 2023, pp. 1-7, doi: 10.1109/CIYCEE59789.2023.10401816.

[6] **Y. Nie**, M. N. Esfahani, Y. Hu, X. Li, M. S. Alkahtani, "Multi-port Energy Router in Mobile Energy Storage for Emergency Power Outage in Urban Cities," in *Energies*, doi: 10.3390/en17122927.

[7] X. Zhang, Y. Liu, C. Gong, **Y. Nie** and J. Rodriguez, "Electric Motor Bearing Fault Noise Detection via Mel-Spectrum-Based Contrastive Self-Supervised Transformer Model," in *IEEE Transactions on Industry Applications*, doi: 10.1109/TIA.2024.3451414.

[8] **Y. Nie**, X. Zhang, Y. Hu and M. Nasr Esfahani, “Automatic Power Direction Control of Dual Active Bridge/Triple Active Bridge Converter in Emergency Energy Supply for Sustainability”, in *Sustainability*, 2024.

Nomenclature

B_1, B_2, B_3	Power sources of port 1, port 2 and port 3 of TAB converter
B_{ii}	Power source of port i of the i-th energy router in EEPS (i is 1, 2, 3)
$C_{1,}$ C_2	Resonance capacitance of FPIC
C_{in}, $C_{M,}$ C_O	the input of FPIC respectively Capacitor, intermediate stage capacitor, and output capacitor
C_{vir}	Virtual capacitance of FPIC
C_{v0}	Initial virtual capacitance of FPIC
C_{ad}	Capacitor of bidirectional AC/DC converter
C_y	Capacitor of PPP TAB converter (y is 1 or 2)
C_{dc12}, C_{dc13}, C_{dc23}	Conducted power flow from port 1 to port 2, from port 1 to port 3, and from port 2 to port 3
C_{i12}, C_{i13}, C_{i23}	Conducted power flow from port 1 to port 2, from port 1 to port 3, and from port 2 to port 3 of the i-th energy router in EEPS (i is 1, 2 or 3)
D	Duty ratio
d_x	Duty ratio of three-level inverter of the MER in 2-3 d)
dr	Output duty cycle of bidirectional AC/DC converter
DS_1, DS_2, DS_3	Value that decides the power transmission direction of the first, second and third ER in EEPS
E_a, E_b, E_c	Grid voltage of the MER in 2-3 d)
E_{xi}	AC voltage of the i-th cascaded H-bridge of the MER in 2-3 d)
ER_1, ER_2, ER_3	The first, second and third energy router in EEPS
f_s	Switching frequency
f_1, f_2, f_3	Energy flow in energy flow model
I_{PV}	Photovoltaic current of a hierarchical control system
I_b	Output current of the battery of a hierarchical control system
I_{load}	Load current of a hierarchical control system
I_{dc}	DC current of a hierarchical control system
i_x	Grid current of the MER in 2-3 d)

i_{dc}	DC output current of FPIC
i_{Lad}	Inductor current of bidirectional AC/DC converter
I_{ref}	Reference current of inductor of bidirectional AC/DC converter
i_{Lc}	Current through the inductance of port 1
i_{L1}, i_{L2}, i_{L3}	Current waveforms of inductor at port 1, port 2 and port 3 of TAB converter
i_1, i_2, i_3	Current waveforms of port 1, port 2 and port 3 of TAB converter
i_{Li1}, i_{Li2}, i_{Li3}	Current waveforms of inductor at port 1, port 2 and port 3 of the i-th energy router in EEPS (i is 1, 2 or 3)
k	Ratio of high-frequency transformer of the MER in 2-3 d)
k_u	Voltage tracking coefficient of FPIC
K	Limited value of the voltage change of FPIC
L_s	Equivalent inductance on the grid side of the MER in 2-3 d)
L_m	Leakage inductance of a high-frequency transformer of the MER in 2-3 d)
L_i	Resonance inductance of the resonator of FPIC
L_r	Resonance resistance of the resonator of FPIC
L_{ad}	Inductor of bidirectional AC/DC converter
L_1, L_2, L_3	Inductor of TAB converter
L_d	Sum of each two inductors of TAB converter
L_{ii}	Inductor of port i of the i-th energy router in EEPS (i is 1, 2 or 3)
MS	A value that decides the power transmission direction of DAB/TAB converter
max	Maximum SOC of B_2 of DAB converter
min	Minimum SOC of B_2 of DAB converter
$maximum_2$	Maximum SOC of B_2 of TAB converter
$minimum_2$	Minimum SOC of B_2 of TAB converter
$maximum_3$	Maximum SOC of B_3 of TAB converter
$minimum_3$	Minimum SOC of B_3 of TAB converter
$maximum_{i2}$	Maximum SOC of B_2 of PPP TAB converter of the i-th energy router in EEPS (i is 1, 2 or 3)
$minimum_{i2}$	Minimum SOC of B_2 of PPP TAB converter of the i-th energy router in

	EEPS (i is 1, 2 or 3)
$maximum_{i3}$	Maximum SOC of B_3 of PPP TAB converter of the i-th energy router in EEPS (i is 1, 2 or 3)
$maximum_{i3}$	Minimum SOC of B_3 of PPP TAB converter of the i-th energy router in EEPS (i is 1, 2 or 3)
n_x	Benchmarking function for the conversion between switch-status of three-level inverter of the MER in 2-3 d)
n_T	Transformer turns ratio of FPIC
N_1, N_2, N_3	The winding of transformer at port 1, 2 and 3 of TAB converter
N_{ii}	Winding of transformer at port i of the i-th energy router in EEPS (i is 1, 2 or 3)
$P_{DC/DC}$	Transmission power of the MER in 2-3 d)
P_{dc12}, P_{dc13}, P_{dc23}	Power flow from port 1 to port 2, from port 1 to port 3, and from port 2 to port 3 of PPP TAB converter
P_{12}, P_{13}, P_{23}	Power flow from port 1 to port 2, from port 1 to port 3, and from port 2 to port 3 of TAB converter
P_{in}	Total input power of PPP TAB converter
P_{out}	Total output power of PPP TAB converter
P_s	Semiconductor loss of PPP TAB converter
P_{tl}	Transformer loss of PPP TAB converter
P_h	Heat loss on passive components
P_+	Forward power of DAB converter
P-	Reverse power of DAB converter
P_1, P_2, P_3	Total power of port 1, port 2, and port 3 of TAB converter
P_{i12}, P_{i13}, P_{i23}	Power flow from port 1 to port 2, from port 1 to port 3, and from port 2 to port 3 of PPP TAB converter of the i-th energy router in EEPS (i is 1 , 2 or 3)
Q_1, Q_2, Q_3,Q_4	Signals controlling the MOSFETs at port 2 of DAB converter
R_s	Equivalent resistance on the grid side of the MER in 2-3 d)
S_k	Switching function of cascaded H-bridge of the MER in 2-3 d)
S_{k1}, S_{k2}	Switching functions of the pre-stage and post-stage of the isolated DC/DC converter of the MER in 2-3 d)
S_{oo}	On/off state value of FPIC
S_{ad1}, S_{ad2}, S_{ad3},	Switch of bidirectional AC/DC converter

S_{ad4}	
S_1, S_2, S_3, S_4	Control signals of switches at port 1
S_5, S_6, S_7, S_8	Control signals of switches at port 2
S_9, S_{10}, S_{11}, S_{12}	Control signals of switches at port 3
SOC_2, SOC_3	SOC value of port 2 and port 3 of TAB converter
SOC_{i2}, SOC_{i3}	SOC value of port 2 and port 3 of PPP TAB converter of the i-th energy router in EEPS (i is 1, 2 or 3)
T_{dc12}, T_{dc13}, T_{dc23}	Total power flow from port 1 to port 2, from port 1 to port 3, and from port 2 to port 3
T_{dc1}, T_{dc2}, T_{dc3}	Total power of port 1, port 2, and port 3
T_s	Switching period
T_{hs}	Half of switching period
T_{i12}, T_{i13}, T_{i23}	Total power flow from port 1 to port 2, from port 1 to port 3, and from port 2 to port 3 of PPP TAB converter of the i-th energy router in EEPS (i is 1, 2 or 3)
T_{ii}	Total power of port i of PPP TAB converter of the i-th energy router in EEPS (i is 1, 2 or 3)
U_{pv}	Photovoltaic voltage of a hierarchical control system
U_b	Terminal voltage of the battery of a hierarchical control system
U_{load}	Load voltage of a hierarchical control system
U_{dc}	DC voltage of a hierarchical control system
$U_{dc1\text{-}xi}$, $U_{dc2\text{-}xi}$	pre-stage voltage, and post-stage voltage of the i-th isolated DC/DC converter of the MER in 2-3 d)
U_{DC1}	Low-voltage side that connects to the renewable energy module of the MER in 2-3 d)
U_{DC}	Medium-voltage side that connects to the medium-voltage DC bus of the MER in 2-3 d)
u_{dc}	DC bus voltage of FPIC
u_{dc}^*	Reference of DC bus voltage of FPIC
V_0	Output voltage of bidirectional AC/DC converter
V_{ref}.	Reference voltage of bidirectional AC/DC converter
V_{ado}	Voltage of DC port of bidirectional AC/DC converter
V_{adin}	Voltage of AC port of bidirectional AC/DC converter

V_1, V_2, V_3	Voltages of port 1, port 2 and port 3
V_{max}	Maximum value of acceptable voltage range of port 1
V_{min}	Minimum value of acceptable voltage range of port 1
V_{ii}	Voltage of port i of PPP TAB converter of the i-th energy router in EEPS (i is 1, 2 or 3)
V_{DC}	DC bus voltage of port 1 in each ER in EEPS
δ	Pulse shift angle of the MER in 2-3 d)
φ_2, φ_3	Phase shift angle of TAB converter
φ_1	Phase shift angle of DAB converter
φ_{i2}, φ_{i3}	Phase shift angle of PPP TAB converter of the i-th energy router in EEPS (i is 1, 2 or 3)

Chapter 1 **Introduction**

1.1 Motivation

The reason people need emergency energy is that there are lots of unexcepted accidents causing the paralysis of the urban power grid, which has a severe effect on people's lives. For example, a significant power scale power failure in China was caused by a snow disaster. About 4.5 million people lived without electricity for about two weeks in 2008 [1]. There was also a large power outage in Northeast Brazil because of an accidental break-down of the dam power supply system [2]. Nearly one-third of the Brazilian population was caught in a power outage for about 4 hours. In addition, 12 million Indians in India suffered from a large power outage for about two days because the power supply could not meet the peak demand [3]. More importantly, some malignant social events can also cause a large power outage. 9 million people living in New York once experienced a period of power failure for a period of 24 hours [4]. Various reasons can lead to a large power outage, and the harm of a large-scale power outage is also severe. Firstly, the most direct impact is the damage to power grid equipment which can require a lot of material, financial and time resource to repair [5]. Secondly, people can be seriously affected such that their life and work will become inconvenient. Because of the power outage, people have to cook by open fire [6]. Besides, a power outage can also be life-threatening. For example, a doctor must operate without the assistance of any electronic medical equipment, which significantly increases the risk and difficulty of operation [7]. Therefore, emergency energy is reasonably necessary because it can replace the urban power grid to supply the power when the urban power grid is abnormal.

Various applications of electricity have been an essential part of human life which means almost all industries need electricity to drive the corresponding electrical equipment to complete the work. This causes a problem that cannot be ignored. When a power outage happens, a severe problem can be caused that people cannot complete the regular work, which further results in economic loss and even loss of life and safety [8]. Considering the above reasons, it is necessary to prevent these losses in an unexpected power failure. So far, emergency electric power sources and related distribution methods which are explained carefully in this review have been considered effective. Up to now, three kinds of emergency

electric power sources and two emergency power distribution methods have been widely used in daily life, but a potential emergency electric power source the battery of electric vehicle and a potential emergency power distribution method energy router which is the energy router have been proposed and proven to be feasible. This emergency power source and energy routers are analysed and explained in detail in this review. In particular, the energy router is also considered as a potential emergency power distribution method [9]. It can apply to multiple different types of emergency electric power sources as the input at the same time [10]. It can also be applied in the current hot research areas: smart power grid and microgrid [11] [12] [13]. Considering its function such as high energy utilization, multiple power forms, energy storage and monitoring the state of the main power grid, the energy router is quite suitable to be the power supply in the smart power grid and microgrid [14].

This research focuses on investigating an emergency energy supply method in microgrid and realize the P2P trading in this emergency energy power system. The progressive objectives of this study can be summarized as follows:

i. To **review the different kinds of emergency electric power sources and the distribution methods that can be used to supply power, including the controlling method**. Their advantages and disadvantages are introduced. Additionally, a potential emergency electric power source and its connecting and controlling method is proposed. Three methods of using the emergency electric power sources are shown when the power grid is paralyzed.
ii. To **propose a topology of multi-port energy router (MER) composed with a bidirectional AC/DC converter and a PPP TAB converter. This design of MER improves the power efficiency significantly through PPP technology to realize the power transmission among the main power grid, emergency electric power sources including a potential emergency electric power source which is the battery of EV and clients' loads.** The control methods of the power transmission of two power electronic converters in MER, are also illustrated. The bidirectional AC/DC converter is used to realize efficient energy management, increased energy efficiency and P2P trading technology. PPP is a technology that uses converters to process part of the total power, while most of the unprocessed system energy is transferred directly through the power cables. a PPP TAB converter has three ports, and power is exchanged between them using a phase-shift pulse-width modulation (PWM) mechanism.
iii. To **propose an automatic power direction control method for dual active bridge**

(DAB)/TAB converters at a microgrid level, enabling bidirectional power transmission without manual intervention. This approach simplifies operations and enhances system safety by eliminating the need for human supervision. A well-implemented model containing an automatic control method ensures efficient and consistent power transfer within the system, replacing manual operations whenever power direction adjustment is necessary especially in emergencies.

iv. To **implements emergency energy power system (EEPS) in microgrids by proposing an automatic power direction control strategy for multiple MERs consisting of TAB converters based on PPP technology in a microgrid.** A well-implemented model containing an automatic control method ensures efficient and consistent power transfer within the system, replacing manual operations whenever power direction adjustment is necessary especially in emergencies.

1.2 Dissertation Outline

The dissertation consists of seven chapters. An outline of the structure is organized as follows:

Chapter 1 introduces the motivation of this study. Besides, the main objectives and a brief introduction of the research contents are illustrated.

Chapter 2 reviews the different kinds of emergency electric power sources and the distribution methods that can be used to supply power, including the controlling method. Additionally, a potential emergency electric power source and its connecting and controlling method is proposed. Three methods of using the emergency electric power sources are shown when the power grid is paralyzed.

Chapter 3 propose a topology of MER composed with a bidirectional AC/DC converter and a PPP TAB converter. The control methods of the power transmission of two power electronic converters in MER, are also illustrated. Power dissipation can be reduced as the PPP converter processes less power, which has the effect of improving system efficiency and power density.

Chapter 4 propose an automatic power direction control method for DAB/TAB converters, enabling bidirectional power transmission without manual intervention for EES. The direction of power transmission varies based on the different lag/lead relationships, as each port of the PPP TAB converter can facilitate bidirectional power flow. Therefore, an automatic power

direction control method can adjust power direction automatically according to the states of the ports of the PPP TAB converter.

Chapter 5 implements EEPS in microgrids by proposing an automatic power direction control strategy for multiple ERs consisting of TAB converters based on PPP technology in a microgrid.

Chapter 6 is the conclusion part. The main contributions of this study are summarized. The future work that can be carried out to further improve the EEPS is also introduced.

Chapter 2 **Review of Emergency Electric Power Sources and Distribution Methods in Cities**

The current emergency power supply measures are not perfect and standardized in response to large-scale power failures [15], such as city-wide ones. This review chapter focuses on reasonably using the emergency electric power source to supply power in case of an abnormal urban power grid, to ensure the regular operation of urban electrical equipment and the daily life of the people. This study first introduces the different kinds of main emergency electric power sources and analyzes their advantages and disadvantages. The battery of an electric vehicle as a potential emergency electric power source is introduced that can also avoid the loss caused by unexpected power failure. Finally, three different emergency power supply methods are explained in detail for different emergency occasions. Among them, the energy router is reviewed comprehensively considering it is the most potential emergency power distribution approach in the future because of its various applications. Through the review work, the author discovered a valuable research topic that can be summarized as energy router for EES for the rest of this research.

2.1 Emergency Electric Power Sources

There are mainly three kinds of emergency electric power sources that are used to supply emergency power. Three types of emergency electric power sources: Diesel/Gas generator set, uninterrupted power supply (UPS) and emergency power supply (EPS) are shown in Fig. 2-1. This section introduces the following types of power supplies used as urban emergency electric power sources: Diesel/Gas generator set, EPS, UPS.

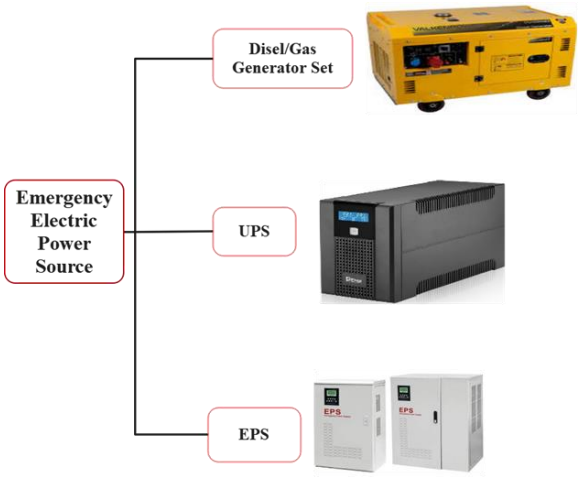

Fig. 2-1. Different kinds of emergency electric power sources.

2.1.1 Diesel/Gas Generator Set

In terms of the Diesel/Gas generator set, the Diesel generator set, and Gas generator set are generator sets that use different fuels but have the same power supply principle. Therefore, these two generator sets are regarded below as the same emergency electric power source.

The diesel generator set is a power generation equipment, which uses diesel as fuel and a diesel engine as a prime mover. Furthermore, the diesel engine is a machine that drives a generator to generate electricity [16]. The whole generator set generally consists of a diesel engine, generator, control box, fuel tank, and other components. The diesel engine comprises two mechanisms and four systems, including a crankshaft connecting rod mechanism, valve train, oil supply system, lubrication system, cooling system, and starting system [17]. The generator set is applicable to various loads with allowable interruption of power supply time greater than 15s [18]. Using a generator set as an emergency electric power source is the most common emergency standby electric power source used in most applications at present. Due to its large capacity, parallel operation, and long continuous power supply time, the generator set has a long application history [19]. However, no matter how fast the generator starts, it takes at least tens of seconds to several minutes to deliver power. This is the starting period from when the generator receives the start signal after a power failure to when the generator voltage and frequency are stable and can supply power [20]. During this period, all connected electrical equipment loses power, which may cause damage to a few pieces of equipment or the life safety and property. On the other hand, the application of diesel generators in emergency electric power sources has the following disadvantages [21], including (1) In high-rise buildings, the

diesel generator set is generally placed in the basement, challenging to design and high cost. The facilities such as air inlet, cooling, smoke exhaust, shock absorption, and silencing need to be fully considered. (2) There is a potential fire hazard, and its oil tank is like an extremely dangerous "bomb" in case of fire. (3) The daily maintenance is frequent, and the workload is heavy. (4) The diesel generator is noisy. (5) There is a large amount of sulfur dioxide and carbon dioxide in the smoke exhaust, which are polluting and affects environmental protection. Although the generator set is practical and ordinary, the risks of the generator set should be considered carefully.

2.1.2 UPS

The second emergency electric power source is UPS. UPS is a constant voltage and constant frequency power supply equipment. It is mainly composed of the rectifier, battery, inverter, and static switch [22] which are shown in Fig. 2-2. (1) Rectifier is a device that converts alternating current (AC) into direct current (DC). It has two main functions: first, converts AC into DC; second, it acts as a charger to provide charging voltage to the battery. (2) Storage battery is a device used by UPS to store power. It is composed of several batteries in series. Its first function is that when the main power is normal, converts the electric power into chemical energy and stores it in the battery. Its second function is that when the main power fails, converts the chemical energy into power and provides it to the inverter or load. (3) Inverter is a device that converts DC into AC. It consists of an inverter bridge, a control logic, and a filter circuit. (4) Static bypass switch is composed of thyristors with positive and negative polarity connected in parallel. When the inverter is overloaded or fails, the inverter will cut off the output and the static switch will be switched on automatically. After that, the main power will directly supply power to the load. The static switch is an intelligent high-power contactless switch with a conversion time of 2-3ms [23].

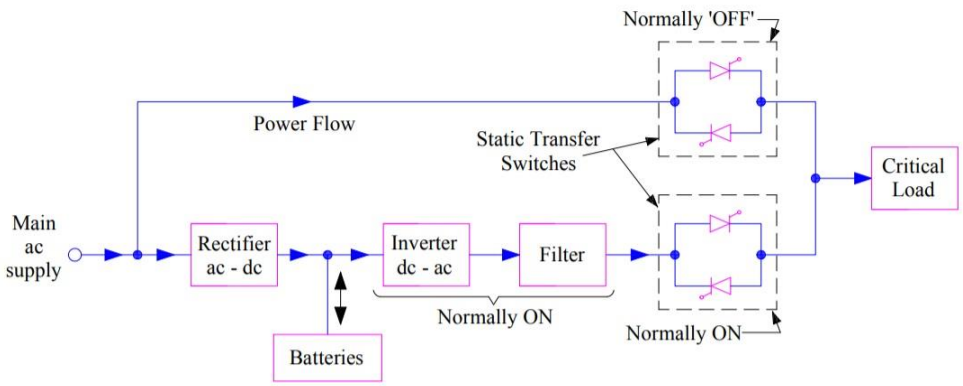

Fig. 2-2. Working principles of UPS [24]

UPS is equipment that can replace the urban power grid supply with a continuous power supply in case of power failure [25]. Its power comes from the battery pack and continues to be supplied to the load. It is mainly used to provide power to a single computer, computer network system or other power electronic equipment [26]. UPS can stabilize the main power grid and supply it to the load when the power grid input is normal. Currently, UPS is an AC main power grid regulator, and it also charges the battery at the same time. However, if the main power grid is interrupted (accidental power failure), UPS will immediately supply the power stored in the battery to the load through inverter conversion for a period. Therefore, there are two advantages of UPS. One is that the power supply is uninterrupted. In the case of typical power failure, the load powered by UPS will not have any impact. The other is that when the normal power supply voltage fluctuates abruptly, UPS also acts as a voltage regulator [27].

2.1.3 EPS

EPS is equipment composed of fire-fighting facilities, emergency lighting, and other first-class load power supply equipment such as the lighting equipment [28]. EPS mainly adopts SPWM (AC pulse band modulation) technology, and the system includes explicitly rectifier charger, battery pack, inverter, mutual switching device, and so on [29]. The function of the rectifier is to convert AC into DC to supply power to the battery and inverter module. The inverter is the core, and the function of the inverter is to convert DC into AC to supply stable and continuous power to load equipment. The mutual switching device ensures the smooth switching of load between the main power grid and inverter output. Battery detection and shunt detection circuits are designed in the system, and the backup operation mode is adopted. There are three modes that the EPS has called main power working mode, battery inverter working mode, and manual maintenance bypass mode [30]. Fig. 2-3 shows the whole function diagram of EPS. The main power working mode of EPS is bypass priority. When the mains power is normal, it is directly from bypass to load. At the same time, charge the battery, and the inverter is on standby. When the main power is abnormal, the electric energy stored by the battery is inverted by the inverter to supply power to the load [31]. Furthermore, when online maintenance is required under the continuous power supply, the manual maintenance bypass switch can be directly closed, and the output switch and bypass switch can be disconnected to completely disconnect the circuit part, input, and output of the EPS power supply without interrupting the user's output [32].

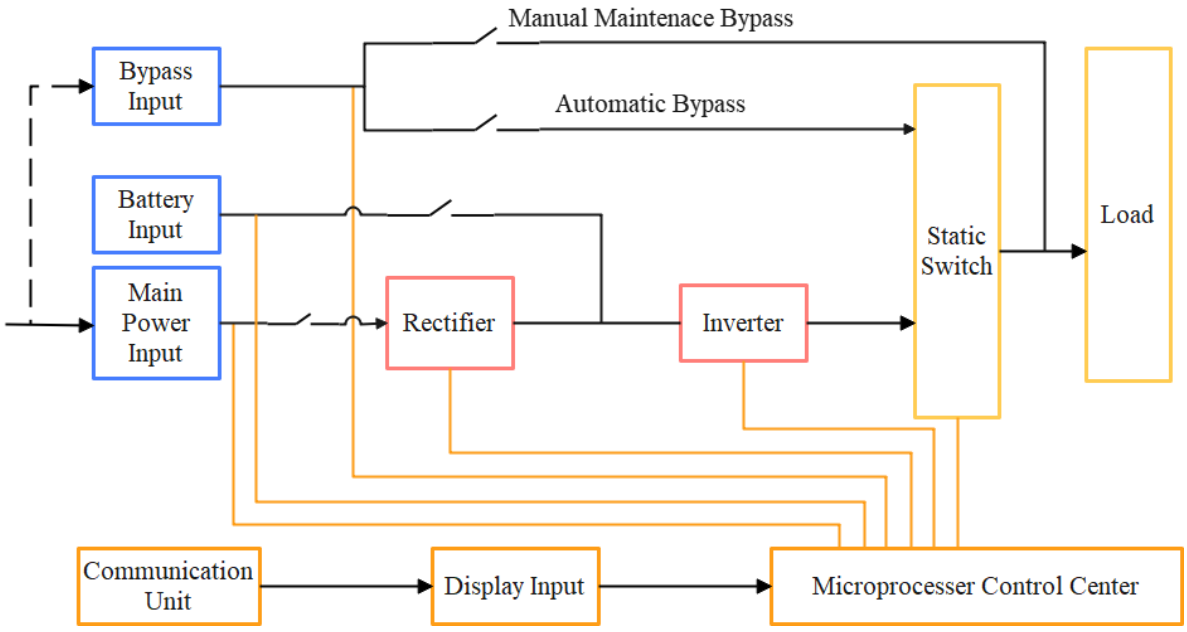

Fig. 2-3. The whole function diagram of EPS

Compared with UPS, EPS has a lot of advantages [33]. The inverter has large redundancy because EPS systems usually have several inverters, which can work simultaneously or as backups, so that in the event of a failure of one of them, the other inverters can immediately take over the power supply task to avoid power interruptions. It can operate normally under 120% load and has incoming and outgoing feeder functions and a multi-channel mutual switching function. There are measures to prevent high and low temperature, damp heat, salt fog, dust, vibration, rat movement, and rat bite. It adopts an off-line operation mode, with high efficiency, energy-saving, and low noise. Thus, the inverter can only be carried out when the power grid is off, which causes the service life of the host to be relatively long, generally 15-20 years. Finally, the total cost of EPS is less expensive than that of UPS of the same capacity [32].

2.1.4 The Comparison among EPS, UPS, and Diesel/Gas Generator Set

Table 2-1 is the comparison between EPS and UPS. EPS is better at many aspects such as structure, power saving, noise, price, and life span. EPS has the advantages of a wide application environment, high power-saving performance, low noise, high economy, long service life, many types of applicable load and wide application. However, UPS has the fastest responding time, which means that if the main power grid is paralyzed, UPS can supply the power to the load immediately. This is the biggest reason that UPS cannot be replaceable by the EPS. EPS is primarily utilised in emergency lighting and security apparatus, among other

applications. Conversely, UPS is extensively employed in data centres, servers and other domains with elevated power demands.

TABLE 2-1 Comparison between EPS and UPS [32]

Characteristic	EPS	UPS
Structure	Large redundancy, and can normally operate for more than 10 min under 120% rated load Incoming cabinet and out-going cabinet, fire protection multi-channel mutual switching function, and special measures for dehumidification, mildew prevention and corrosion prevention	Small redundancy, generally required to work at 80% of the rated current No incoming cabinet and outgoing cabinet, fire protection, and mutual switching functions
Power saving	the bottom power consumption state when the power grid is normal. Efficiency is > 90% when there is no power grid	When the supply of the power grid is normal, the efficiency is only 80 ~ 90%
Noise	the grid is normal, no static noise. When there is no power supply on the grid, its noise is less than 55dB	55～65 dB
Price	Low maintenance price	Expensive maintenance price
Life span	Generally, > 20 years	Generally, 5 ~ 8 years
Load adaptability	Especially suitable for inductive load	Only suitable for capacitive and resistive load (computer load)

Table 2-2 compares EPS, and Diesel/Gas Generator Set. EPS performs better than Generator Set in terms of the start time, environment protection, maintenance cost, power supply status, overload and protection, and construction and operation cost. The generator cannot be started in time. The generator also needs to add environ-mental protection facilities of about 11000-14000 pounds/set, fire prevention facilities of 5800-7000 pounds/set, and labor-management fee and regular maintenance fee of 3500 pounds/set. In addition, the power supply quality of the generator is poor, and the ap-applicable environmental capacity is poor. On the contrary, EPS has a low comprehensive cost, easy management, more stable and reliable power generation, and a small floor area. EPS are utilised in a multitude of applications, including the safeguarding of essential apparatus such as computers, communication devices, medical equipment, and so forth. Additionally, they are employed in the protection of vital structures and infrastructure, ensuring the continuity of operations and the safety of personnel in the event of a power outage. However, the most significant advantage of the Diesel/Gas Generator Set is a long-time power supply. EPS and UPS can only supply the power for a few hours de-

pending on their capacities. A generator set can usually supply the power for a few days without interruption.

TABLE 2-2 Comparison between EPS and Diesel/Gas Generator Set [34]

Characteristic	EPS	Diesel/Gas Generator Set
Start time	<0.2s	5~30s
Environment protection	No smoke exhausts, noise, vibration, and pollution	A large amount of harmful gas, great noise, and vibration, and required to be fireproof
Maintain	Simple maintenance, unattended automatic operation, and computer monitoring	Special personnel shall be assigned to take care of and maintain regularly
Power supply status	Strong voltage stability, Stable frequency, no interference, and high efficiency	Unstable voltage and frequency, and low efficiency
Overload and protection	Strong overload capacity, perfect protection function, and low power capacity and load power, generally 1:1	Weak overload capacity, general protection function, and high ratio of standby generator set to load power, generally at least 1:1.5 times
Construction cost and operation cost	One time investment, basically no follow-up operation cost	The lower procurement cost of generator set equipment, but the high cost of auxiliary facilities, and many subsequent operation costs

The allowable power failure time of load and the site of load are two the most important factors when considering how to choose and use the appropriate emergency electric power source. Based on the different needs of various loads, the combination of UPS, EPS and generators can also be applied [35].

2.2 Emergency Electric Power Sources

There are always some unexpected situations such as the shortage of reserves for emergency electric power sources that the current emergency power supply technology cannot solve. Thus, discovering a potential emergency electric power source can also be extremely meaningful. With the development of the electric vehicle industry, more and more electric vehicles are running in the cities. This means that the power source of each electric vehicle can be a potential emergency power source to deal with power failure. Table 2-3 shows the daily electricity consumption of an ordinary family and the specific energy of the battery of an electric vehicle. According to Table 2-3, the daily electricity consumption of a typical family is 10-20 kWh,

and the specific energy of the battery of an electric vehicle is 15-60 kWh [36]. This means that one battery of an electric vehicle can meet 2 to 3 families' daily electricity demands [36].

TABLE 2-3 The daily electricity consumption of an ordinary family and the specific energy of the battery of an electric vehicle

The daily electricity consumption of an ordinary family (kWh)	10-20
Specific energy of the battery of an electric vehicle (kWh)	15-60

The most significant advantage of the battery of the electric vehicle is that it almost has no cost because it is only needed to be the emergency electric power source when an unexpected power failure occurs, and in a normal situation, it is can also be used as the power source of the electric vehicle [37]. This means that people do not need to buy an emergency electric power source. The electric vehicle can also be maintained by the electric vehicle company considering that it is also one part of an electric vehicle. There are some other advantages, such as decreasing the pressure of supplying emergency power of the government when a large-scale power outage occurs in view that some families have the electric vehicle to supply emergency power on their own. With the amounts of the electric vehicle increasing, the battery of electric vehicles has the full potential to become a kind of emergency power source.

To ensure the private electric vehicle can be used as an emergency electric vehicle, vehicle-to-grid (V2G) is a technology that is firstly proposed by W. Kempton [38] ensuring the bidirectional energy flow between the EVs and the power grid. V2G has improved the efficiency and profitability of the power grid, and made significant progress in environmental protection, such as reducing greenhouse gas emissions. In addition, it also effectively reduces the cost of power consumption of each user. However, as explained in the article [39], V2G still needs a lot of research in the technical level. Once the V2G technology can be applied in the multi-port energy router, the battery of the EV is a significant emergency electric power source.

2.3 Power Supply and Control Methods

2.3.1 Distributed Power

To use the above three kinds of emergency electric power sources in the emergency power failure situation, there are two of the most popular ways to supply emergency electric power. Distributed generation is an emergency measure prepared in advance before power failure occurs. It means that the emergency electric power source is set near the facilities requiring power supply after the power failure. The emergency electric power source is also connected to the power grid to test if the power grid is normal [40]. The basic principle of distributed power is that when the urban power grid is normal, the load is supplied by the urban power grid directly through the bypass, and UPS is charged by the urban power grid through the charger, too. Once the urban power grid is abnormal, the switch will be switched to the other side and the distributed power will turn on the emergency electric power source to supply power to the load instead of the urban power grid which is shown in Fig. 2-4.

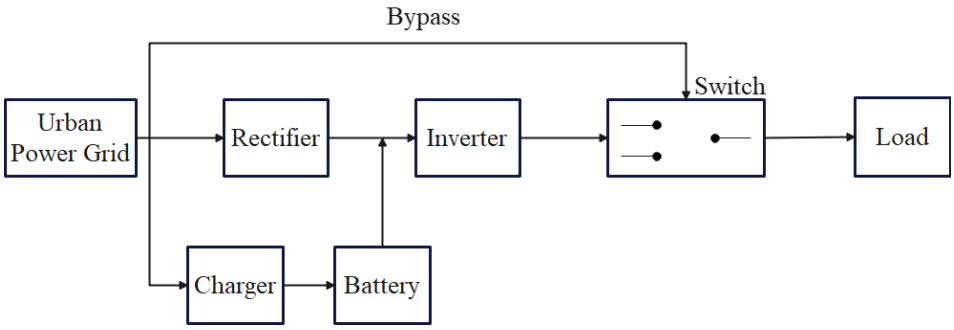

Fig. 2-4. Function diagram of distributed power

The choice of the emergency electric power source of distributed power depends on the allowable time failure time of the load. If the load is a computer system or medical facility, UPS is the best choice. However, if the load is a first-class load such as lighting systems, EPS can be the most suitable choice [41]. The advantages of distributed power are various. The first advantage is easy construction and less costly. The single unit capacity and power generation scale are small, and there is no need to build large power plants, substations, and distribution stations. The civil engineering and installation cost is low, the construction period is short, and the investment is small. Distributed power is also close to users and has simple power transmission and distribution and low loss. Close to power users, it can generally directly supply power to the load nearby without long-distance high-voltage transmission lines. The loss of transmission and distribution is small, and the construction is simple and cheap. The third advantage is less pollution and good environmental compatibility. It also has the advantage of high energy efficiency. Combined with cogeneration, the waste heat of power generation can be recycled for heating and refrigeration, to realize the cascade utilization of

energy scientifically and reasonably. The fifth advantage is flexible operation and guaranteed safety and reliability. The startup and shutdown of small units are fast and flexible. It can be used as a standby power supply. Finally, distributed power can make network operation, with the ability to provide auxiliary services. It can operate jointly with the power grid and complement each other, which can not only improve its power supply reliability but also provide auxiliary services for the large power grid [42].

2.3.2 Emergency Power Vehicle

The second method is the emergency power vehicle whose main function is to supply the power load that needs to be able to reply quickly and extend the power supply time to a certain time due to the power failure after the accident. Emergency power vehicles are suitable for use in large-scale civil construction projects, such as some hospitals, high-rise office buildings, airports, satellite launch measurement and control bases, large stadiums, archives, more important scientific research buildings and so on. The emergency power vehicle has two advantages. On the one hand, the vehicle can quickly arrive at the site which has a power failure when emergency electric power source is not prepared in advance. On the other hand, it has a fast start power supply performance after the failure of the urban power grid when the emergency power vehicle is connected to the loads [38]. The rapid start-up power supply of the power supply vehicle is one of the important characteristics of the emergency power supply vehicle. Shoown in TABLE 2-4, its speed can be divided into three levels according to the reaction time: (1) Instantaneous power supply, (2) Power supply within 5 seconds, (3) Power supply for 5 minutes. In terms of instantaneous power supply, UPS is equipped in the power supply vehicle to automatically detect the municipal electric signal. After the urban power grid is cut off, the UPS will be automatically started immediately. After the generator set is started for power supply, it will automatically switch to the generator set for power supply without interruption. This mode is applicable to class 1 load and power protection operations in major public activity places. In terms of power supply within 5 seconds, EPS is equipped in the power supply vehicle to automatically detect the municipal electric signal. In the hot standby state of the generator set, after the urban power grid is cut off, it will automatically switch to the generator set aside for power supply within 3 ~ 5 seconds. After the urban power grid is restored, it can automatically switch back to the urban power grid within 3 ~ 5 seconds. In terms of power supply for 5 minutes, for ordinary power supply vehicles, the Generator Set starts to supply power from the cold standby state [43]. The warm-up time of the Generator Set is

generally more than 3 minutes, and it is switched on manually. This mode is applicable to power maintenance operations in public activity places and temporary power supply for emergencies [44].

TABLE 2-4 The Starting time of emergency electric power sources

Disel/Gas generator set	About 5minutes
EPS	Within 5 seconds
UPS	Instantaneous power supply

2.3.3 Energy Router and Related Working Method

Sometimes, there is more than one kind of emergency electric power source that can supply the emergency power to the load at the same time. However, the emergency power from different emergency power sources cannot connect to the load directly at the same time. This can cause damage to the load and increase the pressure bearing the burden of circuit lines. Thus, to integrate and distribute these emergency power from different kinds of emergency power sources, an energy router is a device that can be useful between different kinds of emergency power sources and load [45]. The concept of the 'energy router' was first proposed by Alex Q. Huang of North Carolina State University. In 2008, he led the US National Science Foundation project FREEDM, which aimed to integrate power electronics and information technology into the power system to realise the concept of the future energy internet at the distribution grid level [46].

a) An AC-DC Hybrid Multi-Port Energy Router (MER)

An energy router is developed from a solid state transformer (SST) [47]. Based on the function of SST, energy routers also need to achieve the intelligent management and real-time communication of the smart grid, electrical power sources, and load. This means that the energy router has obvious advantages in many aspects such as active management of bidirectional power flows [48], convenient access to electrical power sources [49], [50], energy management optimization [51], [52], etc. Fig. 2-5 is the structure of an AC-DC hybrid MER which includes five parts: grid-connected part, energy storage part, medium voltage DC part, AC part, and low voltage DC part [53].

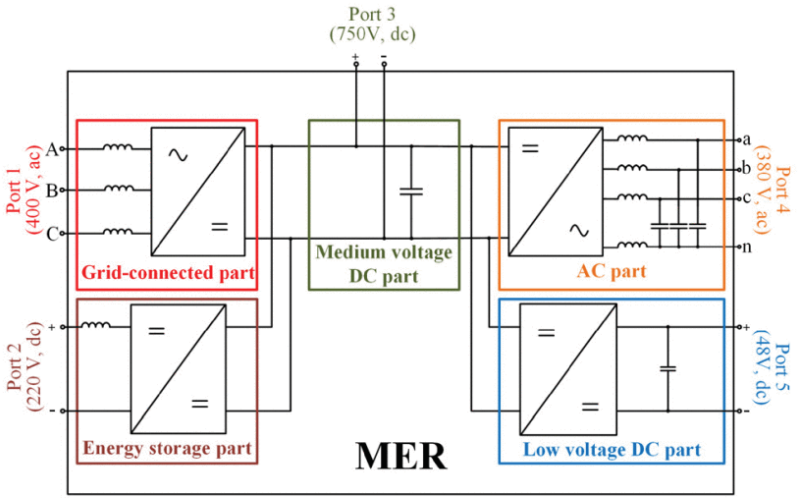

Fig. 2-5. Structure of MER [53]

In the grid-connected part, there are two components: a filter and an AC/DC converter to realize bidirectional power flow between the power grid and the MER. The energy storage part which is an essential bidirectional power part to make the energy management and high power supply reliability come true consists of a DC/DC converter and filter inductance. The medium voltage DC part is a unidirectional power part that comprises some support capacitors and provides a 750V DC port to get access to the other parts. The AC part is a unidirectional power part that is composed of a DC/AC converter and a filter to transfer DC power into AC power to satisfy the needs of the AC load. The low voltage DC part is a unidirectional power part that is made up of a DC/DC converter and filters which decrease the DC voltage to supply a lower DC voltage to the DC load [53].

There are mainly four modes to operate this MER: standby mode, grid-connected mode, islanded mode, and fault mode. The relationship between these four modes is shown in Fig. 2-6.

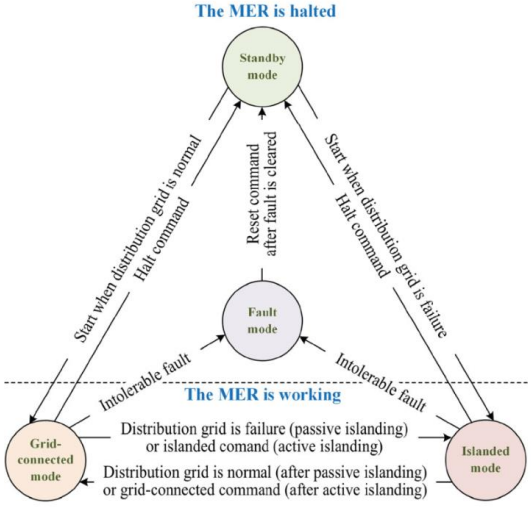

Fig. 2-6. Operation mode transition of MER [53]

In the standby mode, the MER is not working until a start command is received. If the power grid is normal, MER will be switched into the grid-connected mode. Otherwise, MER will be switched into the islanded mode [53].

When MER is in the grid-connected mode, the ports in the grid-connected part are connected to the power grid. The controllers in the gird-connected part ensure the voltage stability of the medium voltage DC link [53]. The controller in the energy storage part will control the charge and discharge state of the battery according to the power that the load need and the power that the power grid supplies.

If MER is in the islanded mode, the grid-connected part will stop working and the energy storage part will be responsible for supplying the power to the load. Besides, the controller in the energy storage part will ensure the voltage stability of the medium voltage DC link instead of the controller in the grid-connected part [53]. There are two situations that make the MER work in the islanded mode. One is the power grid is abnormal, the MER must work in the islanded mode to ensure safety. The other is that MER receives a command that asks it to work in the islanded mode.

When a local fault occurs in the energy storage part, AC part and low voltage DC part, MER will shut down the part which has a fault to make sure the normal working of the rest of the parts. However, if an unboreable fault such as overvoltage of medium DC bus occurs, MER will be switched into fault mode to protect all the systems and shut down all the ports. In fault mode, MER will not be switched into the standby mode until the fault is fixed and a reset command is received [53]. With these four operation modes, MER can work regularly and make sure reliable power is supplied to the load.

b) An Energy Router Based on A Power Electronic Transformer and Related Control Method

This section introduces an energy router based on a power electronic transformer [54]. This energy router can connect the medium voltage distribution network and low-voltage regional network, regulate the low-voltage DC bus, and provide a low-voltage DC bus for renewable energy equipment, energy storage devices, and load to realize the two-way flow of energy. Based on the above requirements, the designed energy router is a multi-input and multi-output plug and play interface circuit, which mainly consists of a power electronic transformer, photovoltaic system, energy storage device, and DC load like what is shown in Fig. 2-7

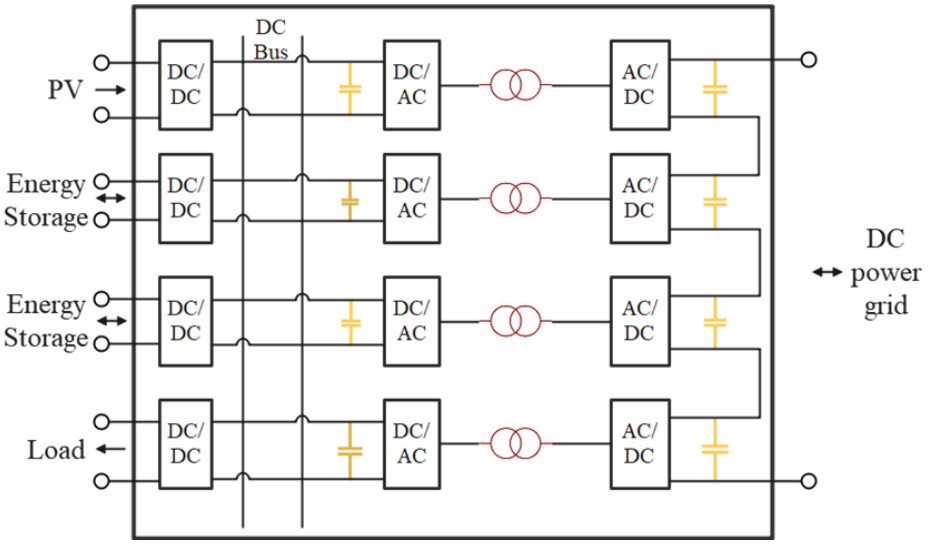

Fig. 2-7. Topology of energy router based on power electronic transformer

If the system is connected to the grid, the high-voltage DC bus can supply power to the load through the power electronic transformer, the DC microgrid can also feed the distribution network through the DC transformer. In case of system failure, photovoltaic power generation and energy storage devices can form a low-voltage DC microgrid and operate in islanded mode. The power electronic transformer here adopts the cascade form of a DAB to realize voltage conversion and electrical isolation [54]. Multiple identical DABs are connected in series to the medium voltage DC distribution network at the high-voltage end and connected in parallel to the low-voltage DC microgrid at the low-voltage end and serve as a plug and play interface for photovoltaic system, energy storage device, and load, compatibility, and flexibility. The interface circuit of the photovoltaic power generation unit is the boost circuit, and the energy storage device consists of a battery and bidirectional Boost /Buck converter.

To control when and which emergency power sources supply the emergency power to the load, the energy router also needs a control system for energy management. This energy router uses a hierarchical control system design. The hierarchical control system design is shown in Fig. 2-8, where I_{PV} is the photovoltaic current; U_{pv} is the photovoltaic voltage; U_b is the terminal voltage of the battery; I_b is the output current of the battery; U_{load} is the load voltage; I_{load} is the load current; U_{dc} is DC voltage, and I_{dc} is the DC current. The control system is divided into three layers: the upper layer is the function customization layer; the middle layer is the energy management layer, and the lower layer is the executive layer [54].

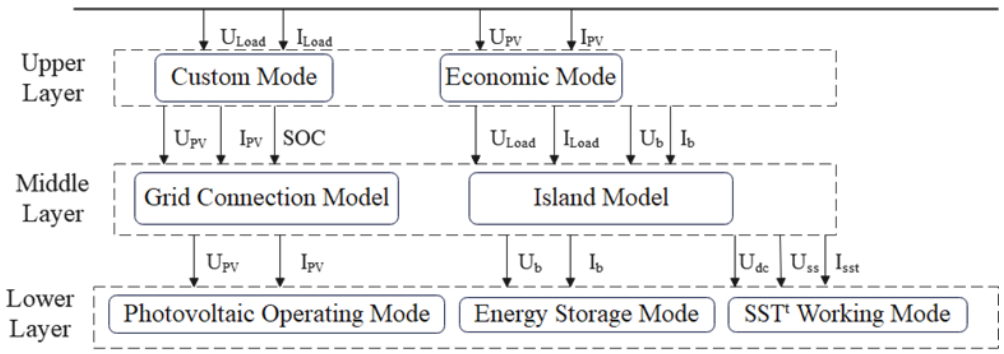

Fig. 2-8. Hierarchical Control System of Working Modes in Threee Layers

To determine the working mode of the energy router, it is necessary to consider each type of three layers in order shown in Fig. 2-8. In detail, the function customization layer takes the photovoltaic output power, the residual capacity of the battery, real-time electricity price, and other information as input signals to determine the system scheduling mode. The system scheduling mode is mainly divided into economic mode and user-defined mode [54]. Under the economic mode, users can sell power to the external power grid to obtain economic benefits if the residual capacity of the energy storage system is sufficient and the electricity price is high. When the remaining capacity of the energy storage system is insufficient and the electricity price is low, absorb power from the external power grid to charge the energy storage system. In terms of the user-defined mode, when the external power grid outputs the specified power, users can determine the energy use strategy according to their own energy use. In both modes, the system operating mode signal will be generated. The energy management layer determines the working mode of the system that is grid-connected mode and islanded mode according to the control signal generated by the upper layer, the output power of the photovoltaic and the residual capacity of the energy storage battery. At the same time, the corresponding logic control signal is generated and transmitted to the execution layer. The main function of the execution layer is to receive the logic control signal, make the logic combination and enable the controller, calculate according to the specific algorithm, further generate the pulse modulation signal, and generate the corresponding drive tube pulse according to the pulse modulation signal. The system only needs to send instructions to the converter, and each converter can execute according to the instructions.

The energy management of this energy router is carried out from two working modes: grid-connected mode and islanded mode [54]. In the grid-connected mode, due to the high cost of renewable energy power generation such as photovoltaic power generation, it is generally set to maximum power tracking (MPPT) mode to fully utilize the electric energy generated. In the

user-defined mode, when the external power grid is in constant power generation if the power currently is higher or lower than the load demand power, the energy storage is responsible for maintaining the power balance and voltage stability in the microgrid. In the economic model, if the electricity price is high and the remaining energy storage capacity is sufficient, the energy storage battery discharges at constant power. In contrast, when the electricity price is low and the remaining energy storage capacity is insufficient, the battery is charged with constant power. Besides, if the output power of distributed generation is greater than the demand power of load, the external power grid can absorb additional power to prevent the rise of bus voltage. However, when the output power of the distributed generation cannot meet the demand of the load, the external power grid can supplement the power shortage of the distributed generation to prevent the drop in bus voltage.

When the DC microgrid is dominated by photovoltaic and energy storage and is disconnected from the external DC bus, the local DC microgrid is in islanded mode. Currently, the power in the system mainly consists of photovoltaic output power, battery output power, and load demand power. Generally, the photovoltaic interface converter works in MPPT mode and only injects power into the bus, while the energy storage unit is used to maintain the bus voltage and balance the power flow in the system. For example, when the power injected into the bus is large, the energy storage battery enters the charging state to suppress the rise of bus voltage. If the power injected into the bus is small, the energy storage battery enters the discharge state to suppress the drop in bus voltage. If the photovoltaic output power is higher than the load demand power and the energy storage charging state reaches the extreme value, the energy storage battery will no longer maintain the bus voltage, and the photovoltaic will be switched from MPPT mode to constant voltage mode. When the total output power does not meet the demand of load, the bus voltage is lower than the minimum required by the DC microgrid. At this stage, the bus voltage of the DC microgrid will decrease significantly, resulting in the paralysis of the microgrid. Therefore, to maintain stability, it is necessary to selectively cut off the unimportant load according to the load shedding algorithm to avoid bus voltage collapse.

c) Energy Router Based on An Integrated Circuit Building Block (ICBB)

An ICBB type of energy router for a power electronic converter can extremely decrease the volume of the component and improve the power processing efficiency [55]. This ICBB consists of two segmented half-bridges and all the components that are used to make mixed-signal current programmed mode (CPM) control come true which are shown in Fig. 2-9.

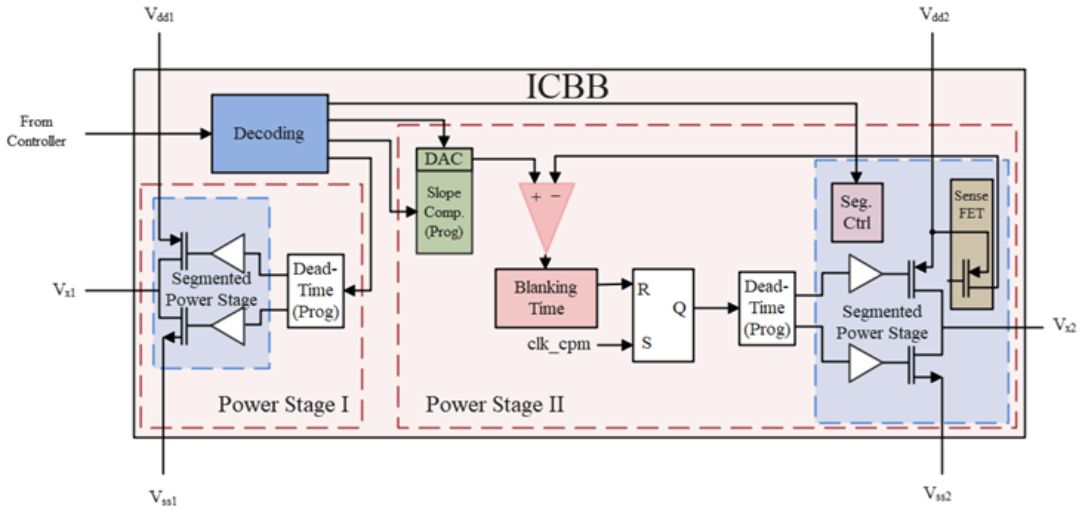

Fig. 2-9. Block diagram of low-power ICBB [55]

These two-segmented half-bridges have the same design. However, power stage II has an extra circuit called Sense Field Effect Transistor (SenseFET) for current sensing which makes mixed-signal CPM controllability possible. This design fulfils two needs which are the possibility of operating at high switching frequencies, and low-power consumption. Besides, this design can be sure to be used with the online efficiency optimization schemes at the same time which can improve the efficiency of power processing by compromising between the ON-resistance and gate charge of the switches. Furthermore, through segmentation, the problems of the limited-speed and high-power consumption caused by the conventional SenseFET current measurement circuits can be solved. To make full use of the multi-levels of different sources. The topology which uses ICBB modules is shown in Fig. 2-10.

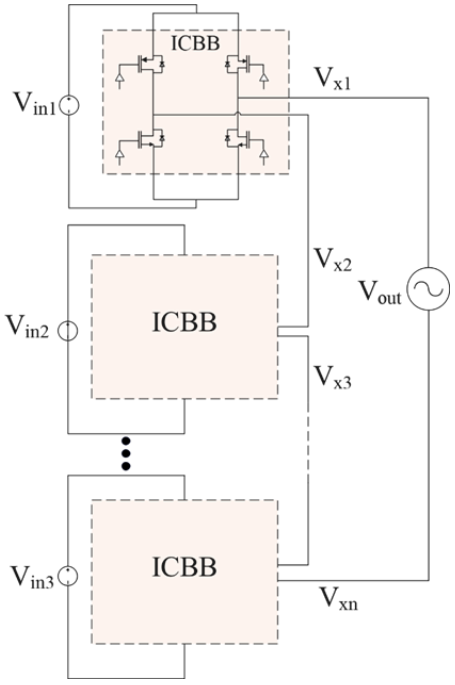

Fig. 2-10. Multilevel inverter implementation utilizing ICBB modules [55]

This converter allows various kinds of DC sources and converts these different input voltages into one output voltage synthesis through ICBB modules which include DC/AC conversion. This design makes the adjusting of voltages easier so that the efficiency of the energy collecting can be improved.

d) An Energy Router Supplying AC and DC Load Separately

Some energy routers can supply the power to the DC load and AC load at the same time [56]. There is a topology that has two imports and two exports. One import is connected to the grid directly, and the other import is connected to renewable energy. With the combination and complementation of these two kinds of energy forms, the problems of one single power form supply and low utilization of renewable energy can be solved [57]. According to Fig. 2-11, this multi-port energy router consists of a three-phase cascaded H-bridge, isolated DC/DC converters, a three-level inverter, and a Buck/Boost converter. The grid transfers its power to the medium-voltage DC bus through a cascaded H bridge and isolated DC/DC converters. DC load can be supplied by the medium-voltage DC bus directly. AC load need the AC power transferred by the three-level inverter from a medium-voltage DC bus. The power from renewable energy can be accessed into the medium-voltage DC bus through Buck/Boost converter.

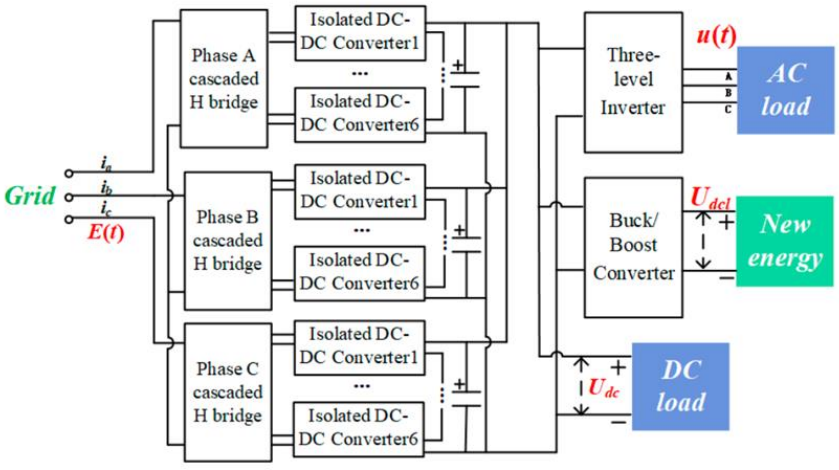

Fig. 2-11. A topology of multi-port energy router [57]

The more detailed topology is shown in Fig. 2-12 on the high-voltage side. The capacitor at the medium-voltage DC side is designed to reduce the voltage ripple and improve power quality [58]. According to Kirchhoff's voltage law, Equation (2-1) and Equation (2-2) can be obtained

$$\begin{cases} E_{xi} = S_k U_{dc1-xi} \\ E_x = L_s \frac{di_x}{dt} + R_s i_x + \sum_{i=1}^{n} E_{xi} \end{cases} \quad (2\text{-}1)$$

$$U_{dc2-xi} = S_{k1} S_{k2} k U_{dc1-xi} \quad (2\text{-}2)$$

where E_x is the grid voltage (x = a, b, c), i_x is the grid current, E_{xi} is the AC voltage of the i-th cascaded H-bridge, $U_{dc1\text{-}xi}$ and $U_{dc2\text{-}xi}$ are pre-stage voltage, and post-stage voltage of the i-th isolated DC/DC converter, S_k is switching function of cascaded H-bridge, L_s and R_s are equivalent inductance and resistance on the grid side, S_{k1} and S_{k2} are the switching functions of the pre-stage and post-stage of the isolated DC/DC converter, and k is the ratio of high-frequency transformer [57]. From Equation (2-1), the output DC voltage can be controlled by changing the value of S_k. According to Equation (2-2) the output voltage at the low-voltage side can be controlled by the value of S_{k1}, S_{k2} and k. Therefore, the transmission power $P_{DC/DC}$ can be obtained.

$$P_{DC/DC} = \frac{U_{dc1-xi} U_{dc2-xi}}{2k\pi f_s L_m} \delta \left(1 - \frac{|\delta|}{\pi}\right) \quad (2\text{-}3)$$

where f_s is switching frequency, L_m is the leakage inductance of a high-frequency transformer and δ is the pulse shift angle [57]. According to Equation (2-3), the $P_{DC/DC}$ can be controlled by changing the value of δ.

In terms of this topology of the high-voltage side, the sub-modules can be turned on or off separately because the bridge arm reduces the voltage and current change rate with the cascade structure existing. This means the switch has less stress and the total output voltage is less possible to distort. Besides, the high-frequency transformers have a significant influence in weakening the high-frequency harmonics and decreasing the noise. Finally, this design can ensure there is no interference between the grid and the secondary sides.

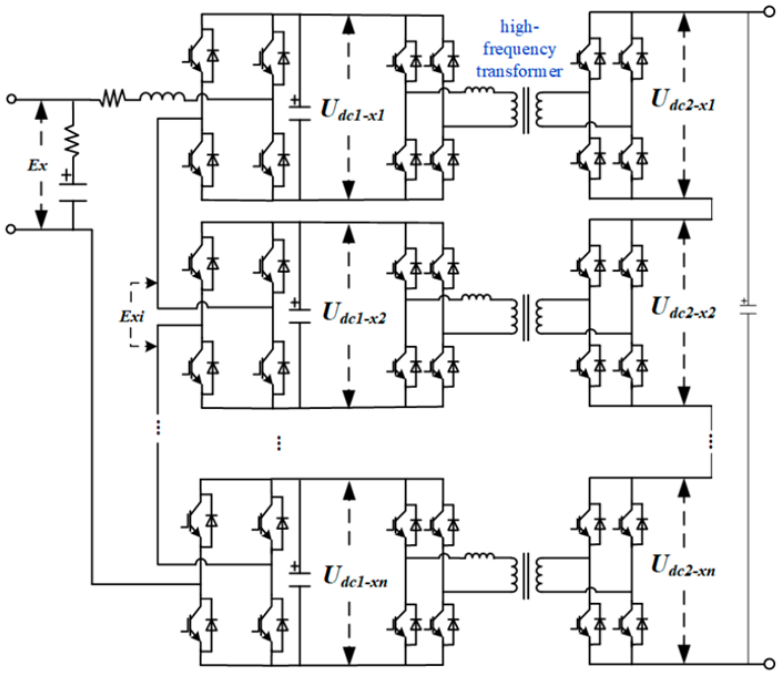

Fig. 2-12. Topology of high-voltage side [57]

On the low-voltage side, there are two topologies: a topology of DC/DC converter and a topology of DC/AC converter. The DC/DC converter is used for the renewable energy to access the medium-voltage DC bus. This DC/DC converter's non-isolated Buck/Boost structure is adopted in this DC/DC converter. The topology of this DC/DC converter is shown in Fig. 2-13. In Fig. 2-13, U_{DC1} is the low-voltage side that connects to the renewable energy module, and U_{DC} is the medium-voltage side that connects to the medium-voltage DC bus. If the renewable energy module can supply power to the medium-voltage DC bus, DC/DC converter works in Boost mode. It can increase the input voltage and supply a stable DC voltage to the medium-voltage DC bus. On the contrary, when the power storage module needs to be charged, the DC/DC converter works in Buck mode. It can charge the power storage module by converting the voltage from the medium-voltage DC bus. Equation (2-4) can calculate the output voltage of this converter

$$U_{DC1} = D\frac{U_{DC}}{1-D} \tag{2-4}$$

where D is the duty ratio of the converter.

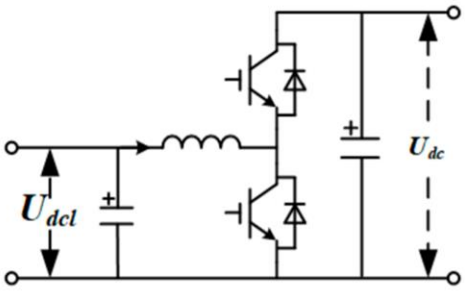

Fig. 2-13. Topology of DC/DC converter [57]

DC/AC inverter is used to convert the DC power in the medium-voltage DC bus into AC power which is supplied to the AC load. This DC/AC converter uses a three-level structure. The topology of this DC/AC converter is shown in Fig. 2-14. According to Fig. 2-14, the output voltage is

$$u(t) = \frac{U_{DC}}{2}(d_x + n_x) \tag{2-5}$$

where d_x is the duty ratio and n_x is the benchmarking function for the conversion between switch-status of three-level inverter, $n_x = \begin{cases} 1, & O \to P \to O \\ 0, & N \to P \to N \end{cases}$ [57]. This three-level structure of DC/AC converter has less harmonic and better power quality than two-level DC/AC converter [59].

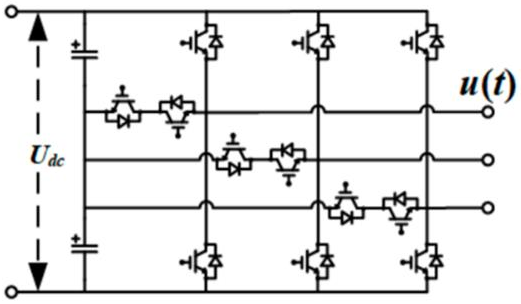

Fig. 2-14. Topology of DC/AC converter [57]

e) A Parallel Coordinated Control Strategy Based on Virtual Capacitor Control in The Four-Port Isolated DC/DC Converter

With the development of renewable energy and batteries, the electric power sources used for an energy router are mostly DC sources. However, the DC micro-grid usually has small inertia. This means that its bus voltage will easily be affected by the power fluctuations caused by intermittent renewable energy and local load changes [60] [61]. Therefore, to control the bus voltage in the DC micro-grid to improve the inertia and stability of the DC micro-grid, there is

a parallel coordinated control strategy based on virtual capacitor control in the Four-port isolated DC/DC converter (FPIC) to make sure that each output power of energy storage unit is allocated according to the remaining capacity and the charge state of each energy storage unit is balanced [62].

According to Fig. 2-15, there is a two-stage isolated bidirectional DC/DC converter that connects the PV source and two energy storage to a 400V DC bus. On the other side, there is also a three-port DC converter connecting with the DC load. The front stage of the two-stage converter is CLLC resonant circuit with the rear stage being the interleaved Buck/Boost circuit. u_{dc} is the DC bus voltage, i_{dc} is the DC output current; n_T is the transformer turns ratio; L_m and L_r are the resonance inductance and resonance inductance of the resonator; C_1 and C_2 are the resonance capacitance; C_{in}, C_M, and C_O are the input of FPIC respectively Capacitor, intermediate stage capacitor, and output capacitor [62].

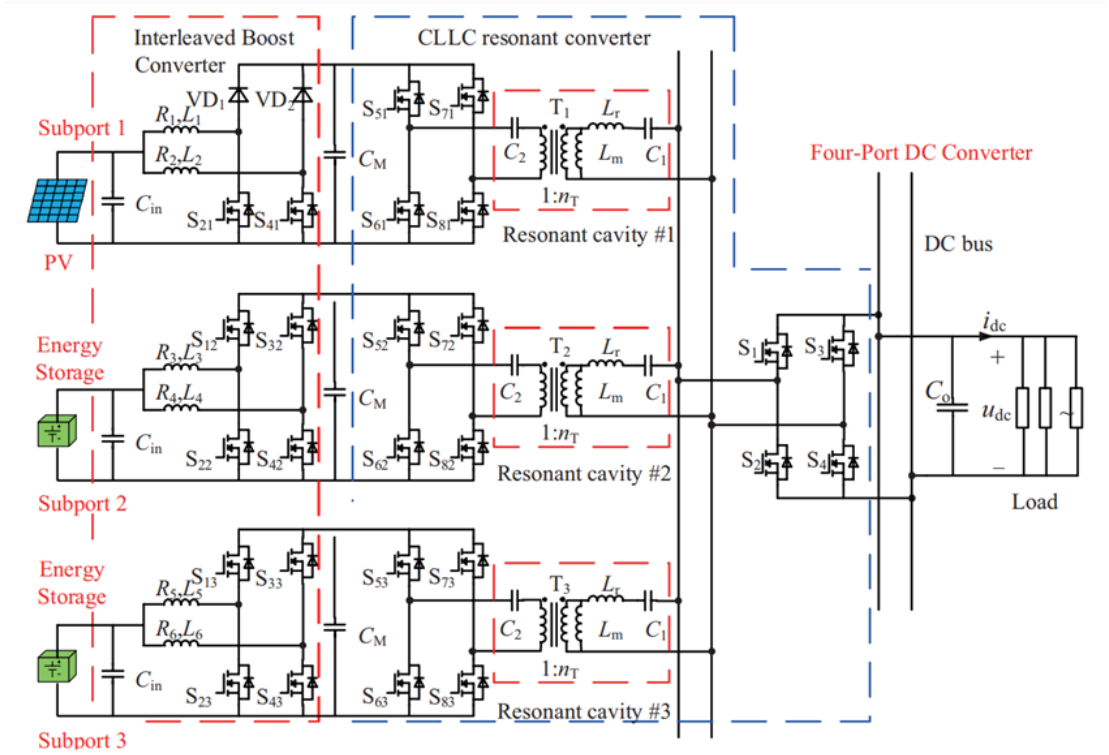

Fig. 2-15. DC micro-grid structure diagram of photovoltaic energy storage with FPIC [62]

The exact control method of this FPIS is as follows. Firstly, In the CLLC resonant circuit, a duty cycle of 50 percent is applied by the high-side full bridge and the two low-side full bridges to the switch tubes S_1, S_4, S_{5i}, S_{8i} $(i = 1,2)$. Its switching frequency is the control signal of resonant frequency (in-phase). The other power transistors S_{53} and S_{83} apply a complementary

control signal. In terms of the post-stage interleaved Buck/Boost circuit, it is assumed that the photovoltaic converter has been working in the MPPT state and the energy storage converter (ESC) operates in IVC mode. For the lower arm switch tubes S_{22} and S_{42}, Apply a driving signal with a phase difference between 180° and the same duty ratio. Besides, control the driving signals of the upper and lower arm switch tubes to be complementary.

Through the design of the virtual capacitor, the droop control of the ESC can simulate the charge and discharge characteristics and damping characteristics of the real capacitor so that the disturbance suppression ability of the DC bus voltage can be enhanced. The final equation of virtual capacitance corresponding to this improved virtual capacitor (IVC) control is:

$$\begin{cases} C_{vir} = C_{v0}, \ \Delta_1 \leq K \\ C_{vir} = C_{v0} + k_u S_{oo}, \ \Delta_1 > K \ and \ \Delta_2 > 0 \\ C_{vir} = C_{v0}, \ \Delta_1 > K \ and \ \Delta_2 \leq 0 \end{cases} \tag{2-6}$$

where C_{vir} is the virtual capacitance, C_{v0} is the initial virtual capacitance, k_u is the voltage tracking coefficient, K is the limited value of the voltage change, $\Delta_1 = |\Delta u_{dc}|$, $\Delta_2 = sgn(du_{dc}^*/dt)\Delta u_{dc}$, u_{dc}^* is the reference of DC bus voltage, S_{oo} is the on/off state value. If $\Delta_1 > K \ and \ \Delta_2 > 0, S_2 = \Delta_2$ [44].

To effectively manage and use energy storage devices in FPIC more efficiently, the multiple energy storage and coordinated control mainly includes IVC control, voltage and current dual-loop control and output current feed-forward control is also applied.

f) An Energy Hub with An Energy Router

An energy hub is also able to supply various kinds of load instead of only electricity load [63]. Fig. 2-17 shows a schematic of an energy hub in which various kinds of electric power sources and gas supplies generate heat and power to satisfy electricity load, cooling load and heat load [64]. Energy router has the advantages such as improved quality of power, a smaller size, tolerance of fault, and reactive power support feature [65]. Fig. 2-16 proposes a topology of energy hub which includes an energy router that realizes the coordination of multiple energy sources and improves the efficiency of energy [64].

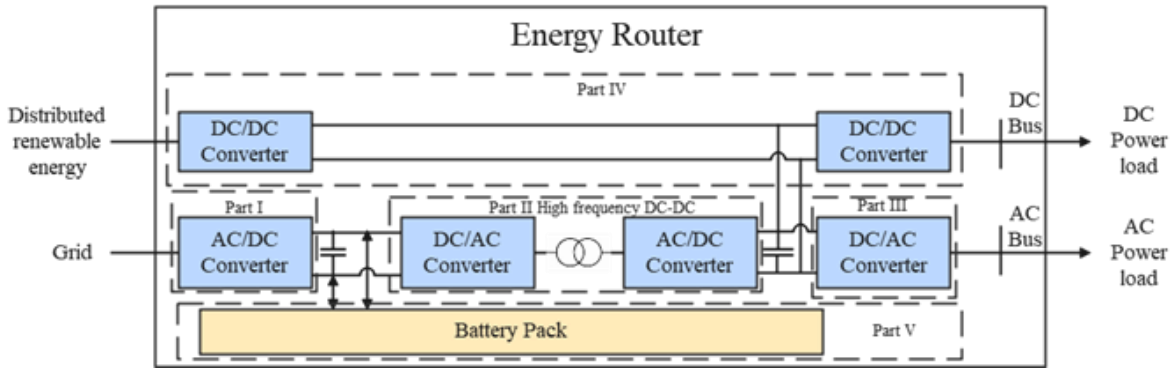

Fig. 2-16. The configuration of the energy hub [64]

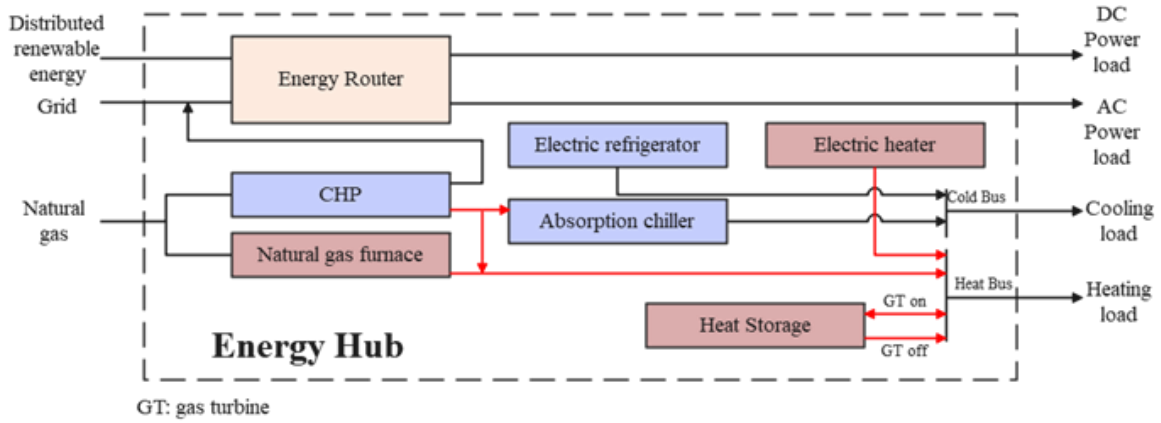

Fig. 2-17. The topology of an energy router [64]

The basic principle of this energy router is that it mainly uses distributed renewable energy to supply power to all load and satisfy the charging demand of the battery pack. However, if the distributed renewable energy is unstable and unable to supply enough power, the power in the energy storage components (battery pack and heat storage) will be used to generate power to satisfy the demands of load. Besides, When the power supplied by the distributed renewable energy is still rest after satisfying the demands of all the load and battery pack, the rest power can be delivered to the power grid so that the rest power can be utilized by the load in other areas. The charging and discharging state of energy storage components can also be controlled [64].

g) Discussion

Table 2-5 compares all the above energy routers from four of the most essential parts: import electric power source, export load, electronic power converter included, and energy storage

function. In terms of the choice of emergency power electric sources, allowable failure time of the loads can be greatly helpful to decide. This is applied by the majority of energy routers. DC load and AC load can both be supplied by the energy routers as long as the correct and suitable power electronic converters are applied. Power electronic converters which are the most important parts of the energy router should be determined and selected according to the types of the power electric sources and the types of the load. The different design circuits of power electronic converters can easily lead to the difference between the function and power transmission performance of the energy routers. Besides, the energy storage function is an essential part of the energy router. It makes sure power management and adjusting. It can supply power to the load when the power of electric power sources is not enough to satisfy the needs of the load. If the power of electric power sources is more than the needs of the load, the energy storage module will be charged by the extra power of electric power sources to improve the efficiency of the power transmission.

TABLE 2-5 The Comparison among Energy Routers

	Import electric power source	Export load	Power electronic converter included	Energy storage function
Example 1	AC Power grid	AC load and DC load	AC/DC converter, DC/DC converter, and DC/AC converter	A power storage part which is charged by the AC power grid
Example 2	DC power grid and photovoltaic power	DC load	AC/DC converter, DC/DC converter, and DC/AC converter	Two energy storage modules charged by the DC power grid and photovoltaic power
Example 3	Various kinds of electric power sources	AC load	An ICBB	No energy storage function
Example 4	AC Power grid and renewable energy	AC Load and DC load	AC/DC converter, DC/DC converter, and DC/AC converter	One energy storage module charged by the AC power grid
Example 5	Photovoltaic power	DC Load	DC converter	Two energy storage modules charged by the photovoltaic power

Example 6	Renewable energy and AC Power grid	AC load and DC load	AC/DC converter, DC/DC converter, and DC/AC converter	One battery pack charged by the AC power grid

Example 1 MER has a lot of advantages such as the plug-and-play access of DERs and loads, various forms of electric energy, unified control and management of the MER-based energy subnet, high power supply reliability, fault isolation between the grid side and the users' side, etc. [66]. However, this kind of MER is only suitable for the low-voltage distribution network. Example 2 energy router realizes flexible control and management of voltage and power, but it can only be used in the DC power grid. Example 3 introduces a ICBB design of emerging low-power, high-frequency multilevel and hybrid converter topologies operating at switching frequencies up to 10 MHz, however, with no power storage function and is only applicable for the AC power grid [67]. MER in example 4 ultizes a free switching control strategy which can accurately transmit the required power and maintain the stability of the DC bus voltage. However, it can only be used in the distribution area with a high penetration rate of the renewable energy. The energy storage system of the energy router in example 5 can accurately distribute the output power according to the proportion of the remaining capacity of each energy storage unit to the total remaining capacity to ensure the safe and reliable operation, but the energy router has no connection with the power grid [68]. Energy router in example 6 has relatively complete functions. However, it is designed for a part of energy hub and renewable energy is the main source of the energy.

According to reviewed energy routers, the energy router is the most effective and potential distribution way that can be used in the emergency electric power supply in the future [69]. Not only it can be set before the emergency occurs and store the power with a power-storage module, but also can connect multi kinds of emergency electric power sources at the same time and utilize and combine them to generate stable and continuous power to the load which suffer from the unexcepted power failure [70]. Thus, to better address the problem of a large-scale sudden power outage, developing a multi-port energy router that can be connected to the power grid and other emergency electrical power sources is essential. This multi-port energy router can detect if the power grid is working normally and combine the power of the power grid with the power of any other emergency electric power source to complete the power adjusting which can ensure to satisfy the needs of the load. The energy storage module in this kind of multi-port energy router can also be charged by both the power grid and the emergency electrical

power sources. Besides, it can supply power to the load when the power grid is paralyzed, or the power supplied by the power sources cannot meet the needs of the load. With this kind of energy router, all kinds of emergency electrical power sources can relate to the power grid to supply power at the same time and minimize the loss caused by power failure.

2.4 Summary

The emergency power source is critical to deal with the unexcepted large-scale power failure of the power grid in the future. Discovering more efficient application schemes and more feasible emergency power sources are the most important work to handle large-scale power failure and decrease economic loss and ensure the life safety of people. At present, the emergency power sources are various and can basically deal with many situations of sudden power failure. Therefore, it is extremely important to have a related complete, and excellent emergency power distribution scheme to supply emergency power to the areas in which occurs power failure. The allowable power failure time of load and the site of load are two of the most important factors when considering how to choose and use the appropriate emergency electric power source. In addition, to be more prepared to deal with sudden power failure, the battery of the electric vehicle is also a potential emergency electric power source considering that electric vehicles have been more and more popular. Besides, the energy router is the most potential device that can connect the emergency power sources to the load fast and is also set near the customers and easy to operate. A multi-port energy router can also connect various kinds of different emergency electric power sources at the same time and adjust and store the output power of each emergency electric power source to meet the needs of the load. This means that the energy router can improve the efficiency of using emergency electric power sources and supply the load with a more stable voltage and current. Therefore, a multi-port energy router that can connect the power grid with various kinds of emergency electric power sources with the function of storing power can be the most important and popular distribution way to explore and research the problems of large-scale unexcepted power failure in cities. Besides, it also needs a lot of research to optimize the connection between the battery of electric vehicle to the energy router to realize bidirectional energy transmission.

Chapter 3 **Multi-port Energy Router in Mobile Energy Storage for Emergency Power Outage in Cities**

This chapter aims to propose a topology for a MER composed of a bidirectional AC/DC converter and a PPP TAB converter. This MER design significantly improves power efficiency by PPP technology, enabling effective power transmission between the main power grid, emergency electric power sources—including the innovative use of EV batteries—and client loads. The control methods for power transmission using the two power electronic converters in the MER are also detailed in this chapter. To validate the practicality of the proposed configuration, MATLAB/Simulink simulations and experimental tests are conducted and meticulously presented.

3.1 Introduction

In the event of an unanticipated power outage, it becomes imperative to mitigate these losses. Up to this point, emergency power sources and their associated distribution techniques, which will be elaborated upon in detail in [71], have been regarded as effective solutions. To date, two prevalent methods for emergency power distribution, namely, distributed power [40] and emergency power vehicles [44] have found widespread use. However, there has been a recent introduction of an alternative approach to emergency power distribution in the form of the energy router. This method has been proposed and demonstrated with several distinctive features [69]. This approach can apply multiple types of different emergency electric power sources as input at the same time [72]. Furthermore, its applicability extends to the smart power grid and microgrid environments [73]. Given its capabilities such as efficient energy utilization, versatile power sources, energy storage, and the ability to monitor the condition of the primary power grid, the energy router is well-suited to serve as a power source within smart power grids and microgrids. Moreover, the battery of EV can be considered as a potential emergency electric power source can be connected more easily and conveniently with energy router to achieve high power management [71].

Compared with two nowadays distribution ways which are distributed power and emergency power vehicle, a MER enables connection to multiple power sources for real-time and efficient energy management. Hence, for a multi-port energy router for emergency supply in cities, it is essential to achieve energy balance between EPPS and the main power grid and ensure the continuous power supply to the loads. In this thesis, the proposed MER consists of a bidirectional AC/DC converter and a PPP TAB converter. The bidirectional AC/DC converter is used to realize the transferring of AC power in the main power grid into DC power to make sure the power transmission in the PPP TAB converter in the normal situation. When the main power grid lacks power, bidirectional AC/DC converter can change the direction of power transmission to meet the demand for power supply to the main grid over a period. This means that power grid will no longer be the power supply only, which realize efficient energy management, increased energy efficiency and P2P trading technology [74] [75].

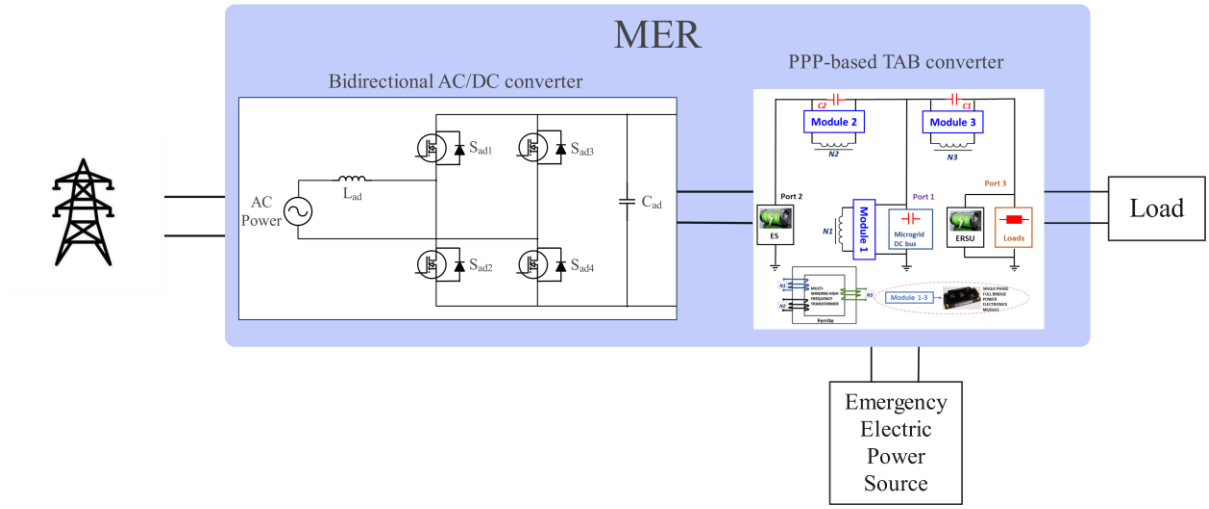

Fig. 3-1. The connection between various power sources, MER and loads

In addition to fulfilling the role of emergency backup power, large-capacity mobile energy storage also possesses the flexibility and ability to regulate energy over long distances to meet different power demand scenarios [76]. By mounting the MER on mobile energy storages, emergency power can be provided to any power outage area regardless of time and location. Also, the required power for various temporary events such as concerts, sports events, construction sites and temporary medical facilities can be supplied [77]. In addition, during periods of peak demand in cities, high-capacity mobile energy storage can be used for peak shaving, helping to maintain grid stability and reduce reliance on traditional energy sources such as fossil fuels [78]. Besides, the battery of EV can also be considered as a mobile emergency electric power source to relate to the large-capacity mobile energy storage [79].

Through combining the large-capacity mobile energy storage and the battery of EV, this makes sure the emergency energy supply is fully prepared in all cases.

PPP is a technology that uses converters to process only a portion of the total power, allowing most of the system's energy to be transferred directly through the power cables [80]. This approach reduces power dissipation as the PPP converter handles less power, resulting in improved system efficiency and power density [81]. Previous research has developed various PPP converters, including those incorporating flyback converters [82], dual-active bridge DAB converters [83], and quasi-Z-source converters [84] based on their equivalent full-power isolated converters. Due to their high energy conversion efficiency, PPP multi-port converters have significant potential and merit further research in both topology design and application, especially within multi-port energy routers. In the context of multi-port energy routers, PPP multi-port converters not only enhance energy transfer efficiency by enabling bidirectional energy flow between ports [85] but also facilitate easier control of energy flow.

In terms of the DC power transfer part in the energy router, a PPP TAB converter is proposed in this chapter. The proposed converter has three ports, and power is exchanged between them using a phase-shift PWM mechanism [86]. Based on the lag/lead relationship of three pulse width waveforms, ports at PPP TAB converter can realize the power transmission. With different lag/lead relationships, the directions of power transmission are also various because each port of PPP TAB converter can make sure the bidirectional power flow [87]. This method allows charging and discharging between ports while inheriting the high efficiency advantages of the PPP converter. Through simulations, this chapter demonstrates the practicality of the power transmission method.

This chapter is structured as follows. First, the power flow control methods and the configuration of the bidirectional AC/DC converter are briefly described. Secondly, the PPP TAB converter is demonstrated. Thirdly, a simulation model containing the proposed MER is implemented in MATLAB/Simulink. Fourthly, an experiment of PPP TAB converter is verified, and a brief conclusion is given at the end of this chapter.

3.2 Topology Configuration

3.2.1 Bidirectional AC/DC Converter

Fig. 3-2 presents the bidirectional AC/DC converter structure. The proposed topology has two ports, each of which is connected separately with the main power gird and one port of the PPP TAB converter. The bidirectional AC/DC converter involves a full bridge with four switches, an inductor L_{ad} and a capacitor C_{ad}. Among them, the inductor L_{ad} is an important factor that makes sure the bidirectional AC/DC converter working in the continuous conduction mode (CCM) and determines the size of the input current ripple. Furthermore, the main functions of capacitor C_{ad} are mainly in two aspects. One of them is filtering of voltage ripples caused by high frequency switching action of switches. The other is keeping bus voltage fluctuations within limits and supplying the load while the bidirectional AC/DC converter is operating in inductive energy storage.

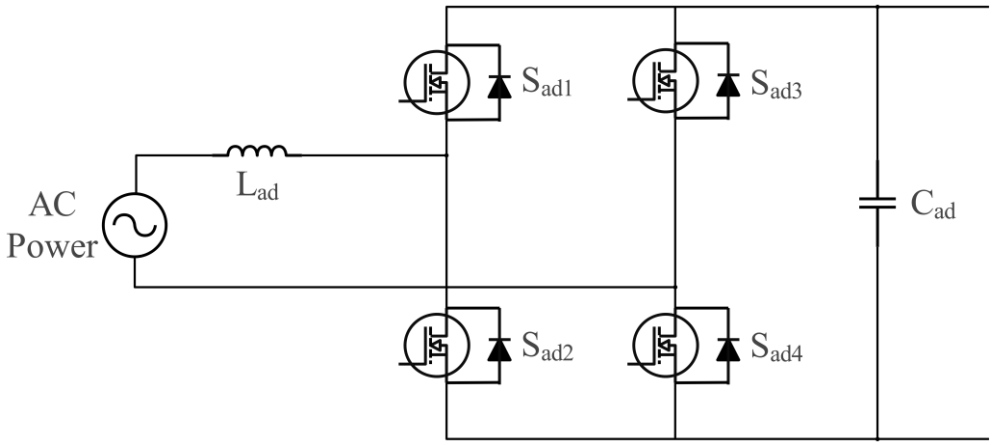

Fig. 3-2. Topology of the proposed bidirectional AC/DC converter

3.2.2 PPP TAB Converter

The depicted configuration, as illustrated in Fig. 3, features three ports. Each of these ports comprises an inductor L_x (where x is 1, 2, or 3), a transformer with winding N_x, and an H-bridge equipped with four switches. Furthermore, capacitors C_y (where y is 1 or 2) at ports 2 and 3 are connected in parallel with their respective H-bridges. Additionally, any type of emergency electric power source *ES* is connected to port 2 through wiring, establishing a circuit for charging and discharging. Port 1 relates to the DC port of the bidirectional AC/DC converter to enable grid connection of MER to the main power grid. Port 3 is connected to the clients' loads and energy router storage unit (ERSU) to realize the power supply for loads. In a multi-port bidirectional MER for emergency energy system, *ES* can be assumed to be any kind of EPPS which is detailed and explained in [71]. In this design, part of the power is transferred between the three ports through the three windings, while the remaining power travels directly

from the input port to the output port. This approach, unlike traditional DC/DC converters, integrates multiple ports to accommodate diverse bidirectional power flow needs. The system can also be flexibly integrated into a multi-port bidirectional energy router to conserve space, utilizing a distributed ERSU.

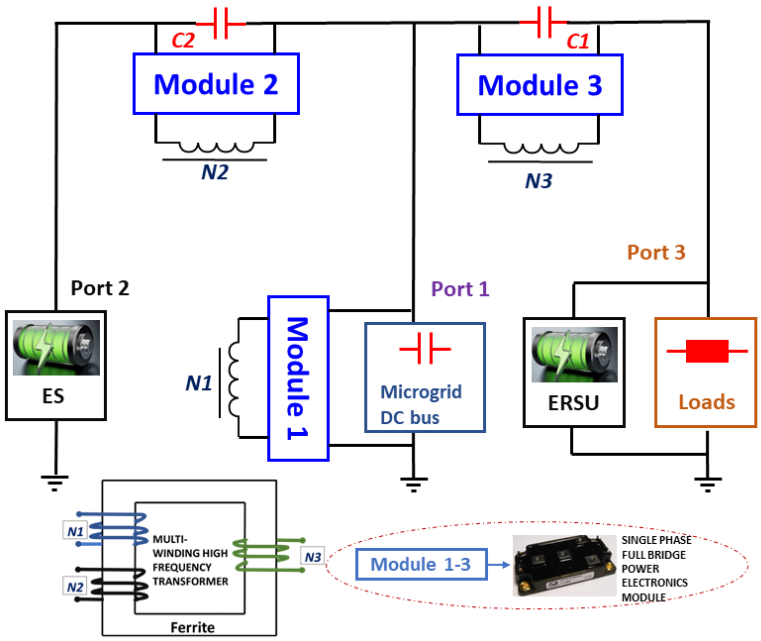

Fig. 3-3. The topology of PPP TAB converter including three ports, where the power grid, emergency electric power source and ERSU are connected.

3.3 Control Method Analysis

3.3.1 Bidirectional AC/DC Converter

In this thesis a full bridge circuit structure consisting of four MOSFET switches is used as the main circuit structure for bidirectional AC/DC converter, thus enabling the bidirectional flow of energy. The control of the four MOSFET switches allows the bidirectional AC/DC converter to always provide a constant and stable output voltage. The working patterns of bidirectional AC/DC converter are shown in Fig. 3-4. For bidirectional AC/DC converter in rectifier mode converting AC power to DC power, when the voltage at the AC port is positive, switch S_{ad3} is always off and S_{ad4} is always on, while switch S_{ad1} and S_{ad2} operate at high frequencies shown in Fig. 3-5, thus contributing to a Boost circuit with the AC input side inductor Lad. S_{ad2} is the main switch and S_{ad1} is the current continuity switch. When S_{ad3} is on and S_{ad1} is off, the

inductor charges and stores energy. When S_{ad1} is on and S_{ad2} is off, the inductor discharges and releases energy to the DC port, thus completing the conversion from AC power to DC power. When the voltage at the AC port is negative, a similar operation to the positive half-cycle can be obtained.

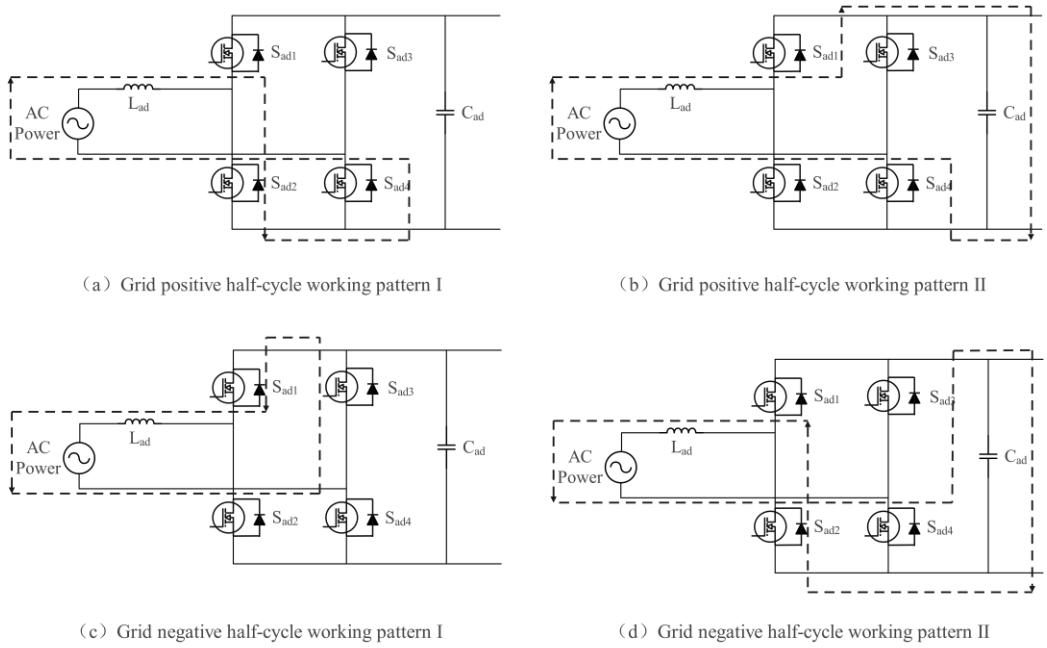

Fig. 3-4. Working patterns of bidirectional AC/DC converter in grid positive half-cycle working pattern (a) I and (b) II, and grid negative half-cycle working pattern (c) I and (d) II

When the topology is in inverter mode, which converts DC power to AC power, the four switches form a Buck circuit in the positive and negative half of the power grid, transferring the energy from the DC side to the AC side. This means that S_{ad3} and S_{ad4} are always on or off during the positive and negative half-cycle of the AC voltage, while the high-frequency switches S_{ad1} and S_{ad2} work as the main switch and continuity switch of the Buck circuit respectively, thus realizing the inverter function.

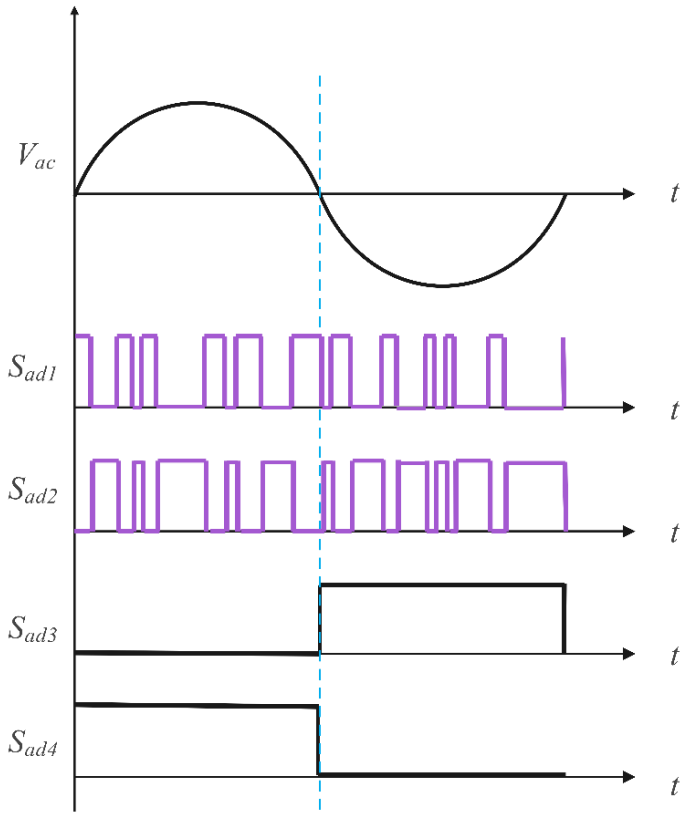

Fig. 3-5. Typical waveforms when bidirectional AC/DC converter conducts forward energy transmission

For the control of switch gate signals, the phase-locked loop (PLL) technique is used in this bidirectional AC/DC converter. PLL is a phase feedback system that obtains the instantaneous phase of a time-varying sine wave. According to Fig. 3-6, the basic PLL consists of three modules, the phase angle detector (PD), the loop filter (LF) and the voltage-controlled oscillator (VCO) [88].

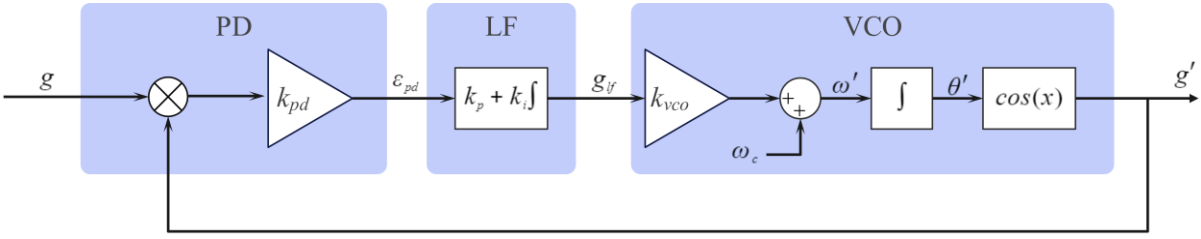

Fig. 3-6. Basic structure of PLL consists of PD, LF and VCO blocks

This topology uses a PLL based on a second-order generalized integrator (SOGI) shown in Fig. 3-7. This PLL omits the VCO and adds a module called the frequency/phase angle generator (FPG), which provides the phase angle for the sinusoidal functions in the Park transform and

can still implement the VCO function in the PLL structure. The combination of the quadrature signal generator (QSG) and the park transform can then be considered a synchronous PD.

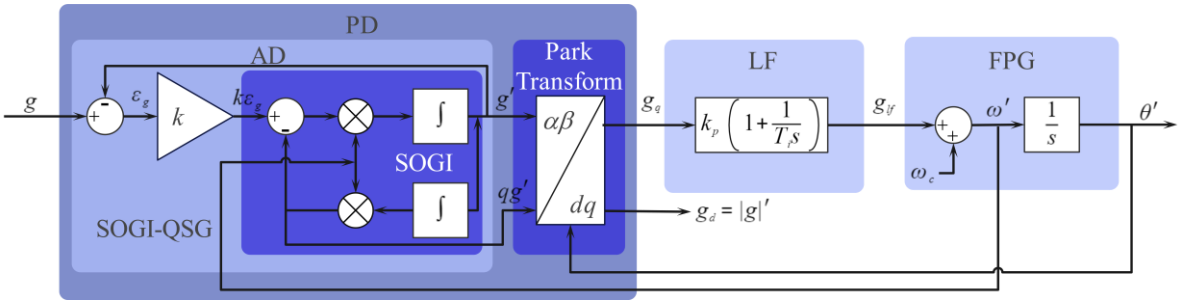

Fig. 3-7. Basic structure of PLL consists of PD, LF and VCO blocks

The transfer functions of SOGI are expressed in equations (3-1), (3-2) and (3-3). These transfer functions show that the bandwidth of the SOGI-based adaptive filter (AD) is not a function of the center frequency, but depends only on the gain. Furthermore, when the center frequency of the filter coincides with the input frequency, the magnitudes of the quadrature signals v and qv coincide with the input signal, so the SOGI-based filter structure will be very suitable for the QSG, also known as the SOGI-QSG system. The SOGI-PLL has a double feedback loop, which means that the FPG provides the phase angle for the Park transform while providing the center frequency for the SOGI-QSG.

$$SOGI(s) = \frac{g'}{k\varepsilon_g}(s) = \frac{\omega_c s}{s^2+\omega_c^2} \tag{3-1}$$

$$D(s) = \frac{g'}{g}(s) = \frac{k\omega_c s}{s^2+k\omega_c s+\omega_c^2} \tag{3-2}$$

$$Q(s) = \frac{qg'}{g}(s) = \frac{k\omega_c}{s^2+k\omega_c s+\omega_c^2} \tag{3-3}$$

The response of the SOGI-PLL differs from that of other PLLs in that both the adaptive filter and the feedback loop of the PLL depend on the same variable, namely the detected phase angle. two variables are involved in the synchronization process of the SOGI-PLL, one is the use of the detected frequency to adjust the SOGI-QSG and the other is the phase angle of the PLL lock input. As a result, the SOGI-PLL detects the input phase angle faster than a conventional PLL and does not contain steady-state oscillations.

The overall control method of the bidirectional AC/DC converter is dual closed loop PI average current control. The controller shown in Fig. 3-8 consists of a voltage change and a current loop. The core of the double closed-loop PI control is to control the switches through the output

duty cycle *dr* and adjust the amplitude and phase of the inductor current to control the output voltage. First, the output voltage error signal is generated by comparing the output voltage V_0 collected by the output voltage sampling circuit with the reference voltage V_{ref}. Then the voltage error signal is multiplied by the input voltage to generate the reference current signal. The reference current signal thus has both the amplitude and phase information of the input voltage as well as the output voltage information. The inductor current i_{Lad} collected by the current sampling circuit is compared with the reference current signal and finally the gate signals of the four switches are generated by the current loop PI controller.

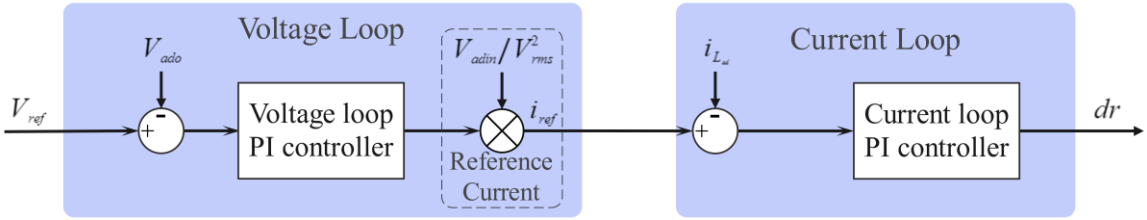

Fig. 3-8. Basic structure of dual closed loop PI average current control consists of voltage loop and current loop

For this topology shown in Fig. 3-2, the block diagram of the double closed loop PI forward and inverse transform control algorithm is shown below.

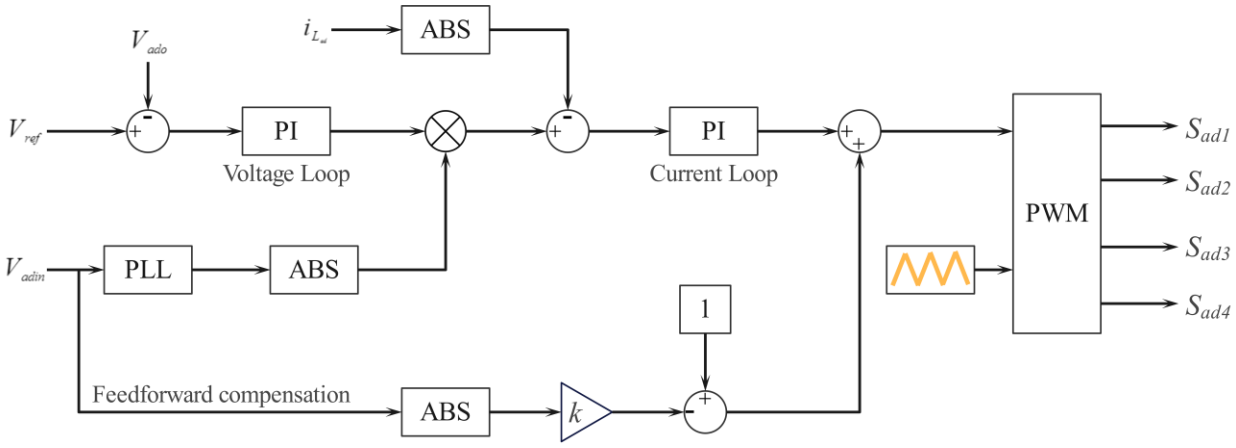

(a)

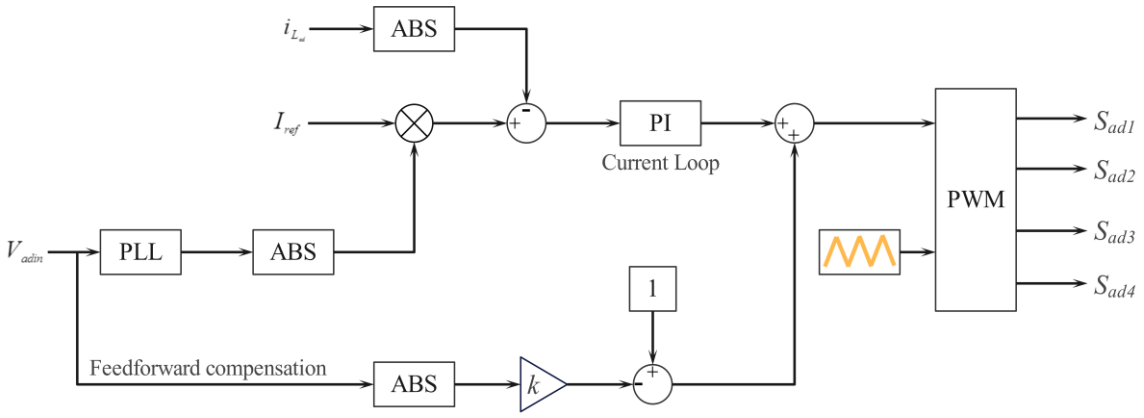

(b)

Fig. 3-9. Dual Closed Loop PI Average Current Control of (a) AC/DC transfer and (b) DC/AC transfer

In terms of the double closed loop PI forward transform control algorithm, the input values are voltage of AC port V_{adin}, voltage of DC port V_{ado}, reference voltage of DC port V_{ref} and current of the inductor i_{Lad}. On the other hand, the double closed loop PI inverse transform control algorithm, the input values are voltage of AC port V_{adin}, reference current of inductor I_{ref} and current of the inductor i_{Lad}.

3.3.2 PPP TAB Converter

To derive the energy flow expression of a PPP TAB converter, the characteristics of power transmission of two ports in an isolated TAB converter are first analyzed. The phase-shift PWM method is applied to control the power flow direction in the proposed converter. According to [87], the equation of power transmission between any two ports in an isolated TAB converter can be obtained as shown in equation (3-4). Taking the control signals of switches S_1 and S_2 as references, the control signals of switches S_7 and S_8 and switches S_{11} and S_{12} are lagged by φ_2 and φ_3 radians, respectively, as exhibited in Fig. 3-8. It's essential to consider that $-\pi<\varphi_2<\pi$, $-\pi<\varphi_3<\pi$. Moreover, each switch operates with a duty ratio equal to half of the switching cycle. Furthermore, the current waveforms of L_1, L_2, and L_3 in a conventional isolated TAB converter are displayed in Fig. 3-8, representing i_{L1}, i_{L2}, and i_{L3}, respectively. For simplicity in analysis, the turns ratio N_1: N_2: N_3 of the transformer is set at 1:1:1.

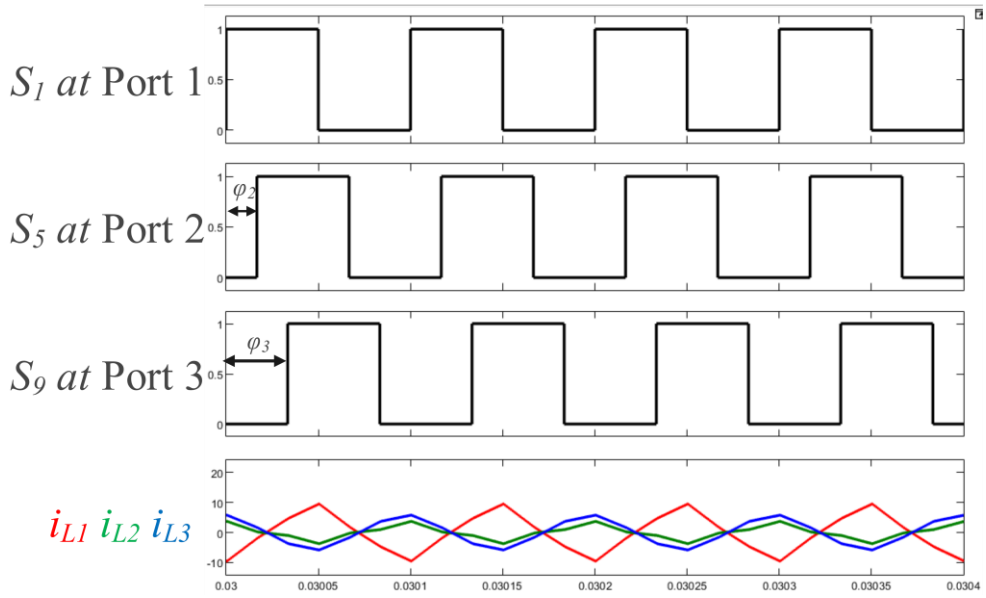

Fig. 3-10. Typical waveforms of an isolated phase-shift TAB converter [87]

$$\begin{cases} P_{dc12} = V_1 I_1 = \frac{\varphi_2(\pi-|\varphi_2|)V_1V_2}{2\pi^2 f_s(L_1+L_2)} \\ P_{dc13} = V_3 I_3 = \frac{\varphi_3(\pi-|\varphi_3|)V_1V_3}{2\pi^2 f_s(L_1+L_3)} \\ P_{dc23} = V_2 I_2 = \frac{(\varphi_3-\varphi_2)(\pi-|\varphi_3-\varphi_2|)V_1V_2}{2\pi^2 f_s(L_2+L_3)} \end{cases} \quad (3\text{-}4)$$

in this expression, V_1, V_2, and V_3 refer to the voltages of port 1, port 2 and port 3, respectively, and P_{dc12}, P_{dc13}, and P_{dc23} are the power flow from port 1 to port 2, from port 1 to port 3, and from port 2 to port 3, respectively. Furthermore, f_s is the switching frequency of gate signals. Considering the proposed PPP TAB converter, since the rest unprocessed energy transfers directly through inductors, the conducted energy in one operation cycle can be obtained in (3-5), where C_{dc12}, C_{dc13}, and C_{dc23} are the conducted power flow from port 1 to port 2, from port 1 to port 3, and from port 2 to port 3, respectively.

$$\begin{cases} C_{dc12} = \frac{(V_1-V_2)}{(L_1+L_2)f_s} \\ C_{dc13} = \frac{(V_1-V_3)}{(L_1+L_3)f_s} \\ C_{dc23} = \frac{(V_2-V_3)}{(L_2+L_3)f_s} \end{cases} \quad (3\text{-}5)$$

Next, the total power transferred among these three ports in one switching period can be acquired from (3-4) and (3-5) by adding together the processed power and conducted power. The equation of the total power converted among various ports is presented in (3-6), where T_{dc12}, T_{dc13}, and T_{dc23} are the total power flow from port 1 to port 2, from port 1 to port 3, and from port 2 to port 3, respectively.

$$\begin{cases} T_{dc12} = \frac{\varphi_2(\pi-|\varphi_2|)V_1V_2+2\pi^2(V_1-V_2)}{2\pi^2 f_s(L_1+L_2)} \\ T_{dc13} = \frac{\varphi_3(\pi-|\varphi_3|)V_1V_3+2\pi^2(V_1-V_3)}{2\pi^2 f_s(L_1+L_3)} \\ T_{dc23} = \frac{(\varphi_3-\varphi_2)(\pi-|\varphi_3-\varphi_2|)V_1V_2+2\pi^2(V_2-V_3)}{2\pi^2 f_s(L_2+L_3)} \end{cases} \quad (3\text{-}6)$$

Suppose each inductor has the same inductance and the sum of each two inductors is L_d, the port power can be derived from

$$\begin{cases} T_{dc1} = T_{dc12} + T_{dc13} \\ = \frac{\varphi_2(\pi-|\varphi_2|)V_1V_2+\varphi_3(\pi-|\varphi_3|)V_1V_3+4\pi^2V_1-2\pi^2(V_2+V_3)}{2\pi^2 f_s L_d} \\ T_{dc2} = -T_{dc12} + T_{dc23} \\ = \frac{-\varphi_2(\pi-|\varphi_2|)V_1V_2+(\varphi_3-\varphi_2)(\pi-|\varphi_3-\varphi_2|)V_2V_3+4\pi^2V_2-2\pi^2(V_1+V_3)}{2\pi^2 f_s L_d} \\ T_{dc3} = -T_{dc13} - T_{dc23} \\ = \frac{-\varphi_3(\pi-|\varphi_3|)V_1V_3-(\varphi_3-\varphi_2)(\pi-|\varphi_3-\varphi_2|)V_2V_3+4\pi^2V_3-2\pi^2(V_1+V_2)}{2\pi^2 f_s L_d} \end{cases} \quad (3\text{-}7)$$

where T_{dc1}, T_{dc2}, and T_{dc3} represent the total power of port 1, port 2, and port 3, respectively.

It is evident that the energy flow at each port is solely influenced by the phase shift angles, as long as the port voltages remain constant. Consequently, the power transmission direction is contingent on both the phase shift angles and the voltage levels of the ports. For instance, Fig. 3-11 displays four typical energy flow scenarios. For example, when $T_{dc1}>0$, $T_{dc2}<0$ and $T_{dc3}<0$ which also means $0< \varphi_2 < \varphi_3$, as depicted in Fig. 3-10, the combined power flow from port 1 to port 2 and port 3 is evident. Consequently, the capacity for multi-directional power flow can be achieved by modulating the phase shift angles of the converter switches within a specific range of variation in the port voltages.

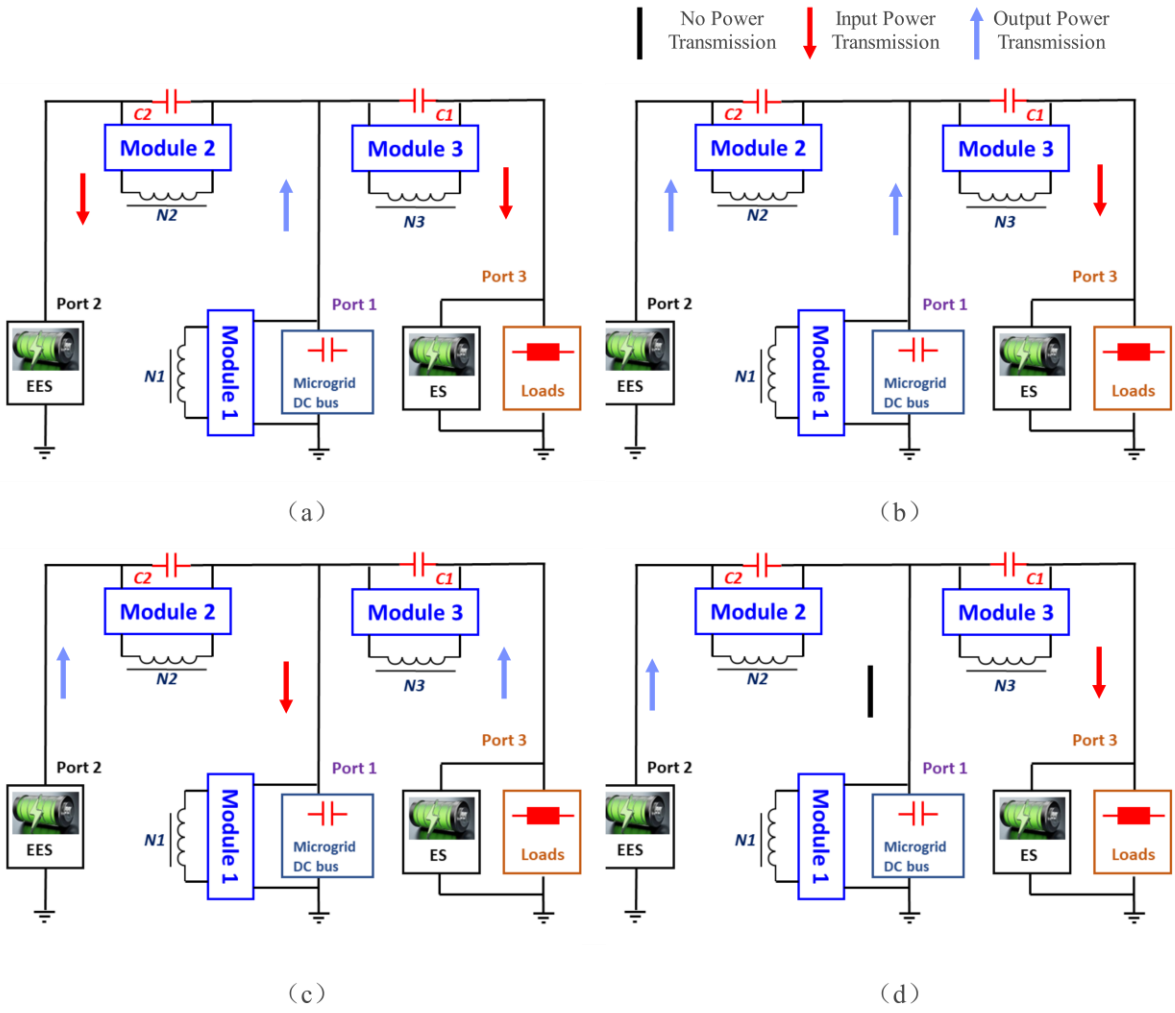

Fig. 3-11. Typical power flow directions of the proposed topology, where (a) $0< \varphi_2 < \varphi_3$; (b) $\varphi_2 < 0 < \varphi_3$ and $|\varphi_2|<|\varphi_3|$; (c) $\varphi_2 < \varphi_3 < 0$; (d) $\varphi_2 < 0 < \varphi_3$ and $|\varphi_2|=|\varphi_3|$

3.3.3 Power Efficiency Analysis

P_{in} is the total input power which can be obtained through pulsing the total output power P_{out}, semiconductor loss P_s, transformer loss P_{tl}, and heat loss on passive components P_h shown in (3-8).

$$P_{in} = P_{out} + P_s + P_{tl} + P_h \tag{3-8}$$

In semiconductor components, there are typically two types of losses: conduction loss and switching loss. Additionally, the losses incurred by transformers consist of iron and copper losses. In the context of the proposed bidirectional AC/DC converter, the Buck/Boost circuit design, characterized by its simplicity, ensures that conduction and switching losses during the

conversion process are minimized. In the case of the proposed PPP TAB converter, only a portion of the power is transferred through the transformer, resulting in lower transformer losses. However, the conduction loss in the proposed converter is relatively higher due to the presence of power cables. By eliminating conduction losses through the use of low-resistance cables with a short distance, the overall losses in the proposed converter can be reduced, thus achieving greater power efficiency compared to the conventional TAB converter. In summary, this design of MER has less loss during the conversion process that others in [13], [89], [90]and [91].

3.4 Simulation Results

To assess the viability of the proposed power transmission method, a MATLAB/Simulink simulation model is developed, featuring three battery packs. The designed models are depicted in Fig. 1. The system configurations are exhibited in Table 1, where the voltages of AC port and DC port of bidirectional AC/DC converter are 311V and 400 V. The reference voltage and reference current of bidirectional AC/DC converter model are 400 V and $30\sqrt{2}$ A The voltages of port 1, port 2 and port 3 of the PPP TAB converter are set to 400 V, 410V, and 420 V, respectively. The initial state of charge of the battery pack at port 2 is considered at 50%. Moreover, the converter switching frequency is 10 kHz and the transformer turns ratio is 1:1:1.

TABLE 3-1 Parameters of the MER Simulation Model

Parameter name	Parameter Value
$V_1/V_2/V_3$ (Port voltages)	400/410/420 V
V_{ac} (Voltage of the main power grid)	311 V
SOC (Initial state of charge)	50%
R_L (Initial resistance of load)	200 Ω
N_1:N_2:N_3 (Transformer turns ratio)	1:1:1
f_s (Converter switching frequency)	10 kHz
f_{ac} (AC power frequency)	50 Hz
L_{ad} (AC/DC converter inductance)	360 μH
$L_1/L_2/L_3$ (Series inductance)	300 μH
C_{ad} (AC/DC converter capacitance)	9 mF

C_2/C_3 (Series capacitance)	100 μF
V_{ref} (Reference voltage)	400 V
I_{ref} (Reference current)	30 √ 2 A

3.4.1 AC/DC conversion of bidirectional AC/DC converter

According to the analysis of the relationship of φ_2 and φ_3 of the PPP TAB converter, when φ_2 and φ_3 satisfy the relationship in Fig. 3-11(a) and Fig. 3-11(b), the bidirectional AC/DC converter is in rectifier mode. This means AC power transfer into DC power in the system.

Fig. 3-12 shows the output voltage of DC port. It is obvious that during the steady state, the voltage can be maintained at 400V. Moreover, there is a negligible fluctuation in the voltage at the steady state condition and it only takes about 0.5s that bidirectional AC/DC converter works in steady state. This shows that the proposed bidirectional AC/DC converter can provide a stable and continuous DC voltage to the port 1 of the PPP TAB converter through transferring the AC power into DC power.

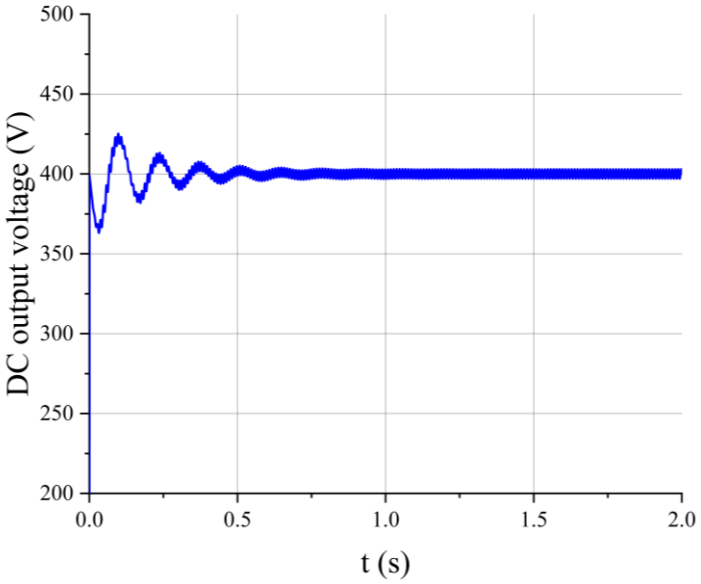

Fig. 3-12. DC output voltage of AC/DC transfer

Fig. 3-13 shows the active power and reactive power and power factor of bidirectional ACDC converter at the AC port. During the steady state, these two values are mainly at about 0W and 6500W respectively. This means that the power factor of the bidirectional AC/DC converter is nearly 1 when transferring the AC power to the DC power according to the circulation by active

power and reactive power.

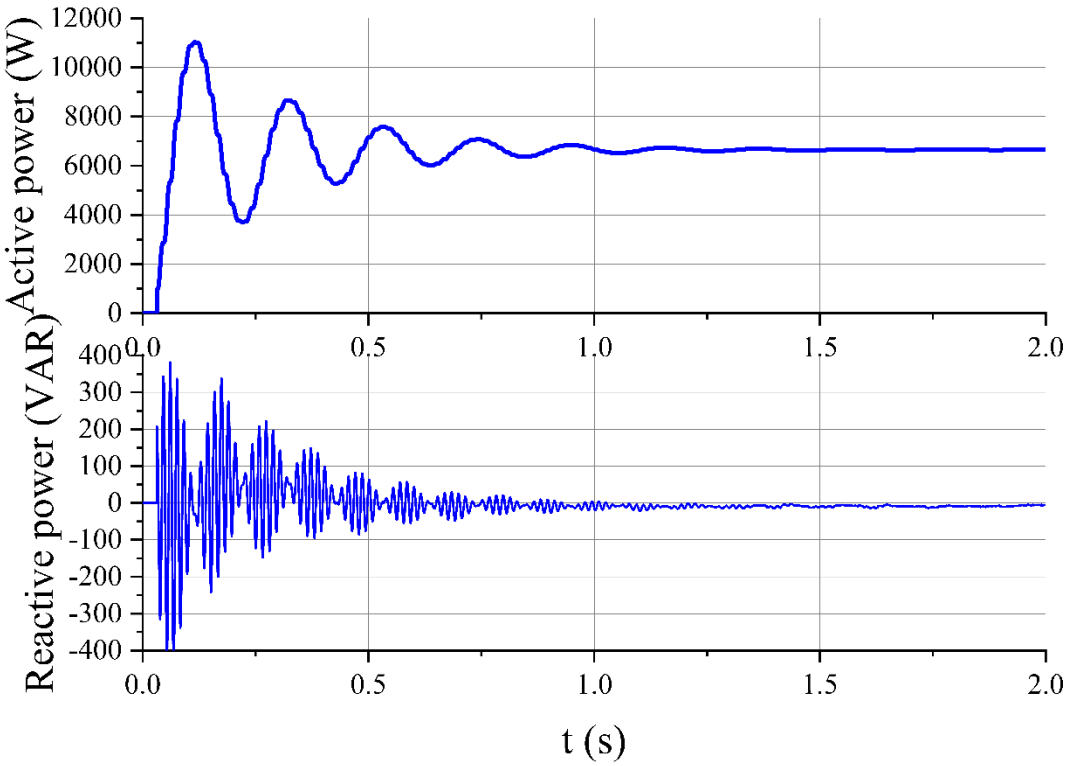

Fig. 3-13. Active power and reactive power of AC/DC transfer at AC port

3.4.2 DC/AC conversion of bidirectional AC/DC converter

When φ_2 and φ_3 satisfy the relationship in Fig. 3-11(c), bidirectional AC/DC converter is in inverter mode which means that it transfers DC power into AC power.

Fig. 3-14 shows the output voltage and current of AC port during the steady state. It is obvious that during the steady state, the voltage and current waveform still conform to the design requirement of the bidirectional AC/DC converter. This means that the PPP TAB converter can provide a stable and continuous AC voltage to the AC port of the bidirectional AC/DC converter through transferring the DC power into AC power.

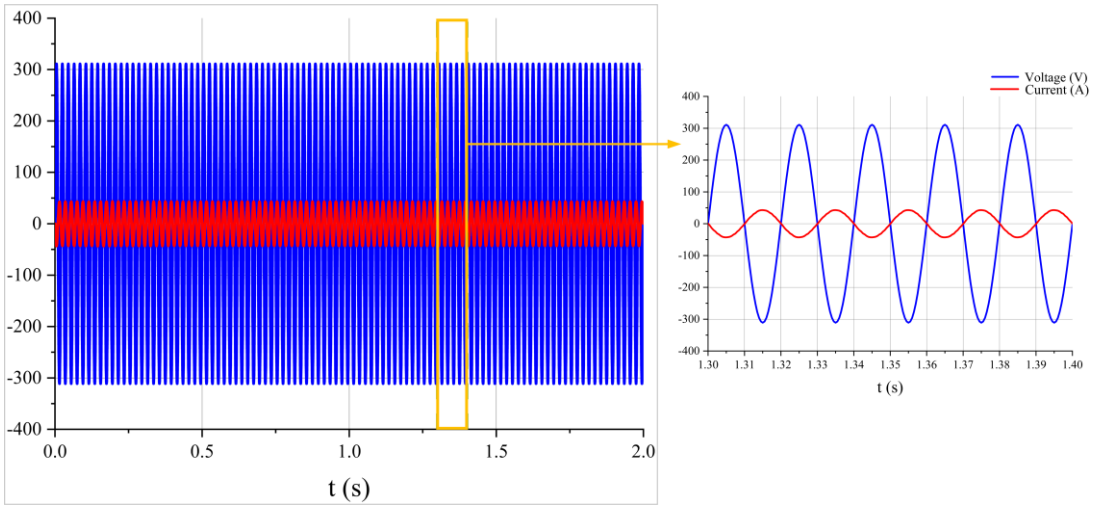

Fig. 3-14. Active power and reactive power of AC/DC transfer at AC port

Fig. 3-15 shows the power factor of bidirectional AC/DC converter at the AC port. During the steady state, power factor is mainly at about -1. This means that the efficiency of the bidirectional AC/DC converter is also high when transferring the DC power to the AC power.

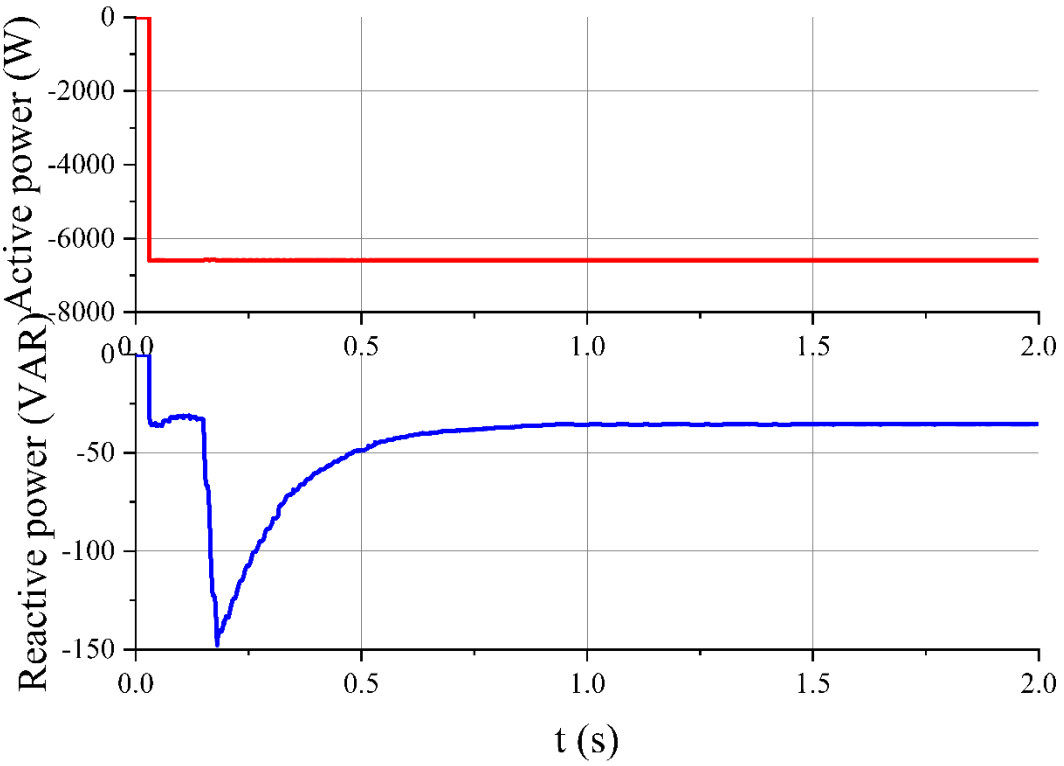

Fig. 3-15. Active power and reactive power of DC/AC transfer at AC port

3.4.3 DC/DC conversion of PPP TAB converter

To ensure the working status of PPP TAB converter in four different kinds of power direction flows shown in Fig. 3-11, the following results are shown in different situations of port 2 and 3.

a) When port 2 and 3 are output ports

In this situation, it means that power grid has enough energy to satisfy the needs of all the loads and the charging of emergency electric power source and ERSU. The direction of power transmission is shown in Fig. 3-11(a). Fig. 3-16 shows the voltage of port 3 when port 2 and 3 are output ports. It is obvious that the voltage of port 3 can be maintained at about 420V in steady states which means that the loads can be supplied by PPP TAB converter continuously and steadily. Besides, because the voltage of port 3 is positive shown in Fig. 3-16, port 3 is the output port of PPP TAB converter.

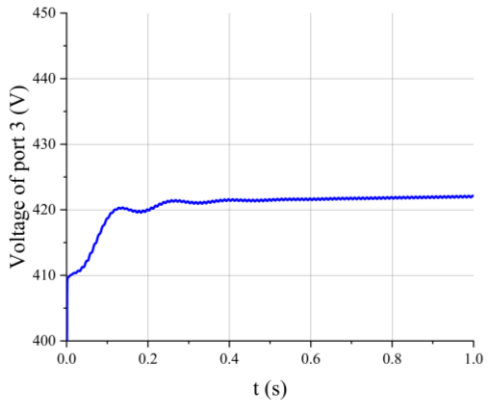

Fig. 3-16. Voltage Waveform of port 3 when port 2 and 3 are output ports

Table 3-2 is the state of charge (SOC) of emergency electric power source at port 2. The emergency electric power source at port 2 can be charged stable and port 2 is the output port in this condition. This means that in this relationship between φ_2 and φ_3, port 1 is the input port, and port 2 and 3 are the output ports which corresponds to the conclusion obtained in Fig. 3-11(a).

TABLE 3-2 SOC of port 2 when port 2 and 3 are output ports

Time (s)	Value of SOC (%)
0	40
20	41.2
30	41.8

40	42.4
60	43.6

b) When port 2 is input port and port 3 is output port

In this situation, it means that power gird does not have enough energy, or the power grid is paralyzed. Port 2 needs to become the input port to supply power to the loads at port 3 to ensure the normal working of all the loads. The direction of power transmission is shown in Fig. 3-11(b) and (d) when port 2 is input port and port 3 is output port. Fig. 3-17 shows the voltage of port 3 when port 2 is input port. It is obvious that the voltage of port 3 can be maintained at about 420V in steady states which means that the loads can still be supplied by PPP TAB converter continuously and steadily.

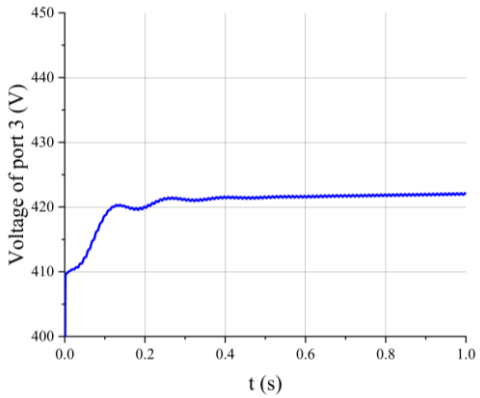

Fig. 3-17. Voltage waveform of port 3 when port 2 is input port and port 3 is output port

Table 3-3 is the SOC of EPPS at port 2. The emergency electric power source at port 2 can be discharged stable and port 2 is the input port in this condition. This means that in these relationships between φ_2 and φ_3, port 2 is the input port, and port 3 is the output port which corresponds to the conclusion obtained in Fig. 3-11(b) and 3-11(d).

TABLE 3-3 SOC of port 2 when port 2 is input port and port 3 is output port

Time (s)	Value of SOC (%)
0	40
20	38.8
30	38.2
40	37.6

60	36.4

c) When port 1 and 3 are output ports

In this situation, it means that emergency electric power source has extra energy to supply to the power gird so that P2P can be realized. The direction of power transmission is shown in Fig. 3-11(c). Fig. 3-18 shows the voltage of port 3 when port 1 and 3 are output ports. It is obvious that the voltage of port 3 can be maintained at about 420V in steady states which means that the loads can be supplied by PPP TAB converter continuously and steadily. Besides, because the current of port 3 is positive shown in Fig. 3-18, port 3 is the output port of PPP TAB converter.

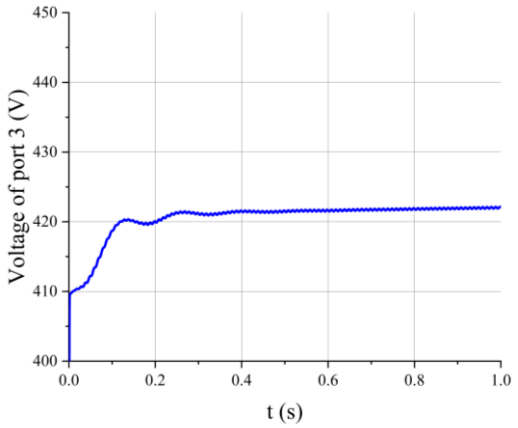

(a) **(b)**

Fig. 3-18. Voltage waveform of port 3 when port 2 is input port and port 3 is output port

Table 3-4 shows the SOC of emergency electric power source at port 2. The emergency electric power source at port 2 can be discharged stable and port 2 is the input port in this condition. This means that in this relationship between φ_2 and φ_3, port 2 is the input port, and port 1 and 3 are the output ports which corresponds to the conclusion obtained in Fig. 3-11(c).

TABLE 3-4 SOC of port 2 when port 1 and 3 are output ports

Time (s)	Value of SOC (%)
0	40
20	38.8
30	38.2

40	37.6
60	36.4

3.5 Experimental Verification of Power Direction of TAB Converter

To verify the inputs and outputs of each port of the TAB converter for different relationships of φ_2 and φ_3, an experimental circuit is set up as shown in Fig. 3-19. The parameters of the experiment are shown in Table 3-5 and model numbers of the parameters used in the experiment are shown in Table 3-6. To ensure the safety of experiment, a lower port voltage is used in the experiment. However, the conclusion of power transmission direction of each port with the relationship of φ_2 and φ_3 is not affected. Besides, the instance L_x is 33 μH and N_1:N_2:N_3=10:8:8.

TABLE 3-5 Parameters of the TAB converter experiment

Parameter name	Parameter Value
V_1/V_2/V_3 (Port voltages)	10/10/10 V
N_1:N_2:N_3 (Transformer turns ratio)	10:8:8
f_s (Converter switching frequency)	10 kHz
L_1/L_2/L_3 (Series inductance)	33 μH

TABLE 3-6 Model Numbers of the Parameters Used in the TAB Converter Experiment

Parameter name	Parameter	Model Number
Si MOSFET	200V/30A	IRFP250MPBF
Transformer	10:8:8	Design
Auxiliary Inductor	33 μH	Design
Driver IC	High Speed Photocoupler	TLP250

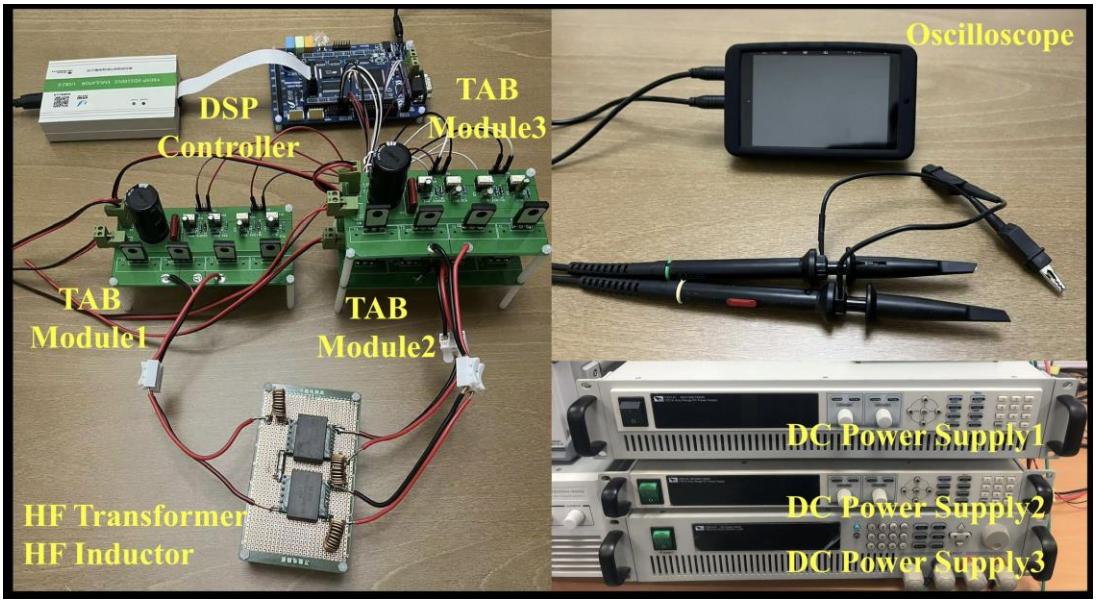

Fig. 3-19. Photograph of the experiment circuit

Fig. 3-20 shows the schematic diagram of one full active bridge in TAB converter. Each switch has a gate control waveform in separate.

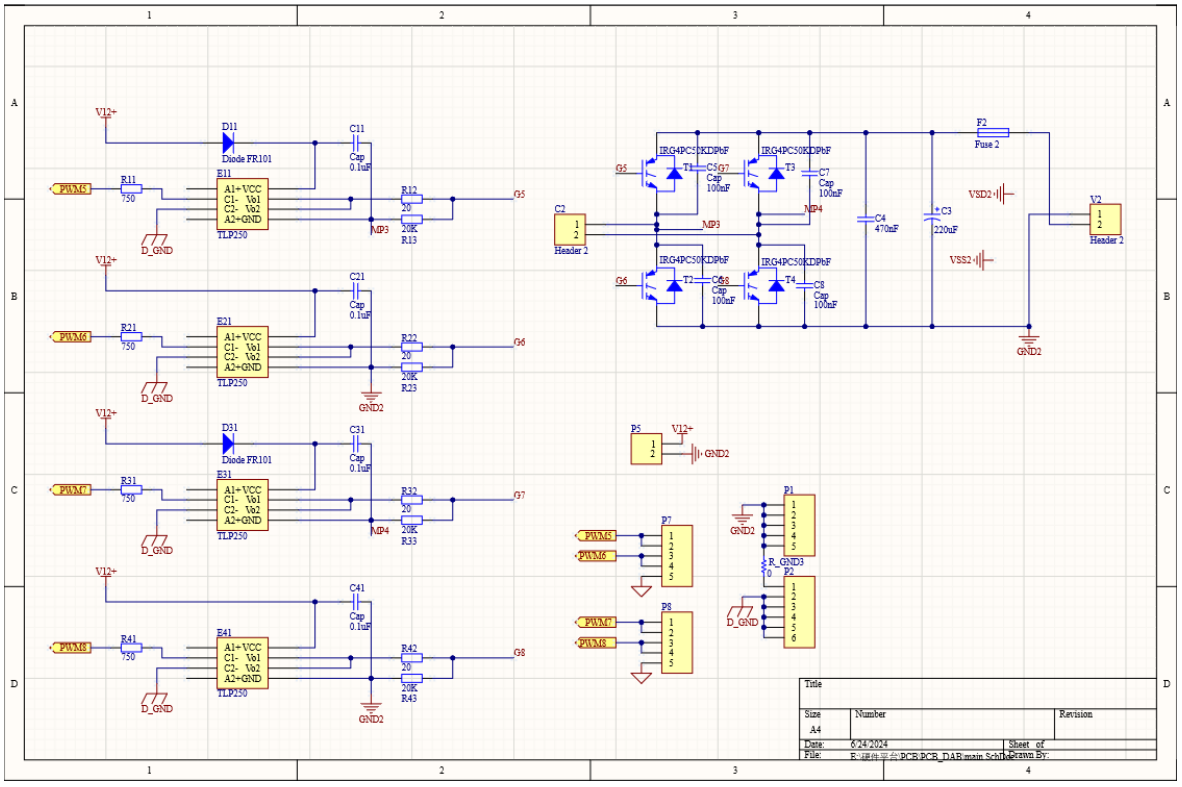

Fig. 3-20. Schematic diagram of one full active bridge in TAB converter

The layout of one full active bridge is shown in Fig. 3-21. Considering that the similarity of each active bridge in TAB converter, the layouts of the other two full active bridge are the

same.

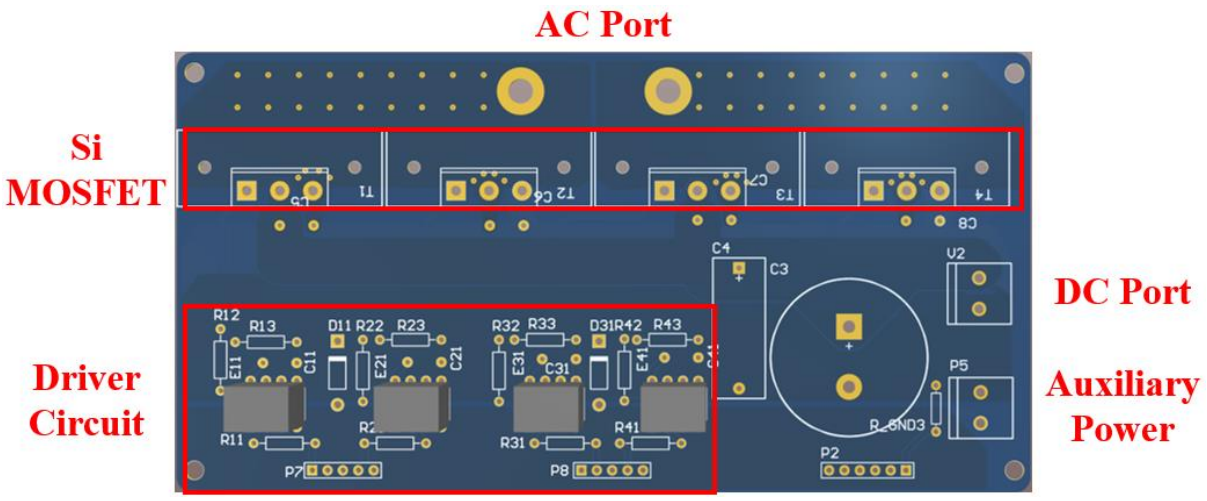

Fig. 3-21. The layout of one full active bridge in TAB converter

Fig. 3-22 shows the four different power flow directions. The left side of each figure shows the switch voltage of each port which shows the relationship of φ_2 and φ_3 and the right side of each figure shows the current of each port which shows the power flow direction. In Fig. 3-22(a), the gate waveforms of switches at port 2 and port 3 are all lagging those at port 1 which means $0< \varphi_2 < \varphi_3$. Fig. 3-22(b) shows $\varphi_2 < 0 < \varphi_3$ and $|\varphi_2|<|\varphi_3|$. It is evident that the gate waveforms of switches at port 2 lead those at port 1, while the gate waveforms of switches at port 3 lag those at port 1., but the absolute value of φ_2 is smaller that that of φ_3 according to the left side of Fig. 3-22(b). The gate waveforms of switches at port 2 and port 3 are all leading those at port 1 in Fig. 3-22(c) which shows $\varphi_2 < \varphi_3 < 0$. When an emergency occurs, TAB converter will be shifted into Fig. 3-22(d). It shows $\varphi_2 < 0 < \varphi_3$ and $|\varphi_2| = |\varphi_3|$. Compared Fig. 3-11 with Fig. 3-22, the relationship between power flow direction and φ_2 and φ_3 is consistent with the theory and simulation.

Furthermore, Fig. 3-22 illustrates four typical power flow scenarios. Fig. 3-22(a) shows power transfers from port 1 to port 2 and port 3 which means that the main power grid is normal and ES and emergency electric power source port are charging. When the energy at emergency electric power source port beyond the needs, TAB converter will be shifted into Fig. 3-22(b). This mode will reduce pressure on main grid transmission and is more economic for the clients. In Fig. 3-22(c), When the energy of ES and emergency electric power source port are all beyond the needs, ES and emergency electric power source port can transfer power to the main power grid which realize the peer-to-peer trading. When an emergency occurs, TAB converter will be shifted into Fig. 3-22(d). The main power grid will be off the grid and emergency electric power

source port and ES port will be the power source to the loads and clients and maintain the normal working of loads until the main grid paralysis is resolved.

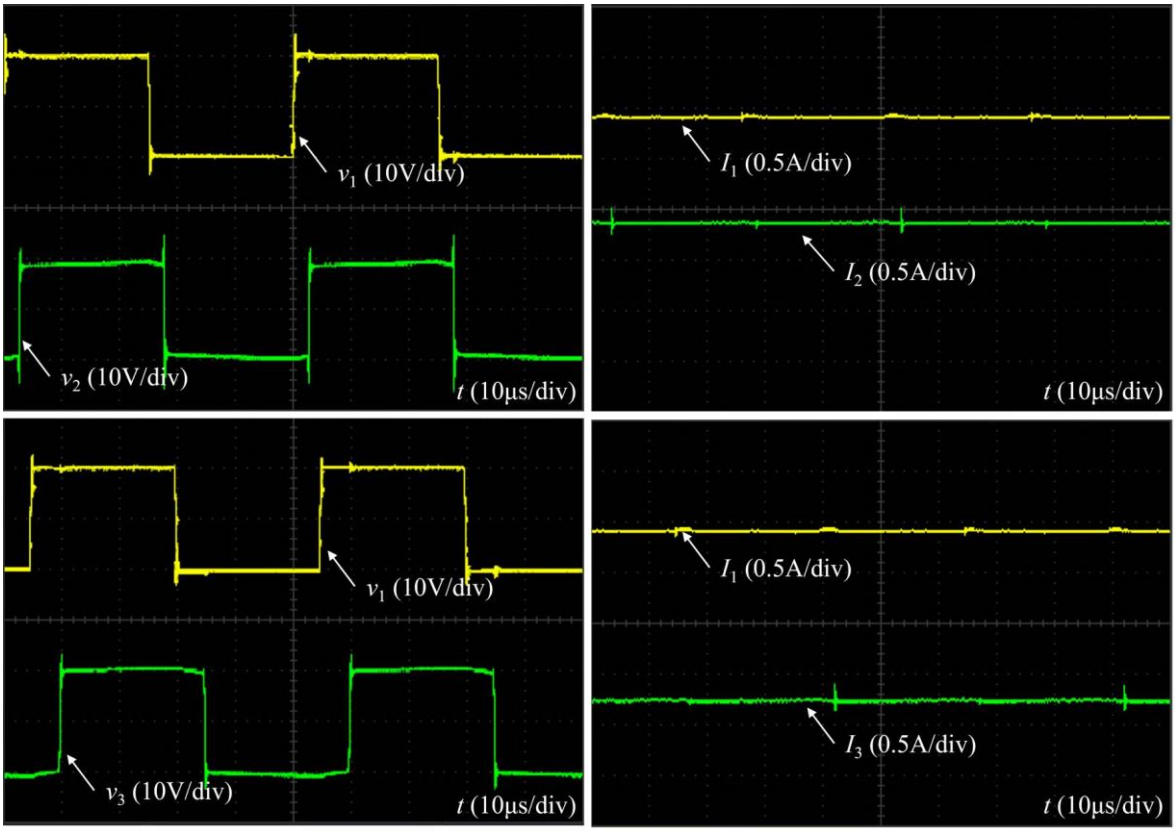

(a)

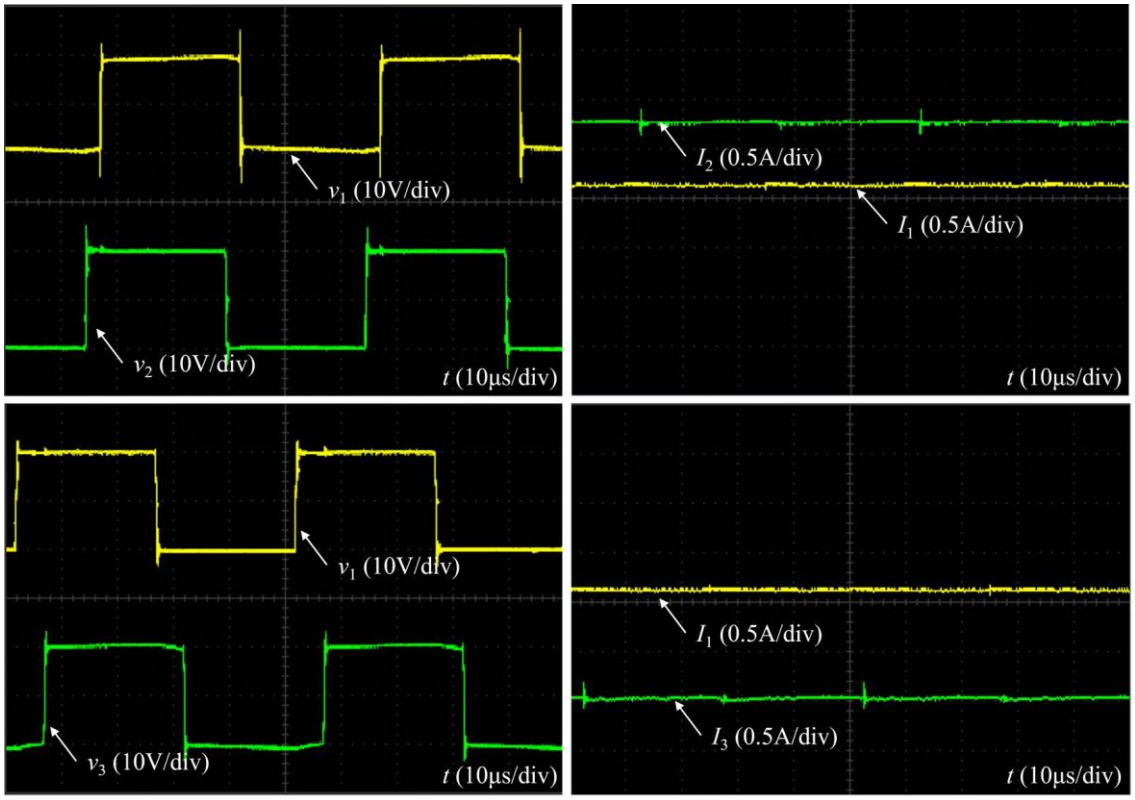
v_1 (10V/div)
v_2 (10V/div)
t (10μs/div)
I_2 (0.5A/div)
I_1 (0.5A/div)
t (10μs/div)
v_1 (10V/div)
v_3 (10V/div)
t (10μs/div)
I_1 (0.5A/div)
I_3 (0.5A/div)
t (10μs/div)

(b)

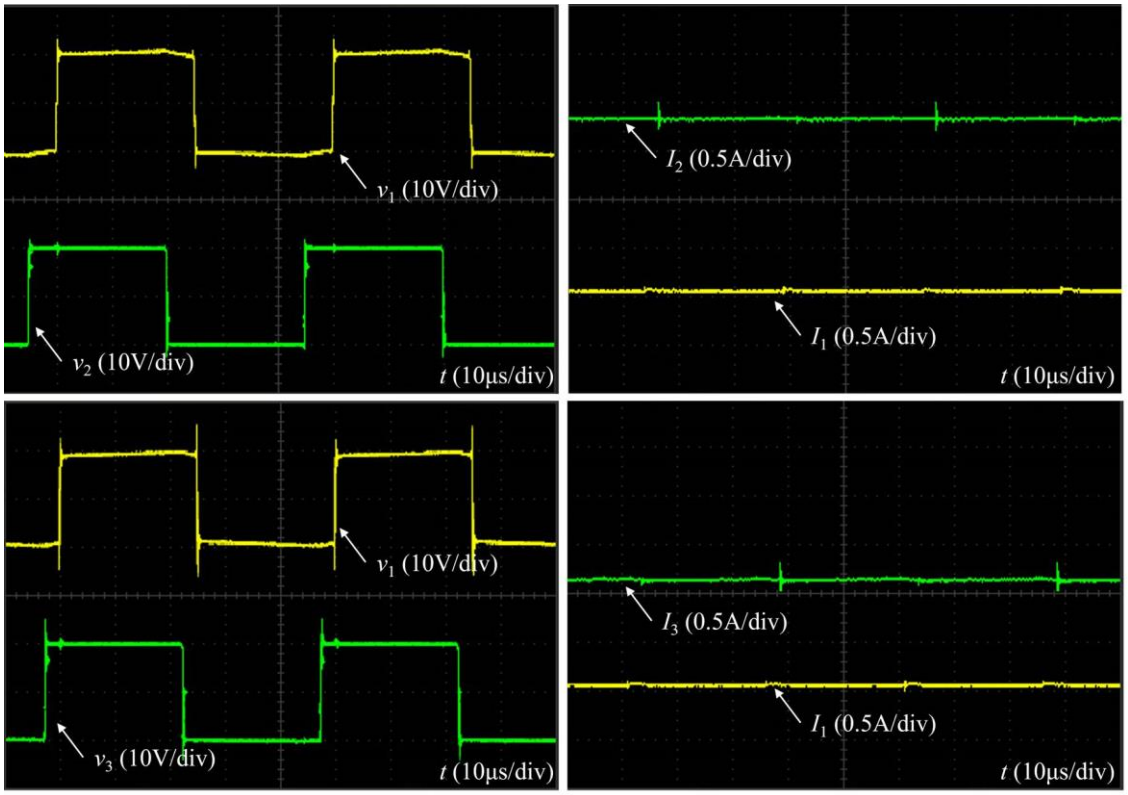
v_1 (10V/div)
v_2 (10V/div)
t (10μs/div)
I_2 (0.5A/div)
I_1 (0.5A/div)
t (10μs/div)
v_1 (10V/div)
v_3 (10V/div)
t (10μs/div)
I_3 (0.5A/div)
I_1 (0.5A/div)
t (10μs/div)

(c)

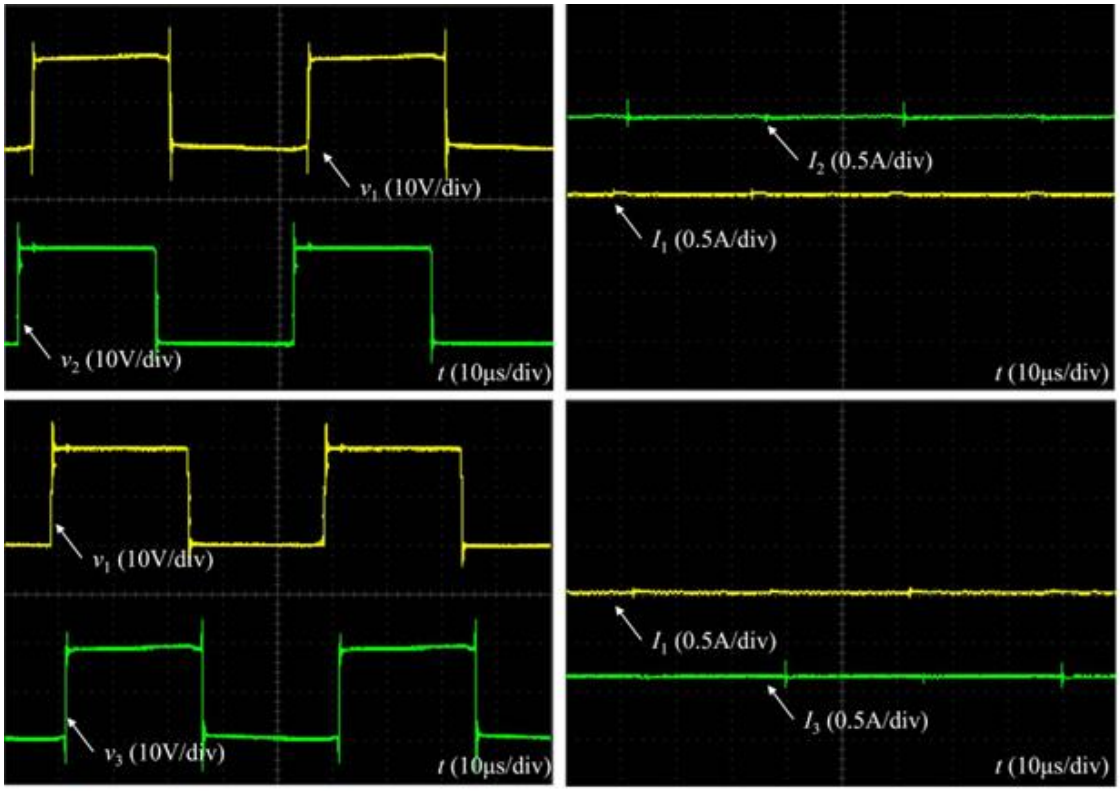

(d)

Fig. 3-22. Experimental switch voltage and current of each port of the TAB converter, where (a) $0< \varphi_2 < \varphi_3$; (b) $\varphi_2 < 0 < \varphi_3$ and $|\varphi_2|<|\varphi_3|$; (c) $\varphi_2 < \varphi_3 < 0$; (d) $\varphi_2 < 0 < \varphi_3$ and $|\varphi_2|=|\varphi_3|$

3.6 Summary

This chapter introduces a MER designed to manage emergency power outages and achieve energy balancing among various power sources and loads. The number of ports in the MER directly influences its capability to manage and supply diverse emergency electric power sources and loads concurrently. Moreover, enhancing urban energy flexibility during emergencies is facilitated by integrating the MER with mobile energy storage units. The MER employs bidirectional AC/DC converters for AC/DC power conversion and PPP TAB converters for DC/DC power transmission. This configuration supports P2P trading and energy balancing, enabling each port in both converter types to serve as either an input or output based on specific operational requirements. Compared to conventional emergency distribution methods and existing ERs, the designed MER exhibits superior power conversion efficiency and accommodates a wide range of emergency electric power sources. Currently, the MER

features three ports. However, expanding the number of ports can be achieved by increasing the ports of the DC/DC converter, thereby enabling the utilization of more emergency electric power sources simultaneously within the MER. A simulation model implemented in MATLAB/Simulink validates the feasibility of the proposed MER. Furthermore, comprehensive testing of the bidirectional AC/DC converter and PPP TAB converter under various operational scenarios demonstrates the efficiency and adaptability of the proposed MER in responding to diverse emergency situations.

.

Chapter 4 **Automatic Power Direction Control of DAB/TAB Converter in Emergency Energy Supply**

With their multi-directional power flow capability, DAB and TAB converters are utilized in energy routers as DC/DC transfer components for emergency energy supply during significant power outages. These converters facilitate stable power transmission across various energy sources while enabling high-power conversion. However, controlling power direction in DAB/TAB converters for EES remains challenging, particularly due to the need for rapid changes in power direction at any port of the converters. This study proposes an automatic power direction control method for DAB/TAB converters, which enables bidirectional power transmission without manual intervention, based on the SOC of the battery for EES. This method allows each port in the DAB/TAB converter to automatically adjust its power direction according to different situations, including emergencies. By simplifying operations and enhancing system safety through the elimination of human supervision, this approach ensures efficient and consistent power transfer within the system. The implementation of this automatic control method replaces manual operations, ensuring reliable and timely adjustments to power direction whenever necessary.

4.1 Introduction

In an energy router designed for emergency supply in urban settings, achieving energy balance among diverse electric power sources is paramount. This necessitates effective control of energy flow within the energy router, which is a critical aspect for managing various emergencies in urban environments. Specifically, in the context of the DC power transfer component within the energy router, this chapter employs DAB and TAB converters due to their inherent advantages. [92]. DAB/TAB converters possess several advantageous features. Firstly, they can automatically adjust bidirectional power flow and are capable of adapting to rapid changes in power flow direction [93]. Moreover, they offer a wide voltage conversion gain range [94]. Additionally, DAB/TAB converters are equipped with zero-voltage switching (ZVS) capability [95], enabling them to achieve high efficiency through power control [96]

[97]. In a study referenced in [98], it was demonstrated that DAB and TAB converters exhibit high power efficiency, reaching up to 97.6%.

Power exchange among DAB/TAB converters is facilitated through a phase-shift pulse width modulation PWM mechanism [99]. Leveraging the lag/lead relationship of two or three pulse width waveforms, ports on DAB/TAB converters enable power transmission. The direction of power transmission varies based on the different lag/lead relationships, as each port of the DAB/TAB converter can facilitate bidirectional power flow [87]. Many control methods such as single-phase shift (SPS), dual-phase shift (DPS) and triple-phase shift (TPS) are used in DAB/TAB converter to realize the high power efficiency and bidirectional power flow [100] [101] [102] [103] [104]. However, for emergency power supply, there is not a proper power direction control method dealing with various emergencies such as power outages to ensure the stability of DAB/TAB converter and normal operation for loads of clients.

Therefore, an automatic power direction control method in this chapter can adjust power direction automatically according to the SOC of battery or EEPS at the port of DAB [105]/TAB converter typically for EES. This eliminates the need for manual monitoring of equipment status and ensures that the equipment can automatically adjust power direction to address different emergencies, thereby saving manpower.

This chapter is arranged as below. Firstly, the principle of power direction of DAB/TAB converter is briefly described. Secondly, the automatic power direction control method is demonstrated. Thirdly, a simulation model that contains a DAB/TAB converter is implemented in MATLAB/Simulink and a summary is provided at the end of this chapter.

4.2 Principle of Power Direction of DAB/TAB Converter

Fig. 1 illustrates the topologies of both the DAB and TAB converters. Each topology features two or three ports, with each port comprising an active bridge consisting of four switches. In the DAB topology, there is a single inductor L and a high-frequency transformer N. On the other hand, each port of the TAB converter includes an inductor L_i (where i = 1, 2, 3) and a transformer with winding N_i. Additionally, a power source B_i is connected to the terminal of each port. For the energy router designed for emergency energy supply in urban areas, B_1 can be considered as the DC bus of the urban power grid, while B_2 represents any source capable of serving as an emergency electric power source. B_3 corresponds to the power storage unit

within the energy router. In this configuration, power is transferred among ports through the magnetic coupling of the windings.

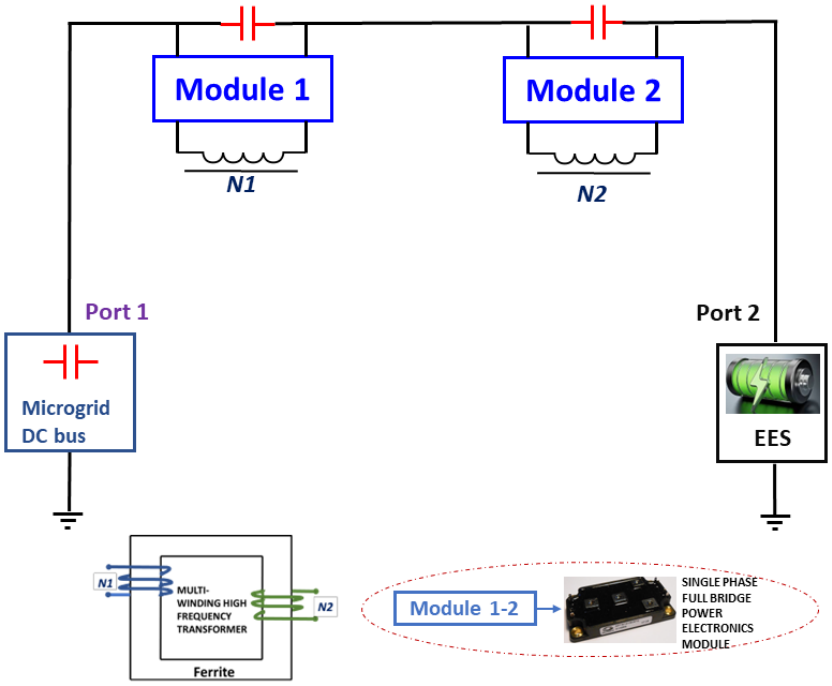

(a)

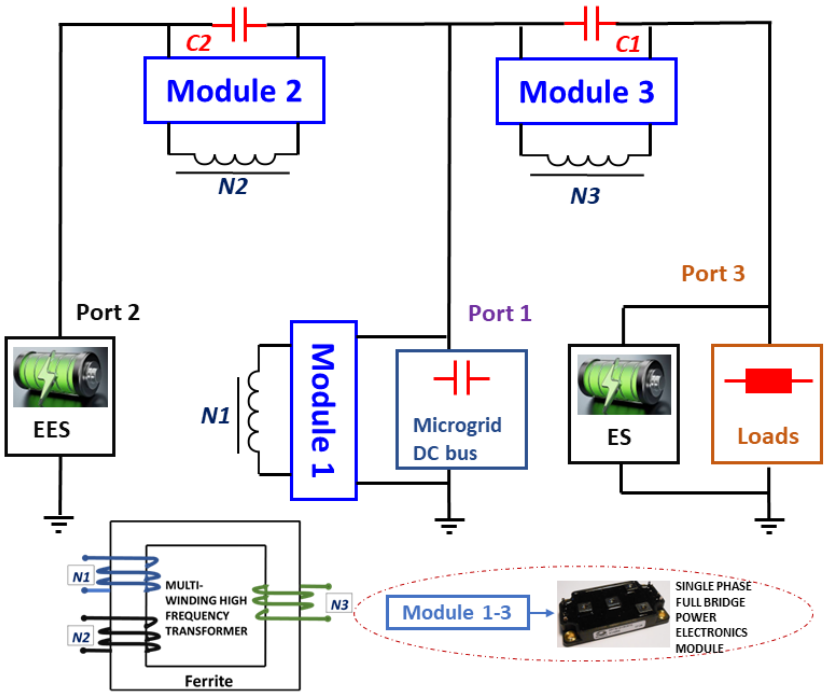

(b)

Fig. 4-1. Topology of (a) the DAB converter; and (b) the TAB converter

4.2.1 DAB Converter

DAB operates primarily through SPS control [104], meaning that energy flow is managed by adjusting the lead/lag relationship between port 1 and port 2 [106]. Fig. 4-2 illustrates an example of forward energy transmission in DAB, where S_1, S_2, S_3, and S_4 represent the signals controlling the MOSFETs at port 1, while Q_1, Q_2, Q_3, and Q_4 represent the signals controlling the MOSFETs at port 2, lagging behind S_1, S_2, S_3, and S_4 by the phase shift angle φ_1. V_1 denotes the voltage at port 1, V_2 denotes the voltage at port 2, and i_{Lc} represents the current through the inductance of port 1. According to Fig. 4-2, within one switching period T_s, there are four different modes of inductor current.

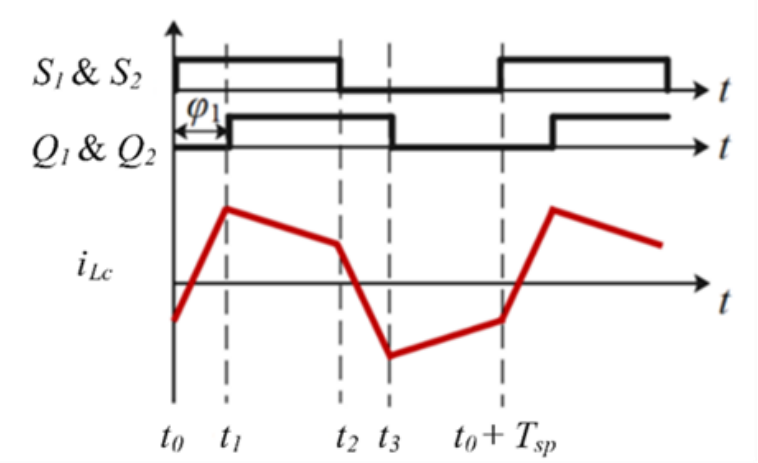

Fig. 4-2. Typical waveforms of a DAB converter

When $t_0 \leq t \leq t_1$,

$$i_{Lc}(t) = \frac{V_1+V_2}{L}(t - t_0) + i_{Lc}(t_0) \tag{4-1}$$

where $t_1 = t_0 + (\varphi_1 T_s)/2\pi$.

When $t_1 \leq t \leq t_2$,

$$i_{Lc}(t) = \frac{V_1-V_2}{L}(t - t_1) + i_{Lc}(t_1) \tag{4-2}$$

where $t_2 = t_0 + T_s/2$.

When $t_2 \leq t \leq t_3$,

$$i_{Lc}(t) = \frac{-V_1 - V_2}{L}(t - t_2) + i_{Lc}(t_2) \tag{4-3}$$

where $t_3 = t_2 + (\varphi_1 T_s)/2\pi$.

When $t_3 \le t \le t_0 + T_s$,

$$i_{Lc}(t) = \frac{-V_1 + V_2}{L}(t - t_3) + i_{Lc}(t_3) \tag{4-4}$$

From Fig. 4-2, the equation $i_{Lc}(t_0) = -i_{Lc}(t_2)$ can be obtained [107]. Through integral, forward power P_+ and reverse power P_- can be circulated.

$$\begin{cases} P_+ = \frac{1}{T_{hs}} \int_0^{T_{hs}} V_1 i_{Lc} dt = \frac{\varphi_1(\pi - \varphi_1) V_1 V_2}{2\pi^2 f_s L} \\ P_- = \frac{1}{T_{hs}} \int_0^{T_{hs}} V_1 i_{Lc} dt = \frac{\varphi_1(\pi + \varphi_1) V_1 V_2}{2\pi^2 f_s L} \end{cases} \tag{4-5}$$

where $f_s = 1/T_s$ represents the switching frequency. D is the phase shift ratio ($D = \varphi_1/180°$) and T_{hs} is the half of the switching period.

Fig. 4-3 depicts the relationship between D and the power P. It is evident that when D falls within the range of -0.5 and 0.5, there exists a positive correlation between P and D. Therefore, D is typically set within the range of -0.5 and 0.5, indicating that φ_1 varies between -90° and 90°.

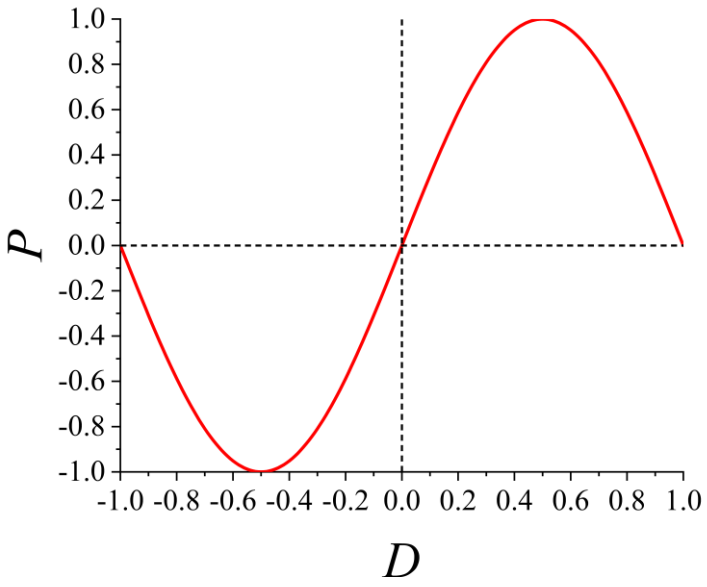

Fig. 4-3. The relationship between P and D

4.2.2 TAB Converter

The phase-shift PWM method employed in the DAB converter is also utilized to control power flow direction in the TAB converter [108]. In Fig. 3-10, the control signals of switches S_1 and S_2 serve as references, while the control signals of switches S_5 and S_6, and switches S_9 and S_{10} are lagged by φ_2 and φ_3 radians, respectively. Here, $-\pi < \varphi_2 < \pi$ and $-\pi < \varphi_3 < \pi$. Moreover, each switch operates with a duty ratio half of the switching cycle. Additionally, Fig. 3-10 illustrates the current waveforms of L_1, L_2, and L_3 for i_{L1}, i_{L2}, and i_{L3}, respectively, in a traditional phase-shift TAB converter. The turns ratio of the transformer N_1: N_2: N_3 is set to 1:1:1.

The power flow characteristics of a phase-shift TAB converter can be derived from those of a DAB converter, and the expression in (4-5) can be extended to (4-6) by analyzing the various operating states of the TAB converter.

$$\begin{cases} P_{12} = \frac{\varphi_2(\pi-|\varphi_2|)V_1V_2}{2\pi^2 f_{sp}(L_1+L_2)} \\ P_{13} = \frac{\varphi_3(\pi-|\varphi_3|)V_1V_3}{2\pi^2 f_{sp}(L_1+L_3)} \\ P_{23} = \frac{(\varphi_3-\varphi_2)(\pi-|\varphi_3-\varphi_2|)V_1V_2}{2\pi^2 f_{sp}(L_2+L_3)} \end{cases} \tag{4-6}$$

in this expression, V_1, V_2, and V_3 refer to the voltages of B_1, B_2, and B_3, respectively, and P_{12}, P_{13}, and P_{23} are the power flow from port 1 to port 2, from port 1 to port 3, and from port 2 to port 3, respectively. Furthermore, f_{sp} is the switching frequency.

Suppose each inductor has the same inductance, and the sum of any two inductors is denoted as L_e. Then, the port power can be derived from

$$\begin{cases} P_1 = P_{12} + P_{13} \\ = \frac{\varphi_2(\pi-|\varphi_2|)V_1V_2+\varphi_3(\pi-|\varphi_3|)V_1V_3}{2\pi^2 f_{sp}L_e} \\ P_2 = -P_{12} + P_{23} \\ = \frac{-\varphi_2(\pi-|\varphi_2|)V_1V_2+(\varphi_3-\varphi_2)(\pi-|\varphi_3-\varphi_2|)V_2V_3}{2\pi^2 f_{sp}L_e} \\ P_3 = -P_{13} - P_{23} \\ = \frac{-\varphi_3(\pi-|\varphi_3|)V_1V_3-(\varphi_3-\varphi_2)(\pi-|\varphi_3-\varphi_2|)V_2V_3}{2\pi^2 f_{sp}L_e} \end{cases} \tag{4-7}$$

where P_1, P_2, and P_3 represent the total power of port 1, port 2, and port 3, respectively.

Therefore, the direction of power transmission is determined by both the port voltages and the phase shift angles of the switching gate signals. For instance, when the difference between port voltages is small or nearly non-existent, Fig. 3-11 illustrates four typical power flow scenarios. Fig. 3-11(a) shows power transfers from port 1 to port 2 and port 3 which means that the main power grid is normal and ES and emergency electric power source port are charging. When the energy at emergency electric power source port beyond the needs, TAB converter will be shifted into Fig. 3-11(b). This mode will reduce pressure on main grid transmission and is more economic for the clients. In Fig. 3-11(c), When the energy of ES and emergency electric power source port are all beyond the needs, ES and emergency electric power source port can transfer power to the main power grid which realize the peer-to-peer trading [109]. When an emergency occurs, TAB converter will be shifted into Fig. 3-11(d), the main power grid will be off the grid and emergency electric power source port and ES port will be the power source to the loads and clients and maintain the normal working of loads until the main grid paralysis is resolved.

4.3 Automatic Power Direction Control Method of DAB/TAB Converter

To address the need for automatic power direction adjustment without manual intervention, this chapter proposes an automatic power direction control method for DAB/TAB converters. In the context of emergency energy supply, numerous unforeseen accidents may occur, making it difficult for individuals to swiftly change the power direction of DAB/TAB converters to address each unexpected situation. An automatic power direction control method can assist in adjusting the power direction according to preset values, thereby enhancing the responsiveness and effectiveness of the system in managing unexpected events. Compared with the automatic modulation methods in [110], this method is easier and more flexible for clients to control the power direction according to their own needs because the power direction is mainly controlled by the SOC of ES and EEPS.

4.3.1 DAB Converter

Based on the preceding explanation of the power direction of the DAB converter, it is evident that when $-90° < \varphi < 0°$, power transfers from port 2 to port 1, whereas when $0° < \varphi < 90°$,

power transfers from port 1 to port 2. Fig. 4-4 illustrates the proposed automatic power direction control method. In this method, two variables, SOC_2 and MS, are employed to control the power direction of the DAB converter. When MS is equal to 0, $-90° < \varphi < 0°$, and power transfers from port 2 to port 1. Conversely, when MS equals 1, $0° < \varphi < 90°$, and power transfers from port 1 to port 2. Here, *max* represents the maximum setting value, and *min* represents the minimum setting value.

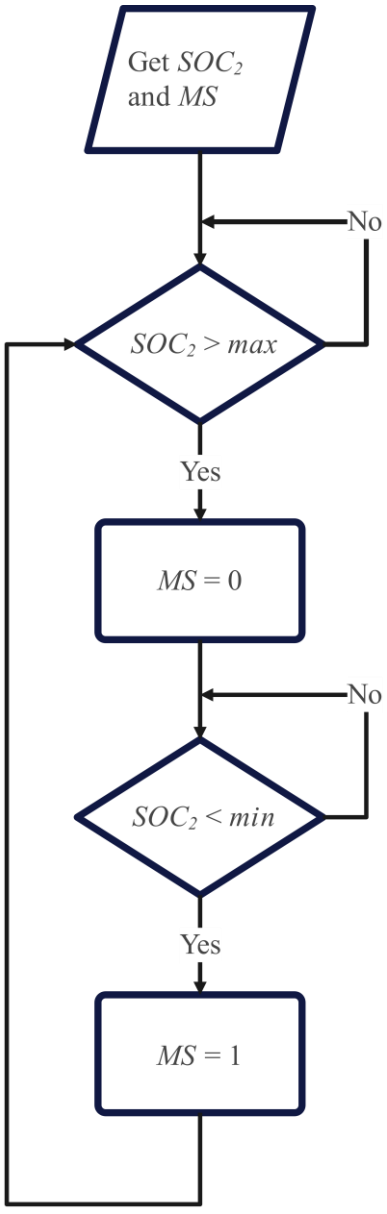

Fig. 4-4. Flow chart of the automatic power direction control method of the DAB converter

According to Fig. 4-4, the process involves two "if" judgments. The first "if" judgment checks if SOC_2 is greater than the maximum setting value and if MS equals 1. If both conditions are

met, then *MS* is set to 0, indicating a change in power direction from forward to reverse. Otherwise, the power direction remains forward. The second "if" judgment examines if SOC_2 is less than the minimum setting value and if *MS* equals 0. If both conditions are satisfied, then *MS* is set to 1, signifying a change in power direction from reverse to forward. Otherwise, the power direction remains reverse. With this automatic power direction control method, the power direction of the DAB converter is regulated by the SOC of Port 2 SOC_2 to ensure bidirectional automatic power transmission within a specified range.

4.3.2 TAB Converter

Considering the similarities between the DAB converter and the TAB converter, this automatic power direction control method can indeed be applied to the TAB converter as well. However, as depicted in Fig. 3-11, the TAB converter presents four different typical power directions determined by the lagging/leading relationship between φ_2 and φ_3. Additionally, scenarios such as Fig. 3-11(d) illustrate instances where power flow occurs solely between port 2 and port 3, with no power transmission at port 1. Therefore, relying solely on two variables may not suffice for the automatic power direction control of the TAB converter.

To address this, three additional controlling variables are proposed for the automatic power direction control of the TAB converter: the voltage of battery 1 V_1, the SOC of port 3 SOC_3, and the SOC of port 2 SOC_2, as illustrated in Fig. 4-5. Incorporating these additional variables ensures more comprehensive and accurate control of power direction in the TAB converter.

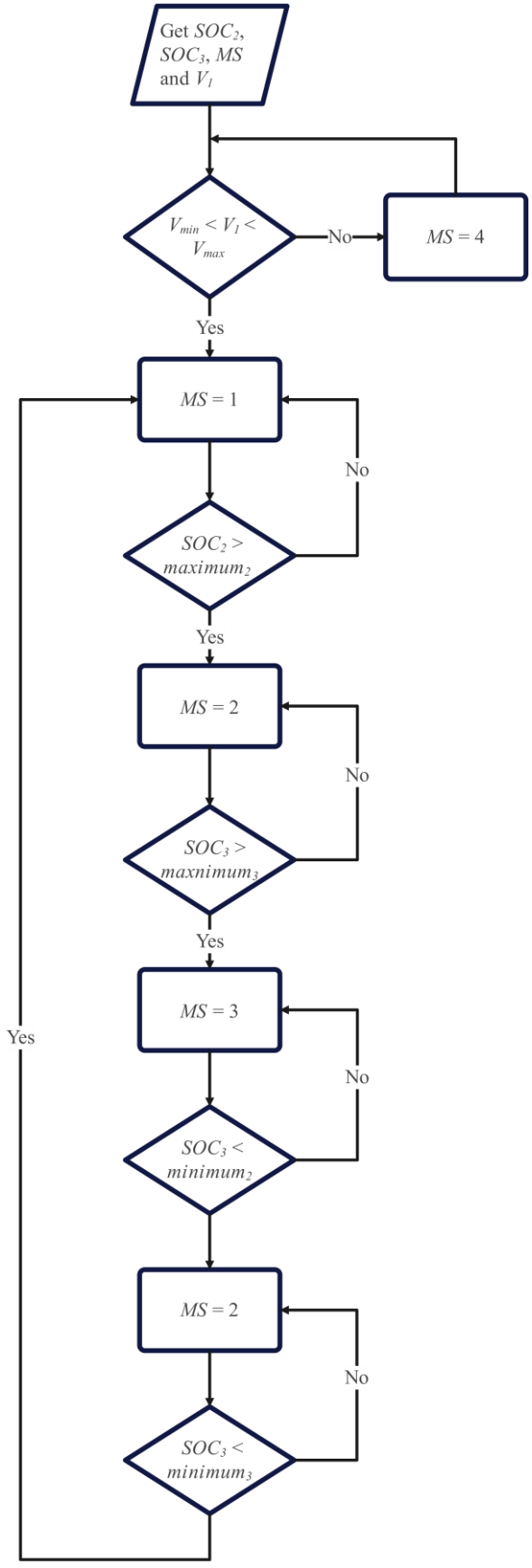
Get SOC_2, SOC_3, MS and V_1
$V_{min} < V_1 < V_{max}$
No
$MS = 4$
Yes
$MS = 1$
No
$SOC_2 > maximum_2$
Yes
$MS = 2$
No
$SOC_3 > maxnimum_3$
Yes
$MS = 3$
No
$SOC_3 < minimum_2$
$MS = 2$
No
$SOC_3 < minimum_3$
Yes

Fig. 4-5. Flow chart of the automatic power direction control method of the TAB converter

Among these controlling variables, the direction of power transmission is ultimately determined by the value of *MS*. The relationship between the direction of power transmission and *MS* is as follows.

MS = 1, power transfers from port 1 to port 2 and port 3.

MS = 2, power transfers from port 1 and port 2 to port 3.

MS = 3, power transfers from port 2 and port 3 to port 1.

MS = 4, power transfers from port 2 to port 3 and there is no power transmission at port 1.

According to Fig. 4-5, the process involves five "if" judgments to accommodate the four different types of power flow in the TAB converter. Assuming the initial value of *MS* is equal to 1, which determines the power flow as shown in Fig. 3-11(a). Here's how the process unfolds. If V_1 is not within the acceptable voltage range between V_{min} and V_{max}, indicating an anomaly at port 1, then *MS* is set to 4, and the power flow is as depicted in Fig. 3-11(d). After the first "if" judgment, if SOC_2 exceeds the maximum setting for SOC_2, *MS* is set to 2, and the power flow is as shown in Fig. 3-11(b). Otherwise, *MS* remains equal to 1. In the third "if" judgment, if SOC_3 surpasses the maximum setting for SOC_3, *MS* is set to 3, and the power flow is as illustrated in Fig. 3-11(c). The fourth "if" judgment checks if SOC_3 falls below the minimum setting for SOC_3. If this condition is met, *MS* is changed to 2, and the power flow is as depicted in Fig. 3-11(b). Otherwise, *MS* remains at 3. During the final "if" judgment, if SOC_2 is lower than the minimum setting for SOC_2, MS is reverted to 1, and the power flow is as shown in Fig. 3-11(a). Similar to the automatic power direction control method of the DAB converter, this method for the TAB converter can automatically adjust the power direction to handle different situations based on the states of each port. This approach significantly reduces the need for manual intervention and ensures the safe and stable operation of the TAB converter

4.4 Simulation Results

Two simulation models of the DAB converter and the TAB converter have been developed in MATLAB/Simulink to evaluate the feasibility of the proposed automatic power direction control method. These simulations aim to validate the direction of power transmission at each

port by monitoring the SOC, *MS*, and current waveforms at each port. Furthermore, by analyzing the timing of changes in waveform values, it is possible to confirm that the change in the direction of power transmission aligns with the proposed method. The simulation models are constructed according to the diagrams presented in Fig. 1. Through these simulations, it is aimed to assess the efficacy and reliability of the automatic power direction control method in ensuring the safe and stable operation of both the DAB and TAB converters.

4.4.1 DAB Converter

The system configurations of DAB converter model are exhibited in Table 4-1, where the voltages of the two battery packs are set to 180 V, 200 V, respectively, with an initial SOC of 50%. Moreover, the transformer turns ratio is N=1 and Initial value of *MS* is 1. The range of SOC_2 is set between 60% and 40% to get the simulation results more quickly.

TABLE 4-1 Parameters of the DAB Simulation Model

Parameter name	Parameter Value
V_1/V_2 (Battery pack voltages)	180/200 V
SOC_1/SOC_2 (Initial SOC)	50%
N (Transformer turns ratio)	1
f_s (Switching Frequency）	50 kHz
L (Series inductance)	82 μH
C_1/C_2 (Series capacitance)	50 μF
SOC_{2max}/SOC_{2min} (Maximum and minimum SOC)	60%/40%
Initial value of *MS*	1

In the Simulink simulation, we set the initial value of MS to 1, and the initial phase-shift angle φ lags the port 1 bridge waveform, as shown in Fig. 4-2. Consequently, power flows from B_1 to B_2, resulting in an increase in SOC_2. Once SOC_2 reaches the maximum setting value, *MS* will be changed to 0, and φ_1 will lead the port 1 bridge waveform, following the automatic power direction control method depicted in Fig. 4-5. During this phase, SOC_2 will decrease, and the power flow will reverse until SOC_2 reaches the minimum setting value. Subsequently, *MS* will revert to 1, and the power flow will return to being forward. Additionally, the current waveform of port 2 i_2 is displayed in Fig. 4-6(b). This simulation scenario allows us to observe

the dynamic behavior of the system and validate the effectiveness of the automatic power direction control method.

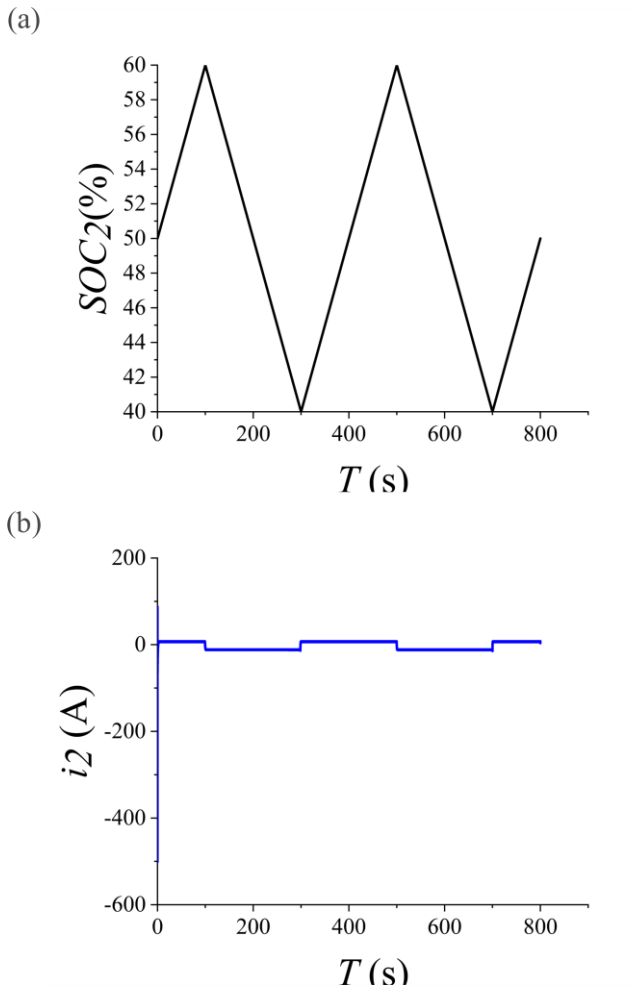

Fig. 4-6. (a) SOC_2 and (b) i_2 waveform in automatic power direction control of DAB converter

In Fig. 4-6(a), the variation of SOC for B_2 throughout the entire simulation process is depicted. It can be observed that B_2 is initially charging, and its charge and discharge status alternate each time SOC_2 reaches the peak point, consistent with the analysis in the previous sections. Furthermore, in Fig. 4-6(b), during the steady state, the current of port 2 switches between positive and negative values, reflecting the power direction of the DAB converter. The timing of the forward and reverse directions aligns perfectly with the conclusions drawn from the SOC_2 waveform analysis. These observations validate the effectiveness of the automatic power direction control method and demonstrate its ability to regulate power flow in the DAB converter accurately and consistently.

Based on the two figures in Fig. 4-6, particularly Fig. 4-6(b), it is evident that the duration of

the power direction change is relatively short. The transition from a positive steady-state value to a negative steady-state value for i_2 takes only 3 seconds. This demonstrates that the proposed automatic power direction control method can swiftly and effectively adjust the power direction without significantly disrupting the normal operation of the DAB converter. Thus, this approach saves manual operation time and ensures the seamless functioning of the converter. Thus, this approach saves manual supervision time and ensures the seamless functioning of the converter for EES. Compared with other automatic power direction control methods [110] and [111] used for batteries or PV energy, this proposed method is easier and more flexible to use for emergency energy supply according to different the needs of clients.

4.4.2 TAB Converter

a) When V_1 is within acceptable voltage range

The first simulation of TAB converter is run when the voltage of B_1 is normal which means that there is no power outage in power station. *MS* will be shifted between 1,2,3 and 4 and will not be equal to 5. This simulation shows automatic change of the TAB converter power transmission direction according to the SOC status and power requirements of the individual ports automatic power direction in the absence of a sudden power failure.

The system configurations of TAB converter model when V_1 is within acceptable voltage range are exhibited in Table 4-2. In Table 4-2, the voltages of three ports are all 180V and the initial SOC of two battery packs are all 50%. Moreover, the transformer turns ratio N_1:N_2:N_3 is 1:1:1 and the initial value of *MS* is 1. To get simulations results more quickly, four peak values of SOC are set 60%, 5%, 91% and 77% respectively.

TABLE 4-2 Parameters of the TAB Simulation Model When V_1 is Within Acceptable Voltage Range

Parameter name	Parameter Value
$V_1/V_2/V_3$ (Port voltages)	180/180/180 V
SOC_2/SOC_3 (Initial SOC)	50%
N_1:N_2:N_3 (Transformer turns ratio)	1:1:1
$L_1/L_2/L_3$ (Series inductance)	300 μH
f_{sp} (Switching Frequency)	50 kHz

Maximum$_2$ (Maximum SOC of port 1)	60%
Minimum$_2$ (Minimum SOC of port 1)	5%
Maximum$_3$ (Maximum SOC of port 2)	91%
Minimum$_3$ (Minimum SOC of port 2)	77%
Initial value of *MS*	1

In TAB Simulink simulation, the initial value of *MS* is 1 and the initial value of phase-shift angles φ_2 and φ_3 is lagging the port 1 bridge waveform and $|\varphi_2|<|\varphi_3|$ shown in Fig. 4-3. Therefore, power is transferred from B_1 to B_2 and B_3 which means that SOC_2 and SOC_3 is increasing. After SOC_2 reaches the maximum setting value, *MS* will be changed into 2 and φ_2 will lead the port 1 bridge waveform and φ_3 will still lag the port 1 bridge waveform with $|\varphi_2|<|\varphi_3|$ according to the automatic direction control method shown in Fig. 4-5. During this period, SOC_2 decreases while SOC_3 increases until the SOC_3 arrives the maximum setting value. After that, *MS* will be changed into 3 and φ_3 will also lead the port 1 bridge waveform with $\varphi_2<\varphi_3<0$. During $MS = 3$, SOC_2 and SOC_3 decrease at the same time until the SOC_3 arrives the minimum setting value. Then, *MS* will be changed back into 2. In this period, SOC_3 increases with SOC_2 decreasing until SOC_2 reaches the minimum setting value. For this reason, MS will be back into 1 and φ_2 will be back to lag the port 1 bridge waveform with $|\varphi_2|<|\varphi_3|$ so that SOC_2 can increase. Additionally, the waveform of *MS* is exhibited in Fig. 4-8.

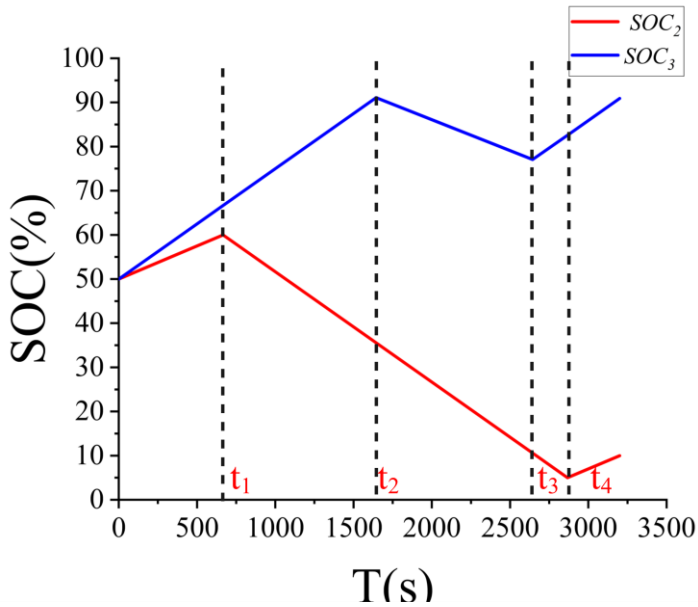

Fig. 4-7. SOC waveforms in automatic power direction control of TAB converter when V_1 is within acceptable voltage range

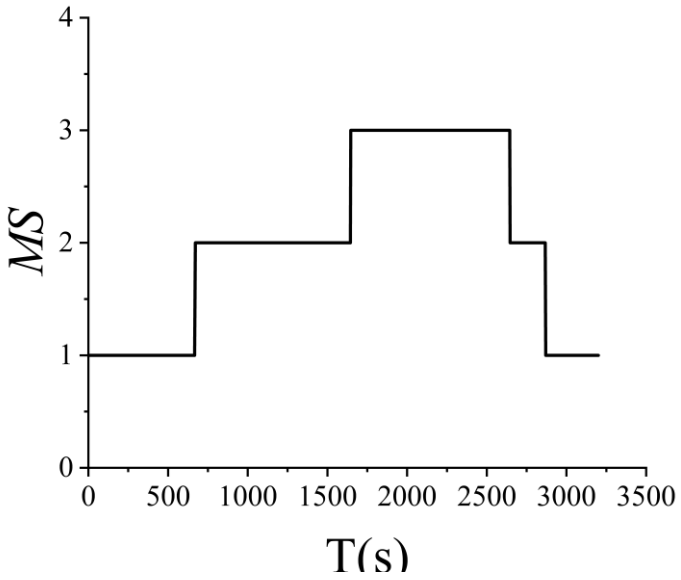

Fig. 4-8. MS waveforms in automatic power direction control of TAB converter when V_1 is within acceptable voltage range

Fig. 4-7 presents the variation of SOC for the B_2 and B_3 in the whole simulation process, from which it can be investigated that SOC_2 and SOC_3 changes corresponding to the proposed analysis and power direction changes corresponding to the proposed automatic power direction control method which is consistent with the analysis in the previous sections. In this whole TAB simulation process, a completed automatic direction control loop is finished and a whole loop can be divided into four modes which are 0-t_1, t_1-t_2, t_2-t_3 and t_3-t_4. In Fig. 4-8, *MS* can also be different values in these four modes and the period of each mode is consistent with that in Fig. 4-7. Through Fig. 4-9, during the steady state, the current waveform of port 1 i_1, port 2 i_2 and port 3 i_3 also switches between positive and negative values which also shows the power direction of TAB converter. When the current is negative, this port is the input port. Conversely, when the current is positive, this port is the output port. Compared Fig. 4-7 with Fig. 4-9, the power direction obtained from SOC status of each port is the same with the power direction obtained from the current value of each port.

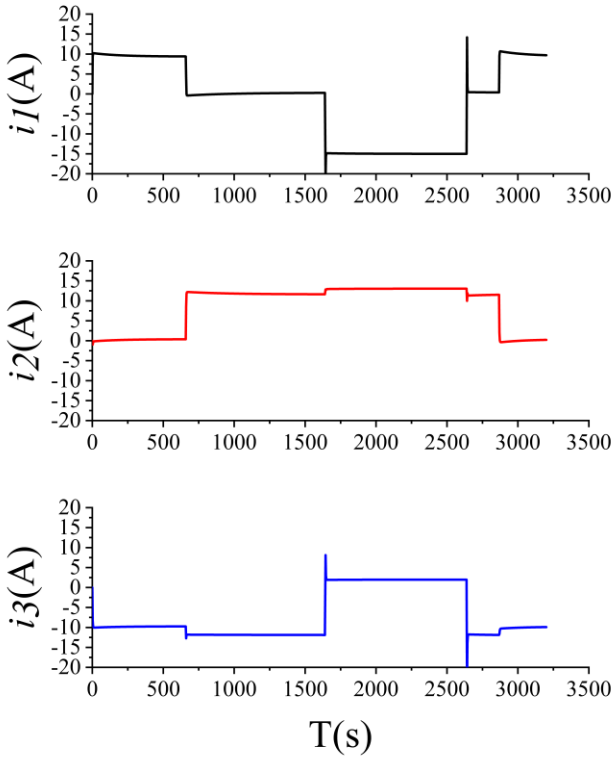

Fig. 4-9. Current waveforms in automatic power direction control of TAB convert when V_1 is within acceptable voltage range

Based on the two figures in Fig. 4-9, it is apparent that the duration of the power direction change at each port is also relatively short, similar to the behavior observed in the DAB converter. The transition from a positive steady-state value to a negative steady-state value for the current at each port takes only 3 seconds. This confirms that the proposed automatic power direction control method can swiftly and effectively adjust the power direction in the TAB converter without significantly disrupting its normal operation. Consequently, this approach saves manual operation time while ensuring the smooth functioning of the converter. Same with the automatic power direction control method for DAB converter, the automatic power direction control method for TAB converter can also save manual supervision time and ensure the seamless functioning of the converter for EES.

b) When V_1 is not within acceptable voltage range

In this scenario, port 1 exhibits an abnormal voltage, indicating an issue that prevents it from effectively carrying out power transmission duties in the TAB converter. Given that port 1 represents the main power grid, an abnormal voltage suggests that the main power grid is

experiencing significant disruptions and is unable to function normally. Prior to resolving the issue with port 1, it is imperative that the TAB converter operates similarly to a DAB converter. This entails transferring power exclusively between port 2 and port 3 while ensuring that no power transmission occurs at port 1. This temporary operational mode allows the TAB converter to maintain critical power flow functionalities within the system until the problem with port 1 is rectified.

The system configurations of TAB converter model when V_1 is not within acceptable voltage range are exhibited in Table 4-3. In Table 4-3, the voltages of battery packs of port 2 and port 3 are both 180V with the initial SOC of them are all 50% while the voltage of port 1 is 100V. Moreover, the transformer turns ratio $N_1:N_2:N_3$ is 1:1:1 and the initial value of *MS* is 1.

TABLE 4-3 Parameters of the TAB Simulation Model When V_1 is Not Within Acceptable Voltage Range

Parameter name	Parameter Value
$V_1/V_2/V_3$ (Port voltages)	100/180/180 V
SOC_2/SOC_3 (Initial state of charge)	50%
$N_1:N_2:N_3$ (Transformer turns ratio)	1:1:1
$L_1/L_2/L_3$ (Series inductance)	300 μH
f_{sp} (Switching Frequency)	50 kHz
Initial value of *MS*	1

Although the initial value of *MS* is 1, because of the abnormal value of V_1, *MS* is rapidly changed into 5. This causes that φ_2 is leading the port 1 bridge waveform and φ_3 is lagging the port 1 bridge waveform at the same time with $|\varphi_2|=|\varphi_3|$. With this relationship between φ_2 and φ_3, power only transfers from B_2 to B_3 and there is no power transmission at B_1. This mode will last until the problem of port 1 is fixed. After that, *MS* will be back to 1 so that TAB converter can work as its own role again and continue the power transmission loop shown in Fig. 4-10. Additionally, the waveform of *MS* is exhibited in Fig. 4-11.

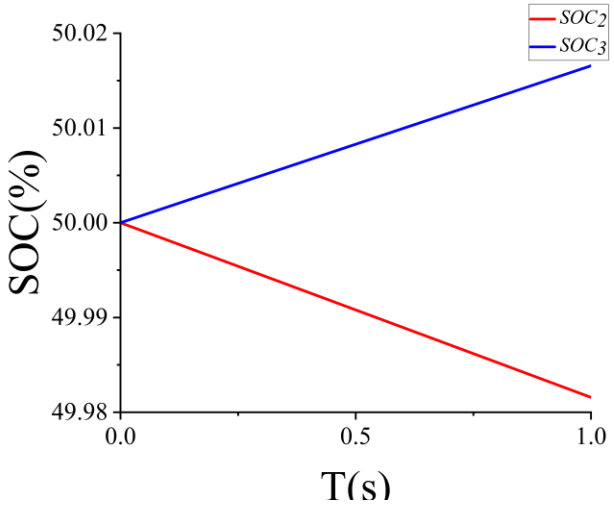

Fig. 4-10. SOC waveforms in automatic power direction control of TAB convert when V_1 is not within acceptable voltage range

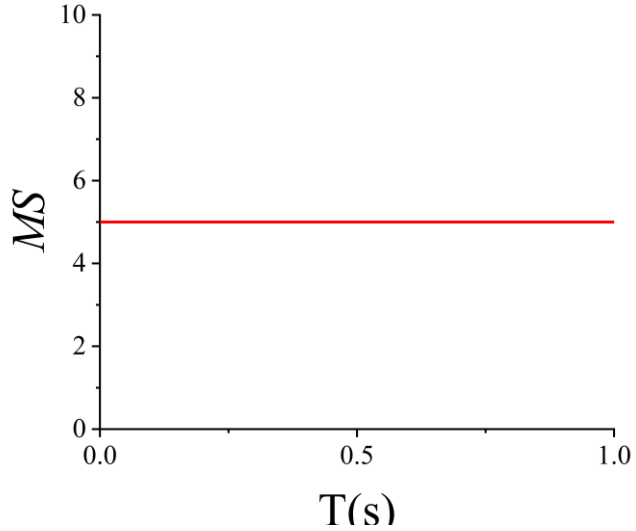

Fig. 4-11. *MS* waveform in automatic power direction control of TAB convert when V_1 is not within acceptable voltage range

Fig. 4-10 presents the variation of SOC for B_2 and B_3 in the whole simulation process, from which it can be investigated that SOC_2 and SOC_3 changes corresponding to the proposed analysis and power direction is stable from port 2 to port 3 corresponding to the proposed automatic power direction control method which is consistent with the analysis in the previous sections. In Fig. 4-11, *MS* is also constant at 1 which corresponds to the SOC waveforms in Fig. 4-10. In this whole TAB simulation process, TAB converter is working as a DAB converter considering the abnormal performance of port 1. Through Fig. 4-12, during the steady state, the currents of port 1 is zero, and the currents of port 2 and port 3 are constant

positive and negative values respectively which also shows the power direction is only from B_2 to B_3. Compared Fig. 4-10 with Fig. 4-12, the power direction obtained from SOC status of each port is the same with the power direction obtained from the current value of each port.

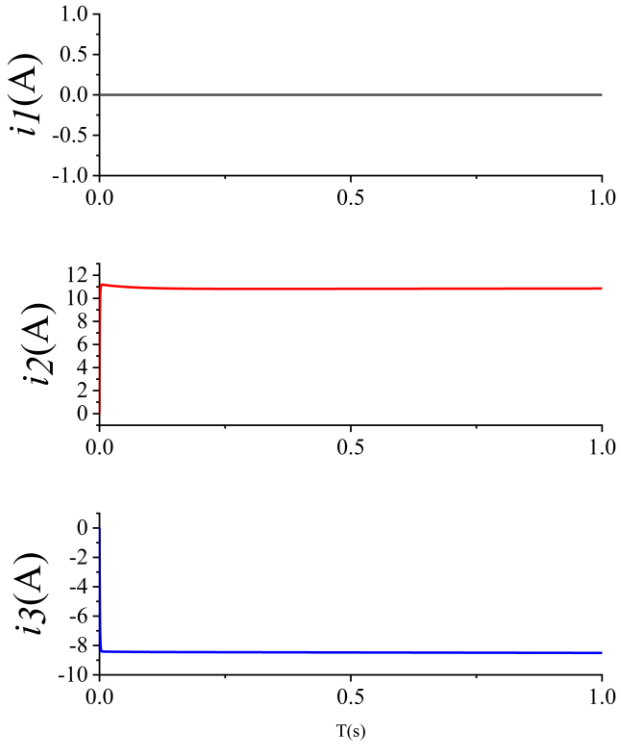

Fig. 4-12. Current waveforms in automatic power direction control of TAB convert when V_1 is not within acceptable voltage range

4.5 Summary

This chapter introduces an automatic power direction control method tailored for DAB/TAB converters, aimed at streamlining energy balancing and automating power direction within an energy router system. Power conversion employs phase-shift PWM, with direction control overseen by the proposed automatic method. The direction of power flow across the three ports is regulated by the lead/lag states of the converter switches and the SOC status of the ES and emergency electric power sources ports. The proposed method offers rapid directional control, leading to significant cost savings by minimizing the need for manual monitoring and regulation of the energy router's status during emergencies. This capability ensures swift

responses to grid emergencies, facilitating prompt resolution. To validate the feasibility of the automatic power direction control method in DAB/TAB converters, several simulation models implemented in MATLAB/Simulink have been employed. Additionally, the method relies solely on the SOC status of individual ports of the DAB/TAB converter, allowing consumers to optimize their power consumption plans based on varying situations. This approach enhances flexibility and efficiency in utilizing energy resources, reducing dependence on the main power grid for supply. Moreover, integrating more energy routers equipped with DAB/TAB converters into an emergency energy power system enables peer-to-peer trading. This advancement fosters a more resilient and responsive energy network capable of adapting to diverse operational scenarios.

Chapter 5 Emergency Energy Power System Composed of Multiple Energy Routers for Peer-to-Peer Trading in Microgrid

As microgrids are becoming more and more prominent in the transmission of power over small areas, the rapid supply of EES is also largely dependent on them. the use of the MER as an efficient multi-port power transmission device in microgrids is also increasing. However, how to better combine MER with emergency power supply in microgrids is still a research problem. This chapter implements EEPS in microgrids by proposing an automatic power direction control strategy for multiple MERs consisting of TAB converters based on PPP technology in a microgrid. An automatic control method ensures efficient and consistent power transfer within the system, replacing manual operations especially in emergencies whenever power direction adjustment is necessary. Besides, in EEPS, in contrast to the existing approach, which merely permits the direction of energy transfer from a single MER to be controlled, the automatic power direction control method facilitates the automatic transfer of energy between multiple MERs for the purpose of enabling P2P trading.

5.1 Introduction

The EEPS will be realized by integrating multiple MERs together to form a microgrid [71] and will still have the various points of MERs such as high energy utilization, versatility in power forms, energy storage capabilities, and grid monitoring functionalities. power transfer can be realized between multiple MERs and in different directions for different needs. This allows the client to choose from a wide range of power sources rather than using the mains grid alone and enables the exchange of energy from client to client shown in Fig. 5-1. Besides, it is free to decide on the size of its own energy storage system in this proposed EEPS, depending on the customer's load and energy storage requirements.

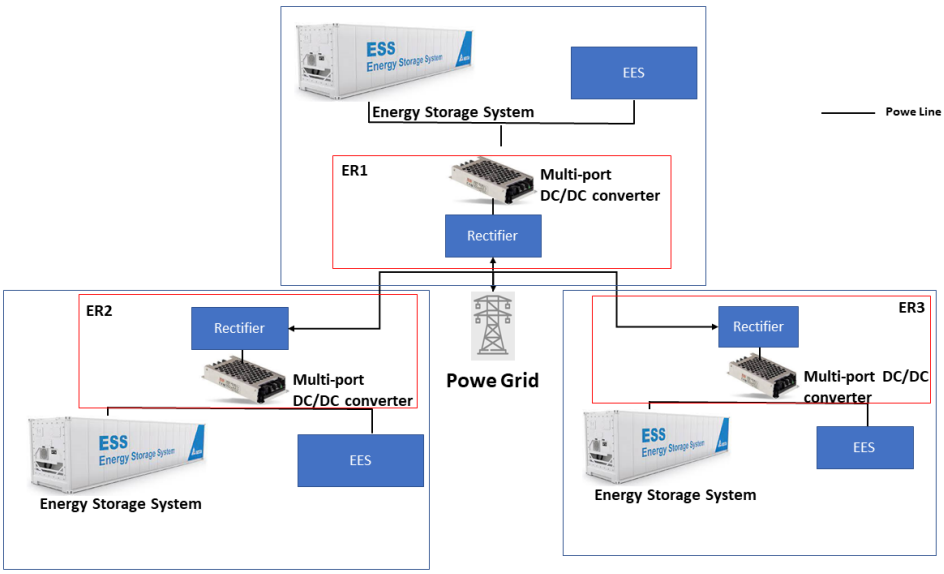

Fig. 5-1. An EEPS consisting of 3 MERs

In an energy router shown in Fig. 3-1 designed for emergency supply in urban settings, achieving energy balance among diverse electric power sources is paramount. This necessitates effective control of energy flow within the energy router, which is a critical aspect for managing various emergencies in urban environments [112]. Specifically, in the context of the DC power transfer component within the energy router, this thesis employs PPP TAB converter due to its inherent advantages. [92]. PPP TAB converter possesses several advantageous features. Firstly, it can automatically adjust bidirectional power flow and are capable of adapting to rapid changes in power flow direction [93]. Moreover, it offers a wide voltage conversion gain range [94]. Additionally, PPP TAB converter are equipped with ZVS capability [95], enabling them to achieve high efficiency through power control [96] [97].

In a study referenced in [98], it was demonstrated that TAB converter exhibits high power efficiency, reaching up to 97.6%. However, PPP TAB converter has a higher efficiency than normal TAB converter because of the PPP technology [113]. PPP is a technology that uses converters to process part of the total power, while most of the unprocessed system energy is transferred directly through the power cables [80]. Power dissipation can be reduced as the PPP converter processes less power, which has the effect of improving system efficiency and power density [81]. As for the multi-port energy routers, the PPP multi-port converters can not only improve the efficiency of energy transfer by realizing the bidirectional energy flow between the ports [85], but also control the energy flow more easily.

Power exchange among PPP TAB converters is facilitated through a phase-shift PWM

mechanism [99]. Leveraging the lag/lead relationship of three pulse width waveforms, ports on PPP TAB converter enable power transmission. The direction of power transmission varies based on the different lag/lead relationships, as each port of the PPP TAB converter can facilitate bidirectional power flow [87]. Therefore, an automatic power direction control method can adjust power direction automatically according to the states of the ports of the PPP TAB converter. This eliminates the need for manual monitoring of equipment status and ensures that the equipment can automatically adjust power direction to address different emergencies, thereby saving manpower and realize the P2P trading [114].

This chapter is arranged as below. Firstly, the principle of power direction of PPP TAB converter is briefly described. Secondly, the automatic power direction control method in EEPS is demonstrated. Thirdly, a simulation model that contains a EEPS is implemented in MATLAB/Simulink and a brief conclusion is provided at the end of this chapter.

5.2 Principle of Power Direction of PPP TAB Converter

Fig. 5-2 illustrates the topology of TAB converter in ER_1. Each topology features two or three ports, with each port comprising an active bridge consisting of four switches. Each port of the PPP TAB converter includes an inductor L_{1i} (where i = 1, 2, 3) and a transformer with winding N_{1i}. Additionally, a power source B_{1i} is connected to the terminal of each port. For the energy router designed for emergency energy supply in urban areas, B_{11} can be considered as the DC bus of the urban power grid, while B_{12} represents any source capable of serving as an EES. B_{13} corresponds to the power storage unit within the energy router. In this configuration, power is transferred among ports through the magnetic coupling of the windings.

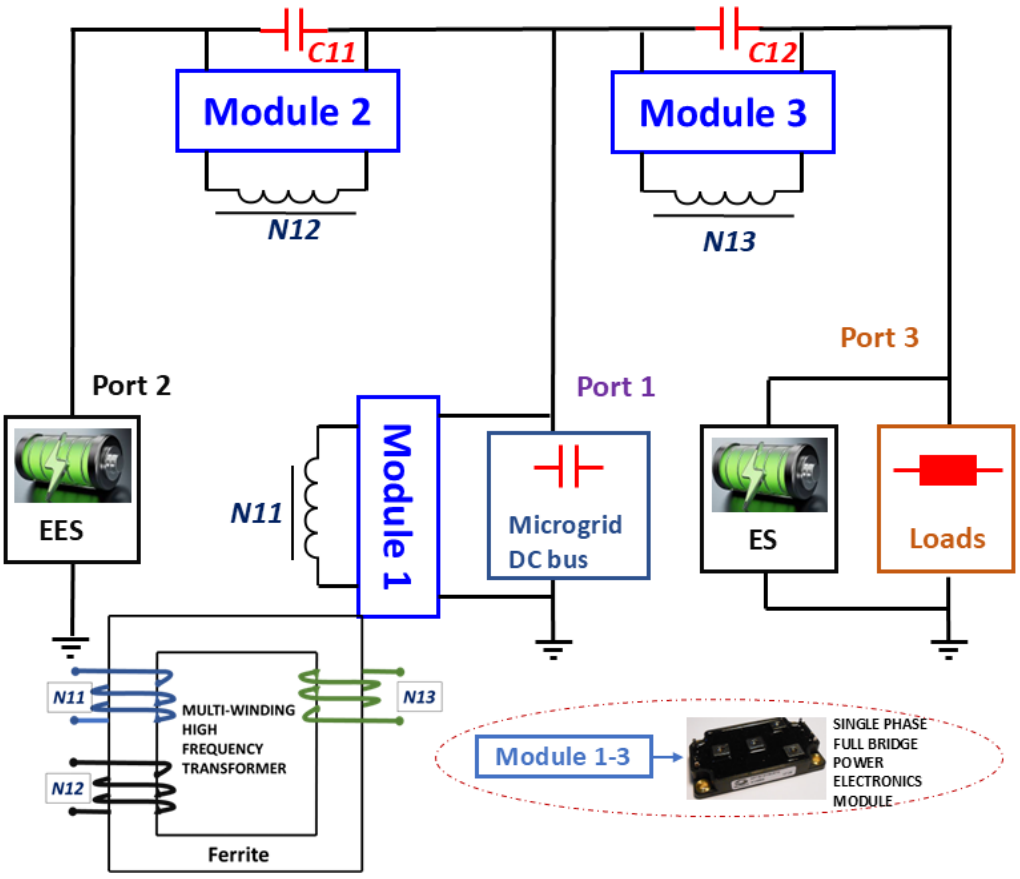

Fig. 5-2. Topology of the PPP TAB Converter in ER_1

The phase-shift PWM method employed is utilized to control power flow direction in the TAB converter. In Fig. 3-10, the control signals of switches S_1 and S_2 serve as references, while the control signals of switches S_5 and S_6, and switches S_9 and S_{10} are lagged by φ_{12} and φ_{13} radians, respectively. Here, $-\pi < \varphi_{12} < \pi$ and $-\pi < \varphi_{13} < \pi$. Moreover, each switch operates with a duty ratio half of the switching cycle. Additionally, Fig. 3-10 illustrates the current waveforms of L_{11}, L_{12}, and L_{13} for i_{L11}, i_{L12}, and i_{L13}, respectively, in a traditional phase-shift TAB converter. The turns ratio of the transformer N_{11}: N_{12}: N_{13} is set to 1:1:1.

The power flow characteristics of a phase-shift TAB converter can be derived from analyzing the inductive current of each port, and the expression (5-1) by analyzing the various operating states of the TAB converter.

$$\begin{cases} P_{112} = \dfrac{\varphi_{12}(\pi-|\varphi_{12}|)V_{11}V_{12}}{2\pi^2 f_S(L_{11}+L_{12})} \\ P_{113} = \dfrac{\varphi_{13}(\pi-|\varphi_{13}|)V_{11}V_{13}}{2\pi^2 f_S(L_{11}+L_{13})} \\ P_{123} = \dfrac{(\varphi_{13}-\varphi_{12})(\pi-|\varphi_{13}-\varphi_{12}|)V_{11}V_{12}}{2\pi^2 f_S(L_{12}+L_{13})} \end{cases} \tag{5-1}$$

in this expression, V_{11}, V_{12}, and V_{13} refer to the voltages of B_{11}, B_{12}, and B_{13}, respectively, and P_{112}, P_{113}, and P_{123} are the power flow from port 1 to port 2, from port 1 to port 3, and from port 2 to port 3 in ER_1, respectively. Furthermore, f_s is the switching frequency. Considering the proposed PPP TAB converter, since the rest unprocessed energy transfers directly through inductors, the conducted energy in one operation cycle can be obtained in (5-2), where C_{112}, C_{113}, and C_{123} are the conducted power flow from port 1 to port 2, from port 1 to port 3, and from port 2 to port 3 in ER_1, respectively.

$$\begin{cases} C_{112} = \frac{(V_{11}-V_{12})}{(L_{11}+L_{12})f_s} \\ C_{113} = \frac{(V_{11}-V_{13})}{(L_{11}+L_{13})f_s} \\ C_{123} = \frac{(V_{12}-V_{13})}{(L_{12}+L_{13})f_s} \end{cases} \tag{5-2}$$

Next, the total power transferred among these three ports in one switching period can be acquired from (5-1) and (5-2) by adding together the processed power and conducted power. The equation of the total power converted among various ports is presented in (5-3), where T_{112}, T_{113}, and T_{123} are the total power flow from port 1 to port 2, from port 1 to port 3, and from port 2 to port 3 in ER_1, respectively.

$$\begin{cases} T_{112} = \frac{\varphi_{12}(\pi-|\varphi_{12}|)V_{11}V_{12}+2\pi^2(V_{11}-V_{12})}{2\pi^2 f_s(L_{11}+L_{12})} \\ T_{113} = \frac{\varphi_{13}(\pi-|\varphi_{13}|)V_{11}V_{13}+2\pi^2(V_{11}-V_{13})}{2\pi^2 f_s(L_{11}+L_{13})} \\ T_{123} = \frac{(\varphi_{13}-\varphi_{12})(\pi-|\varphi_{13}-\varphi_{12}|)V_{11}V_{12}+2\pi^2(V_{12}-V_{13})}{2\pi^2 f_s(L_{12}+L_{13})} \end{cases} \tag{5-3}$$

Suppose each inductor has the same inductance and the sum of each two inductors is L_d, the port power can be derived from

$$\begin{cases} T_{11} = T_{112} + T_{113} \\ = \frac{\varphi_{12}(\pi-|\varphi_{12}|)V_{11}V_{12}+\varphi_{13}(\pi-|\varphi_{13}|)V_{11}V_{13}+4\pi^2V_{11}-2\pi^2(V_{12}+V_{13})}{2\pi^2 f_s L_d} \\ T_{12} = -T_{112} + T_{123} \\ = \frac{-\varphi_{12}(\pi-|\varphi_{12}|)V_{11}V_{12}+(\varphi_{13}-\varphi_{12})(\pi-|\varphi_{13}-\varphi_{12}|)V_{12}V_{13}+4\pi^2V_{12}-2\pi^2(V_{11}+V_{13})}{2\pi^2 f_s L_d} \\ T_{13} = -T_{113} - T_{123} \\ = \frac{-\varphi_{13}(\pi-|\varphi_{13}|)V_{11}V_{13}-(\varphi_{13}-\varphi_{12})(\pi-|\varphi_{13}-\varphi_{12}|)V_{12}V_{13}+4\pi^2V_{13}-2\pi^2(V_{11}+V_{12})}{2\pi^2 f_s L_d} \end{cases} \tag{5-4}$$

where T_{11}, T_{12}, and T_{13} represent the total power of port 1, port 2, and port 3 in ER_1, respectively.

Therefore, the direction of power transmission is determined by both the port voltages and the

phase shift angles of the switching gate signals. For instance, when the difference between port voltages is small or nearly non-existent, Fig. 3-11 illustrates four typical power flow scenarios to satisfy the needs of EEPS.

Since the PPP TAB converter is the same in each ER, the four typical power transmission directions derived from ER_1 apply to ER_2 and ER_3 as well. since port 1 of each ER is connected to the mains grid, then by arranging the power transmission directions of the ERs in different scenarios, power can be exchanged between the ERs, which means that P2P trading can be realized.

5.3 Automatic Power Direction Control Method of EEPS

To address the need for automatic power direction adjustment without manual intervention, this chapter proposes an automatic power direction control method for EEPS. In the context of emergency energy supply, numerous unforeseen accidents may occur, making it difficult for individuals to swiftly change the power direction of PPP TAB converters to address each unexpected situation. An automatic power direction control method can assist in adjusting the power direction according to preset values, thereby enhancing the responsiveness and effectiveness of the system in managing unexpected events.

Based on the preceding explanation of the power direction of the PPP TAB converter, as depicted in Fig. 3-11, the TAB converter presents four different typical power directions determined by the lagging/leading relationship between φ_{12} and φ_{13}. Additionally, scenarios such as Fig. 3-11(d) illustrate instances where power flow occurs solely between port 2 and port 3, with no power transmission at port 1. Therefore, Fig. 5-3 illustrates the proposed automatic power direction control method. In this method, ten variables, SOC of port 2 in ER_1 SOC_{12}, SOC of port 3 in ER_1 SOC_{13}, SOC of port 2 in ER_2 SOC_{22}, SOC of port 3 in ER_2 SOC_{23}, SOC of port 2 in ER_3 SOC_{32}, SOC of port 3 in ER_3 SOC_{33}, DC bus voltage of port 1 in each ER V_{DC}, a variable that decides the power transmission direction of ER_1 DS_1, a variable that decides the power transmission direction of ER_2 DS_2 and a variable that decides the power transmission direction of ER_2 DS_3, are employed to control the power direction of the EEPS. Among these controlling variables, the direction of power transmission of each MER is ultimately determined by the corresponding value of *DS*. The relationship between the direction of power transmission of each MER and the corresponding value of *DS* is as follows.

DS_1 = 1, power transfers from port 1 to port 2 and port 3 in ER_1.

DS_1 = 2, power transfers from port 1 and port 2 to port 3 in ER_1.

DS_1 = 3, power transfers from port 2 and port 3 to port 1 in ER_1.

DS_1 = 4, power transfers from port 2 to port 3 and there is no power transmission at port 1 in ER_1.

DS_2 = 1, power transfers from port 1 to port 2 and port 3 in ER_2.

DS_2 = 2, power transfers from port 1 and port 2 to port 3 in ER_2.

DS_2 = 3, power transfers from port 2 and port 3 to port 1 in ER_2.

DS_2 = 4, power transfers from port 2 to port 3 and there is no power transmission at port 1 in ER_2.

DS_3 = 1, power transfers from port 1 to port 2 and port 3 in ER_3.

DS_3 = 2, power transfers from port 1 and port 2 to port 3 in ER_3.

DS_3 = 3, power transfers from port 2 and port 3 to port 1 in ER_3.

DS_3 = 4, power transfers from port 2 to port 3 and there is no power transmission at port 1 in ER_3.

These ten variables ensure comprehensive and accurate control of power direction in the PPP TAB converter. In addition to this, the power transmission direction of each MER is controlled by the respective corresponding *DS*, which ensures the independence and stability of each MER in the EEPS.

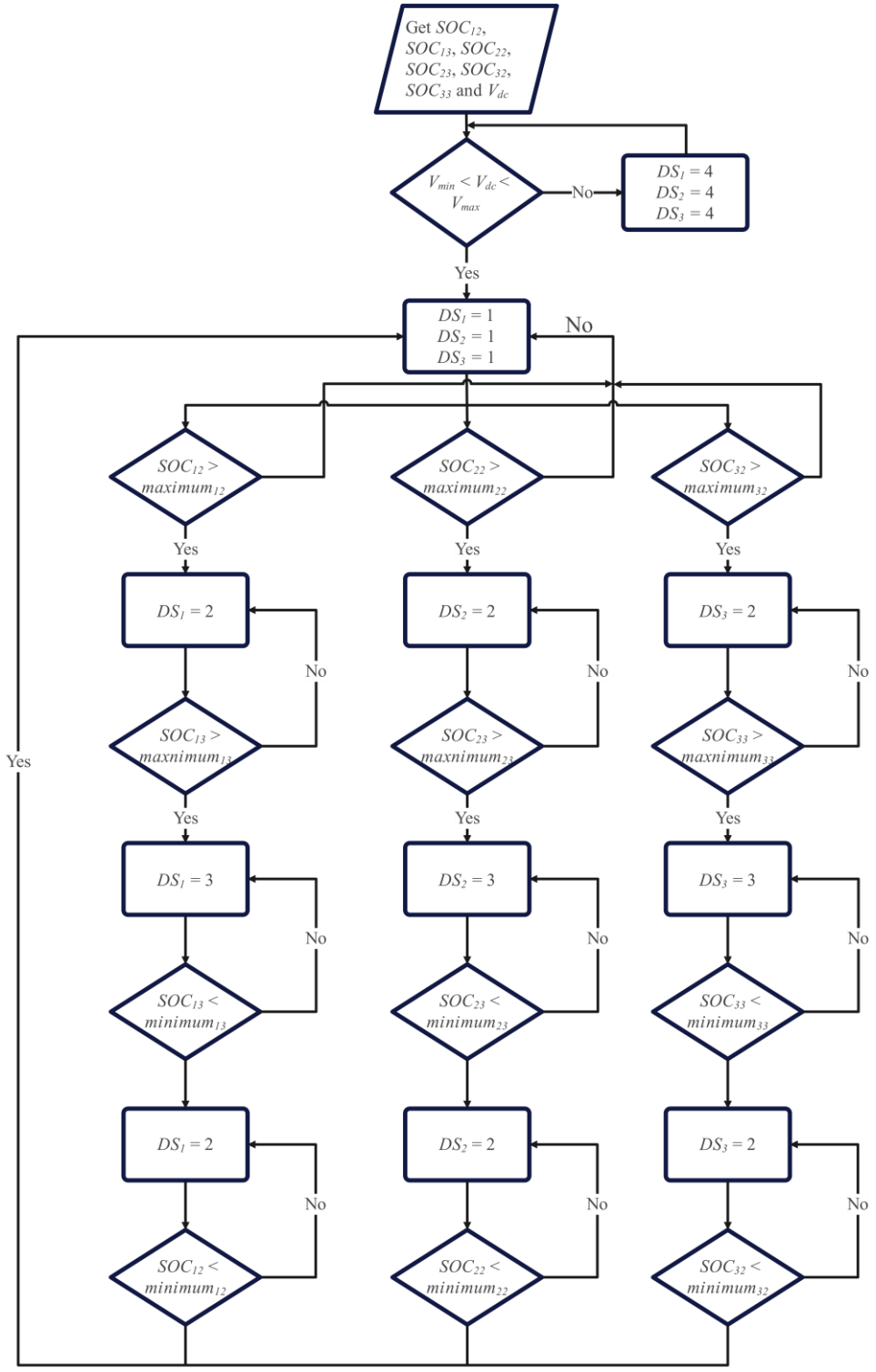

Fig. 5-3. Flow chart of the automatic power direction control method of the TAB converters in EEPS

According to Fig. 5-3, the process of each MER involves five "if" judgments to accommodate the four different types of power flow in the PPP TAB converter. Assuming the initial value of DS_1, DS_2 and DS_3 are equal to 1, which determines the power flow as shown in Fig. 3-11(a). If

V_1 is not within the acceptable voltage range between V_{min} and V_{max}, indicating an anomaly at port 1, then three DS_1, DS_2 and DS_3 are set to 4, and the power flow is as depicted in Fig. 3-11(d). After the first "if" judgment, the power transmission direction of each MER will be based on the real-time SOC values of port 2 and port 3 to determine the respective corresponding *DS* values. Using ER_1 as an example, if SOC_{12} exceeds the maximum setting for SOC_{12}, DS_1 is set to 2, and the power flow is as shown in Fig. 3-11(b). Otherwise, DS_1 remains equal to 1. In the third "if" judgment, if SOC_{13} surpasses the maximum setting value of SOC_{13}, DS_1 is set to 3, and the power flow is as illustrated in Fig. 3-11(c). The fourth "if" judgment checks if SOC_{13} falls below the minimum setting for SOC_{13}. If this condition is met, DS_1 is changed to 2, and the power flow is as depicted in Fig. 3-11(b). Otherwise, DS_1 remains at 3. During the final "if" judgment, if SOC_{12} is lower than the minimum setting value of SOC_{12}, DS_1 is reverted to 1, and the power flow is as shown in Fig. 3-11(a). This method for the PPP TAB converter can automatically adjust the power direction to handle different situations based on the states of each port. This approach significantly reduces the need for manual intervention and ensures the safe and stable operation of the PPP TAB converter. Considering that the remaining ER_2 and ER_3 have the same structure as ER_1, ER_2 and ER_3 also have the same power transmission direction control strategy as ER_1. Moreover, Fig. 5-3 shows that when the DC bus voltage of port 1 is stable, each MER determines its own power transmission direction according to the usage of its own remaining ports and does not receive any influence from other MERs on its own power transmission direction. This ensures that the respective MERs prioritize the satisfaction of their own needs when they are used by individual clients. When each client's demand is satisfied and there is excess power available for transmission, each MER is connected to each other through port 1 and can realize power transmission between MERs, which is P2P trading.

5.4 Simulation Results

The simulation model of the EEPS have been developed in MATLAB/Simulink to evaluate the feasibility of the proposed automatic power direction control method. These simulations aim to validate the direction of power transmission at each port by monitoring the SOC, *DS*, and current waveforms at each port. Furthermore, by analyzing the timing of changes in waveform values, it is possible to confirm that the change in the direction of power transmission aligns with the proposed method. The simulation model is constructed according to the diagrams

presented in Fig. 5-1, Fig. 3-1, and Fig. 5-2. Through these simulations, it is aimed to assess the efficacy and reliability of the automatic power direction control method in ensuring the safe and stable operation of EEPS and MERs in it.

5.4.1 When V_{dc} is within acceptable voltage range

The first simulation of EEPS is run when the voltage of V_{dc} is normal which means that there is no power outage. *DS* will be shifted between 1,2 and 3 and will not be equal to 4. This simulation shows automatic change of each port's power transmission direction according to the SOC status and power requirements of the individual ports automatic power direction in the absence of a sudden power failure.

The system configurations of EEPS model when V_{dc} is within acceptable voltage range are exhibited in Table 5-1. In Table 5-1, the voltage of port 1, port 2 and port 3 at each MER are 400 V, 100V and 120V respectively. The initial SOC of six battery packs is 80%, 90%, 5%, 10%, 50% and 10%, in order. Moreover, the transformer turns ratio N_{i1}:N_{i2}:N_{i3} of each MER is 1:1:1 and the initial value of DS_1, DS_2 and DS_3 are all 1. To get simulations results more quickly, four peak values of SOC are set 60%, 20%, 80% and 45% respectively.

TABLE 5-1 Parameters of EEPS Simulation Model When V_{dc} is Within Acceptable Voltage Range

Parameter name	Parameter Value
$V_{i1}/V_{i2}/V_{i3}$ (Port voltages in each MER)	400/100/120 V
$SOC_{12}/SOC_{13}/SOC_{22}/SOC_{23}/SOC_{32}/SOC_{33}$ (Initial SOC)	80%/90%/5%/10%/50%/10%
N_{i1}:N_{i2}:N_{i3} (Transformer turns ratio of PPP TAB converter in each MER)	1:1:1
$L_{i1}/L_{i2}/L_{i3}$ (Series inductance of PPP TAB converter in each MER)	300 μH
f_s (Switching Frequency)	50 kHz
$maximum_{i2}$ (Maximum setting SOC of port 1)	60%
$minimum_{i2}$ (Minimum setting SOC of port 1)	20%
$maximum_{i3}$ (Maximum setting SOC of port 2)	80%
$minimum_{i3}$ (Minimum setting SOC of port 2)	45%
Initial value of DS_1, DS_2 and DS_3	1

In EEPS Simulink simulation, the initial value of DS_1, DS_2 and DS_3 are all 1 and the initial value of phase-shift angles φ_{i2} and φ_{i3} are lagging the port 1 bridge waveform and $|\varphi_{i2}|<|\varphi_{i3}|$ shown in Fig. 3-10. Therefore, power is transferred from B_{i1} to B_{i2} and B_{i3} which means that SOC_{i2} and SOC_{i3} is increasing. However, according to the automatic direction control method in Fig. 5-3 and the setting value of maximum and minimum, DS_1 is changed into 3 at the start because SOC_{12} and SOC_{13} both are beyond $maximum_{12}$ and $maximum_{13}$. So, before t_1, SOC_{12} and SOC_{13} is decreasing while the rest SOC waveforms are increasing shown in Fig. 5-4 with port 1 bridge waveform is lagging the port 2 and port 3 bridge waveform in ER_1 with $\varphi_{12}<\varphi_{13}<0$. During t_1 and t_2, SOC_{32} has been reached the $maximum_{32}$ which causes that DS_3 is changed into 2 and φ_{32} will lead the port 1 bridge waveform and φ_{33} will still lag the port 1 bridge waveform with $|\varphi_{32}|<|\varphi_{33}|$. This means that SOC_{32} is decreasing until t_2. After t_2, SOC_{32} arrives the $minimum_{32}$ and SOC_{33} is still increasing. DS_3 is changed back into 1 and SOC_{32} can increase. When t_3, since neither SOC_{12} nor SOC_{13} is greater than $minimum_{12}$ and $minimum_{13}$, DS_1 changes from 3 to 1. Both SOC_{12} and SOC_{13} also change from decreasing to increasing. Additionally, the waveforms of DS_1, DS_2 and DS_3 are exhibited in Fig. 5-5.

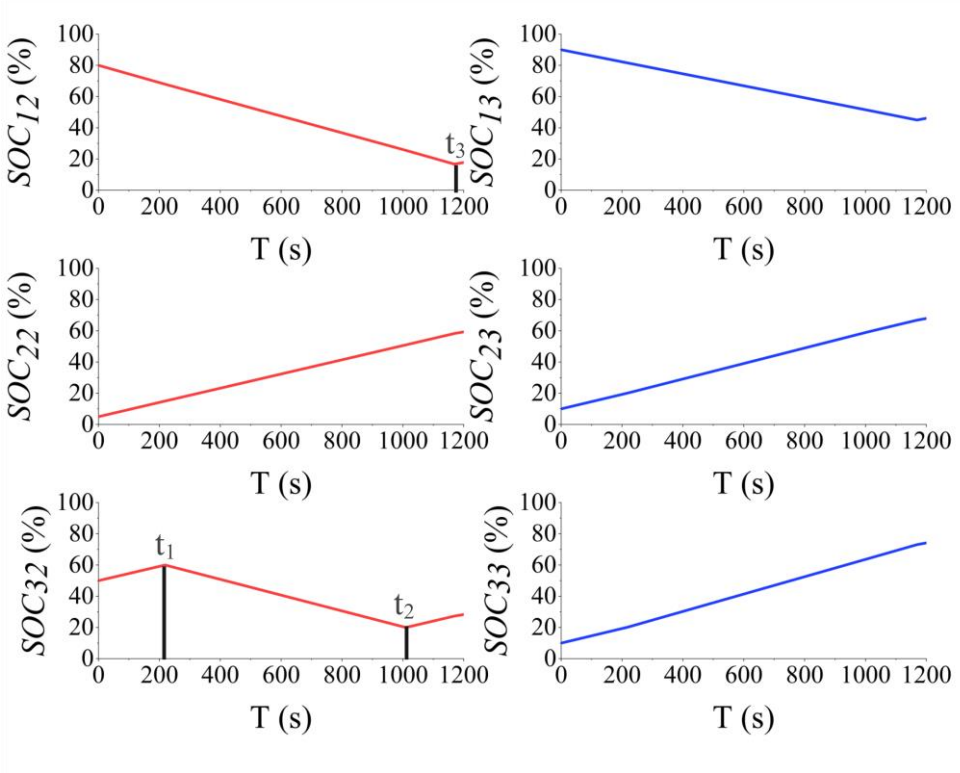

Fig. 5-4. SOC waveforms in automatic power direction control of EEPS when V_{dc} is within acceptable voltage range

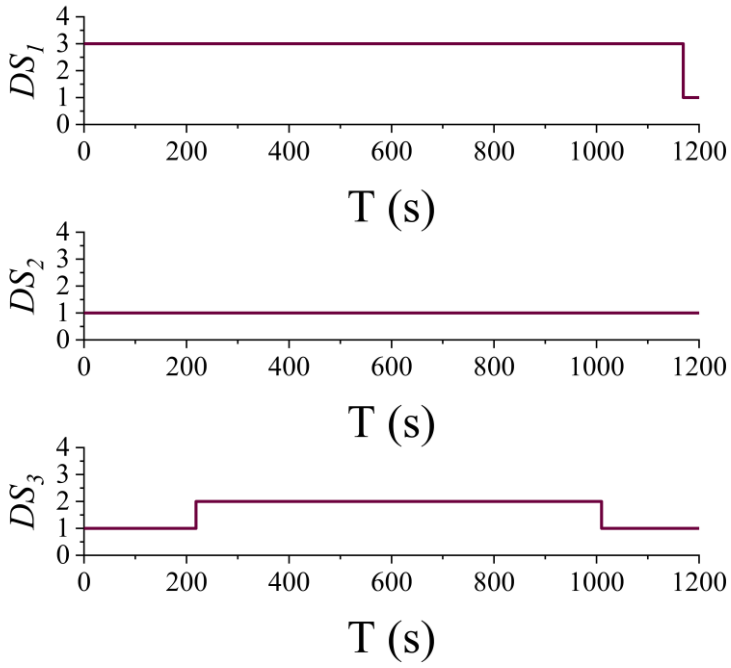

Fig. 5-5. *DS* waveforms in automatic power direction control of EEPS when V_{dc} is within acceptable voltage range

Fig. 5-4 presents the variation of SOC for the B_{i2} and B_{i3} in the whole simulation process, from which it can be investigated that SOC_{i2} and SOC_{i3} changes corresponding to the proposed analysis and power direction changes corresponding to the proposed automatic power direction control method which is consistent with the analysis in the previous sections. In this whole EEPS simulation process, it can be clearly seen that the port of each MER decides the direction of power transmission only by the SOC value of its own port and is not affected by other MERs. This ensures the independence of MERs in EEPS. In addition to this, comparing the time periods 0 to t_1 and t_2 to t_3, the incremental rates of SOC_{22}, SOC_{23}, and SOC_{33} are higher from t_2 to t_3 than from 0 to t_1 because of the extra B_{32} as an input. This shows that there is power transfer between MER and MER in the EEPS. In Fig. 5-5, *DS* can also be different values in these three modes and the period of each mode is consistent with that in Fig. 5-4. Through Fig. 5-7, during the steady state, the current waveform of port 2 i_{i2} and port 3 i_{i3} in each MER also switches between positive and negative values which also shows the power direction. When the current is negative, this port is the input port. Conversely, when the current is positive, this port is the output port. Compared Fig. 5-4 with Fig. 5-6, the power direction obtained from

SOC status of each port is the same with the power direction obtained from the current value of each port.

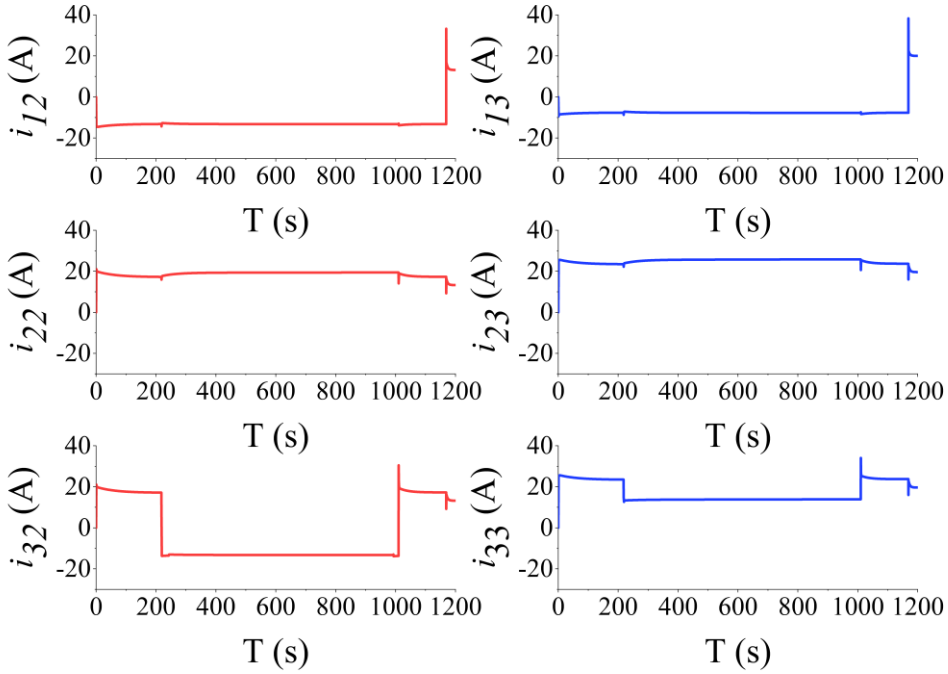

Fig. 5-6. Current waveforms in automatic power direction control of EEPS when V_{dc} is within acceptable voltage range

Based on the figures in Fig. 5-6, it is apparent that the duration of the power direction change at each port is also relatively short. The transition from a positive steady-state value to a negative steady-state value for the current at each port takes only 2 seconds. This confirms that the proposed automatic power direction control method can swiftly and effectively adjust the power direction in EEPS without significantly disrupting its normal operation. Consequently, this approach saves manual operation time while ensuring the smooth functioning of EEPS.

5.4.2 When V_{dc} is not within acceptable voltage range

In this scenario, DC bus of the main power grid exhibits an abnormal voltage, indicating an issue that prevents it from effectively carrying out power transmission duties in EEPS. An abnormal voltage suggests that the main power grid is experiencing significant disruptions and is unable to function normally. Prior to resolving the issue with the main power grid, it is imperative that the PPP TAB converter in each MER operates similarly to a dual active bridge converter. This entails transferring power exclusively between port 2 and port 3 while ensuring that no power transmission occurs at port 1. This temporary operational mode allows each

MER to maintain critical power flow functionalities within EEPS until the problem with port 1 is rectified.

The system configurations of EEPS model when V_{dc} is not within acceptable voltage range are exhibited in Table 5-2. In Table 5-2, the voltages of port 2 and port 3 in each MER are 100V and 120V with the initial SOC of them are all 50% while the voltage of port 1 is 300V.

TABLE 5-2 Parameters of EEPS Simulation Model When V_{dc} is Within Acceptable Voltage Range

Parameter name	Parameter Value
$V_{i1}/V_{i2}/V_{i3}$ (Port voltages in each MER)	300/100/120 V
$SOC_{12}/SOC_{13}/SOC_{22}/SOC_{23}/SOC_{32}/SOC_{33}$ *(Initial SOC)*	50%
$N_{i1}:N_{i2}:N_{i3}$ (Transformer turns ratio of PPP TAB converter in each MER)	1:1:1
$L_{i1}/L_{i2}/L_{i3}$ (Series inductance of PPP TAB converter in each MER)	300 μH
f_s (Switching Frequency)	50 kHz
Initial value of DS_1, DS_2 and DS_3	1

Although the initial value of DS_1, DS_2 and DS_3 are all 1, because of the abnormal value of V_{dc}, DS_1, DS_2 and DS_3 are all rapidly changed into 4. This causes that φ_{i2} is leading the port 1 bridge waveform and φ_{i3} is lagging the port 1 bridge waveform at the same time with $|\varphi_{i2}|=|\varphi_{i3}|$. With this relationship between φ_{i2} and φ_{i3}, power only transfers from B_{i2} to B_{i3} and there is no power transmission at port 1. Each MER will work independently and there is no power transfer between them. This mode will last until the problem of V_{dc} is fixed. After that, DS_1, DS_2 and DS_3 will be back to 1 so that each MER can work as its own role again and again power transmission between MERs namely P2P trading is realized. Additionally, the waveforms of DS_1, DS_2 and DS_3 are exhibited in Fig. 5-8.

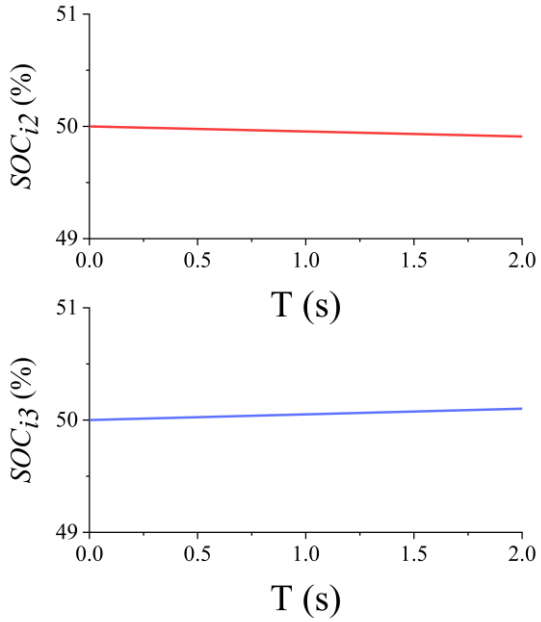

Fig. 5-7. SOC waveforms in automatic power direction control of EEPS when V_{dc} is not within acceptable voltage range.

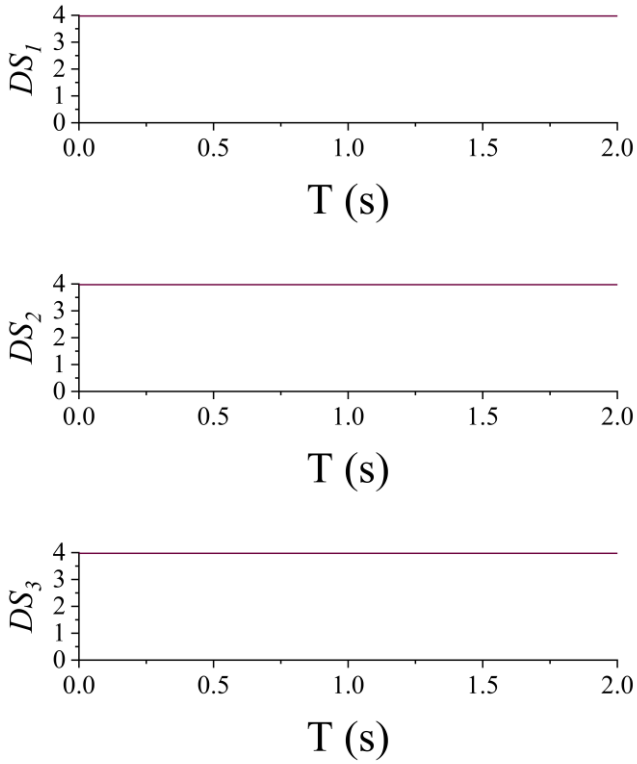

Fig. 5-8. *DS* waveforms in automatic power direction control of EEPS when V_{dc} is not within acceptable voltage range.

Fig. 5-7 presents the variation of SOC for B_{i2} and B_{i3} in the whole simulation process, from which it can be investigated that SOC_{i2} and SOC_{i3} changes corresponding to the proposed analysis and power direction is stable. In Fig. 5-8, DS_1, DS_2 *and* DS_3 are all also constant at 1 which corresponds to the SOC waveforms in Fig. 5-7. In this whole simulation process, each MER is working identically and independently. Through Fig. 5-9, during the steady state, the currents of port 1 is zero, and the currents of port 2 and port 3 in each MER are constant positive and negative values respectively which also shows the power direction is only from B_{i2} to B_{i3}. Compared Fig. 5-7 with Fig. 5-9, the power direction obtained from SOC status of each port is the same with the power direction obtained from the current value of each port. In addition, each MER has the same rate of increase and decrease of SOC_{i2} and SOC_{i3} for each MER because it has the same structure.

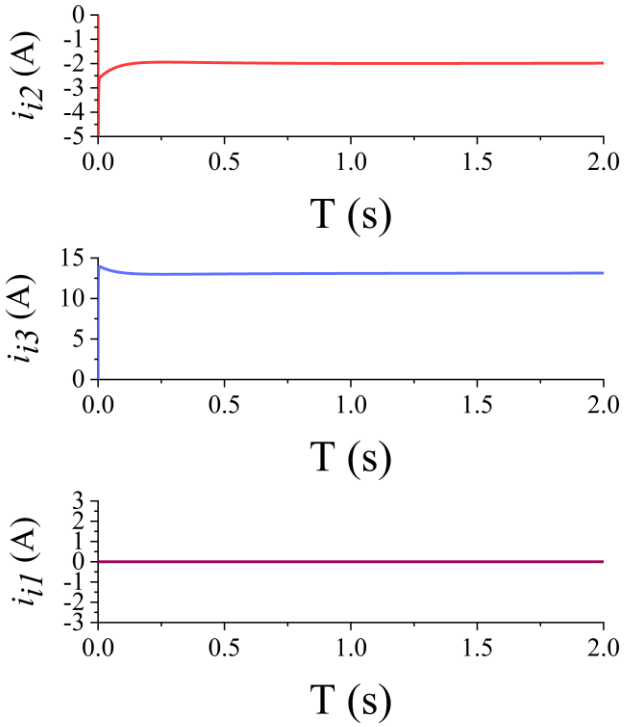

Fig. 5-9. Current waveforms in automatic power direction control of EEPS when V_{dc} is not within acceptable voltage range.

5.5 Summary

This chapter introduces an EEPS designed for emergency energy supply, along with an automatic power direction control method aimed at facilitating energy balancing and automating power direction within the EEPS. This enables automatic energy transfer not only from port to port in a single MER, but also between multiple MERs. The proposed EEPS enables each MER to stabilize independently for power transfer and reserve, adapting to diverse operational scenarios. This flexibility allows for direct power transfer between MERs, reducing reliance on the main grid. Besides, as a consequence of the fact that automatic energy transfer from MER to MER is a reality, it is also possible to engage in P2P trading between users. The automatic power direction control method manages power direction across ports based on the SOC status of the ES and EES ports. This method ensures swift directional control, leading to significant cost savings by minimizing the need for manual monitoring and regulation of the energy router's status during emergencies. This capability enhances the EEPS's responsiveness in addressing grid emergencies promptly. To validate the feasibility of the EEPS and its automatic power direction control method, simulation models implemented in MATLAB/Simulink have been utilized. The method relies on the SOC status of individual ports of the MER, enabling clients to optimize power consumption plans based on varying situations. This approach enhances the flexibility and efficiency of energy resource utilization, thereby reducing dependence on the main power grid.

.

Chapter 6 Conclusions and Future Work

6.1 Conclusions

A MER can simultaneously connect various emergency electric power sources, adjusting and storing their output to meet load requirements. This improves the efficiency of emergency power usage and provides a more stable voltage and current supply. Thus, MERs, which can link the power grid with diverse emergency sources and store power, are crucial for addressing large-scale unexpected power failures in urban areas. The main contributions of this study are summarized as follows:

In Chapter 2, emergency power sources are critical for managing large-scale power failures, reducing economic loss, and ensuring public safety. Identifying efficient application schemes and feasible sources is vital. Current emergency power sources can handle many sudden outages, but a comprehensive and excellent distribution scheme is essential. Key factors in choosing the appropriate emergency power source include the allowable power failure time and the load's location. Electric vehicle batteries, increasingly popular, offer potential as emergency power sources. Energy routers, capable of quickly connecting emergency power sources to loads and positioned near consumers, are highly promising.

In Chapter 3, this chapter presents a multi-port energy router designed to handle emergency power outages and balance energy between various sources and loads. The MER's multiple ports allow it to manage and energize different emergency electric power sources and loads simultaneously, facilitating flexible urban energy management for emergencies. Power conversion is achieved through a bidirectional AC/DC converter and a PPP TAB converter. The MER supports P2P trading and energy balancing, with ports that can function as either input or output based on requirements. Compared to conventional emergency distribution methods and existing energy routers, the MER offers higher power conversion efficiency and compatibility with various emergency power sources.

In Chapter 4, an automatic power direction control method for DAB/TAB converters is proposed to facilitate energy balancing and automation within an energy router system. Power conversion is managed through phase-shift PWM, while the proposed control method regulates

power flow direction based on the SOC of the ES and EEPS ports. This method provides rapid directional control and significant cost savings by reducing the need for manual monitoring and regulation, allowing for prompt resolution of grid emergencies especially in emergencies.

In Chapter 5, An EEPS for emergency energy supply, incorporating the automatic power direction control method, is proposed. This system stabilizes each MER independently for power transfer and reserve management in various situations. Power can be transferred between ERs, not just relying on the main grid. The control method manages power direction based on the SOC of the ES and EES ports, ensuring efficient and automated energy balancing within the EEPS and reducing the need for manual supervision especially in emergencies.

All in all, in terms of the topic about MER for EES, this research combines both theoretical analysis and simulation/experimental validation to investigate and develop an EEPS to avoid the effect of large power outages. In this area, the following achievements have been made in this study:

- The current distribution method of EES and future potential emergency electric power sources and distribution method are clearly explained.
- Compared with the current MERs, an MER consisting of a bidirectional AC/DC converter and PPP TAB converter is prosed for EES with high efficiency and high adaptability to various situations especially in emergencies. To realize P2P trading and energy balancing, both ports in the bidirectional AC/DC converter and PPP-based TAB converter can be input port or output port according to different situations and working requirements. In addition, because the MER is multi-port, two customers can also exchange energy with each other through two ports so that the customers' dependence on the mains grid can be reduced and the distribution of power can be rationalized according to their needs
- An automatic power transmission direction control method algorithm of DAB/TAB converter are proposed for savings in manpower especially in emergencies and reduction in response time of DAB/ TAB converter in case of changes in electricity usage. The proposed method offers a swift directional control solution and leads to significant cost savings by reducing the need for manual monitoring and regulation of the energy router's status when an emergency occurs. Consequently, emergencies within the grid can be promptly addressed and resolved.

- An EEPS in microgrid composed of multiple MERs and its related automatic power direction control method is proposed to resolve sudden power outages within a certain range and provide emergency power and automate the system and P2P trading. The direction change is solely based on the SOC status of the individual ports of the MER, enabling clients to make informed decisions about their power consumption plans depending on various situations. This approach ensures a more flexible and efficient utilization of energy resources, reducing reliance on the main power grid。

6.2 Future Work

Based on the conclusions above and considering the limitations of the existed work, future research could be carried out in the following areas.

- **Further investigation is needed for more potential emergency electric power sources**

  Chapter 2 proposes the use of EV batteries as a potential EEPS. Additionally, it suggests that other emergency electric power sources can be investigated in the future for EES during sudden power outages. Identifying and exploring these sources is crucial for enhancing the reliability and efficiency of emergency power systems.

- **More Efficient converters need to be used in energy router**

  introduces a combination of a bidirectional AC/DC converter and a PPP TAB converter. However, in this configuration, clients only receive high DC voltage at the load port, which does not meet the diverse needs of customers with a wide range of loads. Additionally, other types of AC/DC and DC/DC converters could potentially fulfil the requirements of MERs for EES. Therefore, further verification is needed to identify the optimal converters for MER in EES applications.

- **A higher efficient switching control signal algorithm can be used in DAB/TAB converter**

  A SPS PWM algorithm is employed in this study for DAB/TAB converters. However, there exist more efficient algorithms for controlling the switches of DAB/TAB converters. Further verification is necessary to determine if these alternative algorithms

can be effectively implemented and improve efficiency in TAB converters within ERs for emergency energy storage systems.

- **More ports and MERs should be added into EEPS for more options for energy use**

  According to Chapter 5, the EEPS is currently equipped with only three ports, with just one designated for emergency electric power sources. Given the diversity of available energy sources today, it is evident that a single port is insufficient. Furthermore, enhancing energy efficiency necessitates interconnecting multiple MERs to create a larger EEPS. This expansion would not only accommodate a broader range of energy sources but also facilitate greater P2P trading capabilities.

References

[1] B. Zhou, L. Gu, Y. Ding, L. Shao, Z. Wu, X. Yang, C. Li, Z. Li, X. Wang, Y. Cao, B. Zeng, M. Yu, M. Wang, S. Wang, H. Sun, A. Duan, Y. An, X. Wang, and W. Kong, "The Great 2008 Chinese Ice Storm: Its Socioeconomic–Ecological Impact and Sustainability Lessons Learned," *Bulletin of the American Meteorological Society,* vol. 92, no. 1, pp. 47-60, 2011.

[2] H. Byrd and S. Matthewman, "Exergy and the City: The Technology and Sociology of Power (Failure)," *Journal of Urban Technology,* vol. 21, no. 3, pp. 85-102, 2014.

[3] P. Garg, "Energy scenario and vision 2020 in India," *Journal of Sustainable Energy & Environment,* vol. 3, no. 1, pp. 7-17, 2012.

[4] S. Graham and N. Thrift, "Out of Order," *Theory, Culture & Society,* vol. 24, no. 3, pp. 1-25, 2007.

[5] S. Bhattacharyya, J. M. A. Myrzik and W. L. Kling, "Consequences of poor power quality - an overview," in *2007 42nd International Universities Power Engineering Conference*, 2007.

[6] D. Nye, When the lights went out, Cambridge: MA: MIT Press, 2013.

[7] D. Halperin, T.S. Heydt-Benjamin, B. Ransford, S.S. Clark, B. Defend, W. Morgan, K. Fu, T. Kohno and W.H. Maisel, "Pacemakers and Implantable Cardiac Defibrillators: Software Radio Attacks and Zero-Power Defenses," *IEEE Symposium on Security and Privacy,* pp. 129-142, 2008.

[8] Z, Song, Y, Wei, Y. Sang, G. Fang, X. He, J, Tang and L. Wang, "Evaluation method of emergency support capacity of urban important power supply units," in *2020 5th Asia Conference on Power and Electrical Engineering (ACPEE)*, Chengdu, 2020.

[9] M. Jia, X. Luo, J. Tuo, H. Hua and X. Chen, "Robust Controller Design for the Emergency Response Module of Energy Router," in *2021 IEEE International Conference on Energy Internet (ICEI)*, Southampton, United Kingdom, 2021.

[10] Yi Xu, Jianhua Zhang, Wenye Wang, A. Juneja and S. Bhattacharya, "Energy router: Architectures and functionalities toward Energy Internet," in *2011*, Brussels, 2011 IEEE International Conference on Smart Grid Communications (SmartGridComm).

[11] X. Zhao, Y. Liu, X. Chai, X. Guo, X. Wang, C. Zhang, T. Wei, C. Shi and D. Jia, "Multimode Operation Mechanism Analysis and Power Flow Flexible Control of a New Type of Electric Energy Router for Low-Voltage Distribution Network," *IEEE Transactions on Smart Grid,* vol. 13, no. 5, pp. 3594-3606, 2022.

[12] T. Wu, C. Zhao and Y. -J. A. Zhang, "Distributed AC-DC Optimal Power Dispatch of VSC-Based Energy Routers in Smart Microgrids," *IEEE Transactions on Power Systems,* vol. 36, no. 5, pp. 4457-4470, 2021.

[13] B. Liu, Y. Peng, J. Xu, C. Mao, D. Wang and Q. Duan, "Design and Implementation of Multiport Energy Routers Toward Future Energy Internet," *IEEE Transactions on Industry Applications,* vol. 57, no. 3, pp. 1945-1957, 2021.

[14] R. Morello, C. De Capua, G. Fulco and S. C. Mukhopadhyay, "A Smart Power Meter to Monitor Energy Flow in Smart Grids: The Role of Advanced Sensing and IoT in the Electric Grid of the Future," *IEEE Sensors Journal,* vol. 17, no. 23, pp. 7828-7837, 2017.

[15] N. Bhusal, M. Abdelmalak, M. Kamruzzaman and M. Benidris, "Power System Resilience: Current Practices, Challenges, and Future Directions," *IEEE Access,* vol. 8, pp. 18064-18086, 2020.

[16] B. A. Kumar, R. Selvaraj, T. R. Chelliah and U. S. Ramesh, "Improved Fuel-Use Efficiency in Diesel–Electric Tugboats With an Asynchronous Power Generating Unit," *IEEE Transactions on Transportation Electrification,* vol. 5, no. 2, pp. 565-578, 2019.

[17] V.W. Wong and S.C. Tung, "Overview of automotive engine friction and reduction trends–Effects of surface, material, and lubricant-additive technologies," *Friction,* vol. 4, no. 1, pp. 1-28, 2016.

[18] R. Arghandeh, M. Pipattanasomporn and S. Rahman, "Flywheel Energy Storage Systems for Ride-through Applications in a Facility Microgrid," *IEEE Transactions on Smart Grid,* vol. 3, no. 4, pp. 1955-1962, 2012.

[19] M.H. Nehrir, C. Wang, K. Strunz, H. Aki, R. Ramakumar, J.Bing, Z. Miao and Z. Salameh, "A Review of Hybrid Renewable/Alternative Energy Systems for Electric Power Generation: Configurations, Control, and Applications," *IEEE Transactions on Sustainable Energy,* vol. 2, no. 4, pp. 392-403, 2011.

[20] P. Kundur, "Power system stability," in *Power system stability and control*, 2007, p. 10.

[21] M. Issam H. Ibrahim, R. Lepage and A. Linca, "A review and comparison on recent optimization methodologies for diesel engines and diesel power generators," *Journal of Power and Energy Engineering,* vol. 7, no. 6, pp. 31-56, 2019.

[22] M. Aamir, K. A. Kalwar and S. Mekhilef, "Uninterruptible power supply (UPS) system," *Renewable and sustainable energy reviews,* vol. 58, pp. 1395-1410, 2016.

[23] A. Muhammad, A. Kalwar, and K.S. Mekhilef, "Review: uninterruptible power supply (UPS) sys-tem," *Renewable and Sustainable Energy Reviews,* vol. 58, pp. 1395-1410, 2016.

[24] "What is UPS? -Working & Types of UPS Explained," Electrical Concepts, 2022. [Online]. Available: https://electricalbaba.com/what-is-ups-working-types-of-ups-explained/.

[25] M. A. Awadallah and B. Venkatesh, "Energy Storage in Flywheels: An Overview," *Canadian Journal of Electrical and Computer Engineering,* vol. 38, no. 2, pp. 183-193, 2015.

[26] A. L. H. Fawaz, Y. Peng, C. H. Youn, J. Lorincz and C. Li , “Dynamic allocation of power delivery paths in consolidated data centers based on adaptive UPS switching,” *Computer Networks,* vol. 144, pp. 254-270, 2018.

[27] Bong-Hwan Kwon, Jin-Ha Choi and Tae-Won Kim, “Improved single-phase line-interactive UPS,” *IEEE Transactions on Industrial Electronics,* vol. 48, no. 4, pp. 804-811, 2001.

[28] C. Martín-Gómez, J. Bermejo-Busto, and N. Mambrilla-Herrero, “Emergency lighting cabinet for fire safety learning,” *Case Studies in Fire Safety,* vol. 3, pp. 17-24, 2015.

[29] Rathore, A.K. and Rajagopal, P.U., “Power electronic applications, grid codes, power quality issues, and electricity markets for distributed generation,” *Handbook of distributed generation,* pp. 631-684, 2017.

[30] A. Emadi, A. Nasiri and S.B. Bekiarov, Uninterruptible power supplies and active filters, CRC press, 2017.

[31] B. Zhang, R. Jiao, X. Li, Y. Zhao, Y. Ding, C. Gong and L. Ma, “Research on the control strategy of EPS provided by parallel operation of traditional EPS and EVs,” in *AIP Conference Pro-ceedings*, 2019.

[32] S. Yang, X. Ding, J. Liu and Z. Qian, “Analysis and design of a cost-effective voltage feed-back control strategy for EPS inverters,” in *2007 IEEE Power Electronics Specialists Conference*, 2007.

[33] T. Wu. Q. Li, Y. Yang, L. Li and N. Ning, “Research on Classification and Application of Comprehensive Energy Load of Important Users,” in *IOP Conference Series: Earth and Environmental Science*, 2021.

[34] S.G. Sigarchian, R. Paleta, A. Malmquist and A. Pina, “Feasibility study of using a biogas engine as backup in a decentralized hybrid (PV/wind/battery) power generation system–Case study Ken-ya,” *Energy,* vol. 90, pp. 1830-1841, 2015.

[35] M. Sabita, Z. Yan, G. Stein, U. Oystein and E. Frank, "Providing Microgrid Resilience during Emergencies Using Distributed Energy Resources," *2015 IEEE Globecom Workshops (GC Wkshps),* pp. 1-6, 2015.

[36] K. Young, C. Wang, L.Y. Wang and K. Strunz, "Electric vehicle battery technologies," Springer, New York, NY, Electric vehicle integration into modern power networks.

[37] M. A. Hannan, M. M. Hannan, A. Mohamed and A. Ayob, "Review of energy storage systems for electric vehicle applications: Issues and challenges," *Renewable and Sustainable Energy Reviews,* vol. 69, pp. 771-789, 2017.

[38] W. Kempton and J. Tomić, "Vehicle-to-grid power fundamentals: Calculating capacity and net rev-enue," *Journal of power sources,* vol. 144, no. 1, pp. 268-279, 2005.

[39] B.K. Sovacool, L. Noel, J. Axsen and W. Kempton, "The neglected social dimensions to a vehi-cle-to-grid (V2G) transition: a critical and systematic review," *Environmental Research Letters,* vol. 13, no. 1, p. 013001, 2018.

[40] W. Yue, C. Zhao, Y. Lu and G. Li, "A scheme of connecting microgird to AC grid via flexible power electronics interface," in *2010 International Conference on Power System Technology*, 2010, October.

[41] J.M. Daley and R.L. Siciliano, "Application of emergency and standby generation for distributed generation. I. Concepts and hypotheses," *IEEE Transactions on Industry Applications,* vol. 39, no. 4, pp. 1214-1225, 2003.

[42] L.H. Willis and W.G. Scott, Distributed power generation: planning and evaluation, Crc Press, 2018.

[43] S. Thangavel and S. Saravanan, "Instantaneous reference current scheme based power man-agement system for a solar/wind/fuel cell fed hybrid power supply," *International journal of electrical power & energy systems,* vol. 55, pp. 155-170, 2014.

[44] Y. Zhao, C. Li, M. Zhao, S. Xu, H. Gao and L. Song, "Model design on emergency power supply of electric vehicle," *Mathematical Problems in Engineering,* 2017.

[45] Y.G. Son, B.C. Oh, M.A. Acquah, R. Fan, D.M. Kim and S.Y. Kim, "Multi energy system with an associated energy hub: a review," *IEEE Access,* 2021.

[46] A. Q. Huang, M. L. Crow, G. T. Heydt, J. P. Zheng and S. J. Dale, "The Future Renewable Electric Energy Delivery and Management (FREEDM) System: The Energy Internet," *Proceedings of the IEEE,* vol. 99, no. 1, pp. 133-148, 2011.

[47] S. Hambridge, A.Q. Huang and R. Yu, "Solid State Transformer (SST) as an energy router: Economic dispatch based energy routing strategy," in *2015 IEEE Energy Conversion Congress and Exposition (ECCE)*, 2015, Semtember.

[48] P.H. Nguyen, W.L. Kling and P.F. Riberiro, "Smart power router: A flexible agent-based converter interface in active distribution networks," *IEEE Transactions on Smart Grid,* vol. 2, no. 3, pp. 487-495, 2011.

[49] X. She, A.Q. Huang, S. Lukic and M.E. Baran, "On integration of solid-state transformer with zonal DC microgrid," *IEEE Transactions on Smart Grid,* vol. 3, no. 2, pp. 975-985, 2012.

[50] Y. Kado, D. Shichijo, K. Wada and K. Iwatsuki, "Multiport power router and its impact on future smart grids," *Radio Science,* vol. 51, no. 7, pp. 1234-1246, 2016.

[51] M. Gao, K. Wang and L. He, " Probabilistic model checking and scheduling implementation of an energy router system in energy Internet for green cities," *IEEE Transactions on Industrial Informatics,* vol. 14, no. 4, pp. 1501-1510, 2018.

[52] M.R. Sandgani and S. Sirouspour, "Coordinated optimal dispatch of energy storage in a network of grid-connected microgrids," *IEEE Transactions on Sustainable Energy,* vol. 8, no. 3, pp. 1166-1176, 2017.

[53] B. Liu, W. Wu, C. Zhou, C. Mao, D. Wang, Q. Duan and G. Sha, "An AC–DC hybrid multi-port energy router with coordinated control and energy management strategies," *IEEE Access,* vol. 7, pp. 109069-109082, 2019.

[54] B. Lai, J. Wu, W. Zhang, W. Wu and Y. Wang, "Research on Energy Router Based on Power Electronic Transformer," *Zhejiang Electric Power,* vol. 36, no. 8, pp. 7-12, 2017.

[55] S.M. Ahsanuzzaman, A. Parayandeh, A. Prodić and D.A. Johns, " A building block IC for design-ing emerging hybrid and multilevel converters," *IEEE Journal of Emerging and Selected Topics in Power Electronics,* vol. 6, no. 2, pp. 500-514, 2017.

[56] J. Li, H. Cai, P. Yang and W. Wei, "A Bus-Sectionalized Hybrid AC/DC Microgrid: Concept, Control Paradigm, and Implementation," *Energies,* vol. 14, no. 12, p. 3508, 2021.

[57] S. Chi, Z. Lv, L. Liu and Y. Shan, "Free Switching Control Strategy for Multi-Operation Modes of Multi-Port Energy Router in Distribution Area," *Energies,* vol. 14, no. 23, p. 7860, 2021.

[58] T. Messo, J. Jokipii, J. Puukko and T. Suntio, "Determining the value of DC-link capacitance to ensure stable operation of a three-phase photovoltaic inverter," *IEEE Transactions on Power Electronics,* vol. 29, no. 2, pp. 665-673, 2013.

[59] A. Choudhury, P. Pillay and S.S. Williamson, "Comparative analysis between two-level and three-level DC/AC electric vehicle traction inverters using a novel DC-link voltage balancing algorithm," *IEEE Journal of Emerging and Selected Topics in Power Electronics,* vol. 2, no. 3, pp. 529-540, 2014.

[60] N. Soni, S. Dolla and M.C. Chandoekar, "Improvement of transient response in microgrids using virtual inertia.," *IEEE transactions on power delivery,* vol. 28, no. 3, pp. 1830-1838, 2013.

[61] T. Dragičević, J.M. Guerrero, J.C. Vasquez and D. Škrlec, "Supervisory control of an adaptive-droop regulated DC microgrid with battery management capability," *IEEE Transactions on power Electronics,* vol. 29, no. 2, pp. 695-706, 2013.

[62] Y. Liang, H. Zhang, M. Du and K. Sun, "Parallel coordination control of multi-port DC-DC converter for stand-alone photovoltaic-energy storage systems," *CPSS Transactions on Power Electronics and Applications,* vol. 5, no. 3, pp. 235-241, 2020.

[63] M. Almassalkhi and I. Hiskens, "Optimization framework for the analysis of large-scale networks of energy hubs," in *Power systems computation conference*, 2011.

[64] P. Li, W. Sheng, Q. Duan, Z. Li, C. Zhu and X. Zhang, "A Lyapunov optimization-based energy management strategy for energy hub with energy router," *IEEE Transactions on Smart Grid,* vol. 11, no. 6, pp. 4860-4870, 2020.

[65] I. Syed, V. Khadkikar and H.H. Zeinedin, "Loss reduction in radial distribution networks using a solid-state transformer," *IEEE Transactions on Industry Applications,* vol. 54, no. 5, pp. 5474-5482, 2018.

[66] N. Nikmehr, M. Bragin, P. Zhang and P. Luh, "Computationally Distributed and Asynchronous Operational Optimization of Droop-Controlled Networked Microgrids," *IEEE Open Access Journal of Power and Energy,* vol. 9, pp. 265-277, 2022.

[67] P. McLaughlin, P. Kyaw, M. Kianim, C. Sullivan and J. Stauth, "A 48-V:16-V, 180-W Resonant Switched-Capacitor Converter With High-Q Merged Multiphase LC Resonator.," *IEEE Journal of Emerging and Selected Topics in Power Electronics,* vol. 8, no. 3, pp. 255-2267, 2020.

[68] H. Mahmood and F. Blaabjerg, "Autonomous Power Management of Distributed Energy Storage Systems in Islanded Microgrids," *IEEE Transactions on Sustainable Energy,* vol. 13, no. 3, pp. 1507-1522, 2022.

[69] Y. Bulatov, A. Kryukov and K. Suslov, “Isolated Power Supply System with Energy Routers and Renewable Energy Sources,” *Vestnik IzhGTU imeni M.T. Kalashnikova,* vol. 24, no. 2, p. 124, 2021.

[70] G. Bedi, G. K. Venayagamoorthy, R. Singh, R. R. Brooks and K. -C. Wang, “Review of Internet of Things (IoT) in Electric Power and Energy Systems,” *IEEE Internet of Things Journal,* vol. 5, no. 2, pp. 847-870, 2018.

[71] Y. Nie, H. Xu, Y. Hu and X. Ye, “Energy Router for Emergency Energy Supply in Urban Cities: A Review.,” *Power Electronics and Drives,* vol. 7, no. 1, pp. 246-266, 2022.

[72] Yi Xu, Jianhua Zhang, Wenye Wang, A. Juneja and S. Bhattacharya, “Energy router: Architectures and functionalities toward Energy Internet,” in *2011 IEEE International Conference on Smart Grid Communications (SmartGridComm)*, Brussels, 2011.

[73] J. Ahmad, M. Tahir and S. K. Mazumder, “Improved Dynamic Performance and Hierarchical Energy Management of Microgrids With Energy Routing,” *IEEE Transactions on Industrial Informatics,* vol. 15, no. 6, pp. 3218-3229, 2019.

[74] S. Ansari, A. Chandel and M. Tariq, “A Comprehensive Review on Power Converters Control and Control Strategies of AC/DC Microgrid,” *IEEE Access,* vol. 9, pp. 17998-18015, 2021.

[75] J. Abdella and K. Shuaib, “Peer to peer distributed energy trading in smart grids: A survey,” *Energies,* vol. 11, no. 6, p. 1560, 2018.

[76] S. S. Hosseini, A. Badri, M. Parvania, “A survey on mobile energy storage systems (MESS): Applications, challenges and solutions,” *Renewable and Sustainable Energy Reviews,* vol. 40, pp. 161-170, 2014.

[77] Z. Bie, Y. Lin, G. Li and F. Li, “Battling the Extreme: A Study on the Power System Resilience,” *Proceedings of the IEEE,* vol. 105, no. 7, pp. 1253-1266, 2017.

[78] F. Nadeem, S. M. S. Hussain, P. K. Tiwari, A. K. Goswami and T. S. Ustun, "Comparative Review of Energy Storage Systems, Their Roles, and Impacts on Future Power Systems," *IEEE Access,* vol. 7, pp. 4555-4585, 2019.

[79] S. Seal, B. Boulet, V. R. Dehkordi, F. Bouffard and G. Joos, "Centralized MPC for Home Energy Management With EV as Mobile Energy Storage Unit," *IEEE Transactions on Sustainable Energy,* vol. 14, no. 3, pp. 1425-1435, 2023.

[80] J. R. R. Zientarski, M. L. d. S. Martins, J. R. Pinheiro and H. L. Hey, "Evaluation of Power Processing in Series-Connected Partial-Power Converters," *IEEE Journal of Emerging and Selected Topics in Power Electronics,* vol. 7, no. 1, pp. 343-352, 2019.

[81] J. Anzola, I. Aizpuru, A. A. Romero, A. A. Loiti, R. Lopez-Erauskin and C. Bernal, "Review of Architectures Based on Partial Power Processing for DC-DC Applications," *IEEE Access,* vol. 8, pp. 103405-103418, 2020.

[82] J. Qi and D. D.-C. Lu, "A flyback converter based partial power processing structure for BESS with voltage/current regulation and battery balancing functionalities," in *2017 IEEE International Telecommunications Energy Conference (INTELEC)*, Broadbeach, QLD, Australia, 2017.

[83] S. Mishra, S. Tamballa, M. Pallantala, S. Raju and N. Mohan, "Cascaded Dual-Active," in *20th Workshop on Control and Modeling for Power Electronics (COMPEL)*, Toronto, ON, Canada, 2019.

[84] S. Honarmand, A. Rajaei, M. Shahparasti, A. Luna and E. Pouresmaeil, "A modified partial power structure for quasi Z-source converter to improve voltage gain and power rating," *Energies,* vol. 12, no. 11, p. 2139, 2019.

[85] Y. Liu, Y. Hu, G. Chen and H. Wen, "Partial Power Processing Multiport DC–DC Converter With Radial Module Connections," *IEEE Transactions on Power Electronics,* vol. 37, no. 11, pp. 13398-13412, 2022.

[86] M. Uno, M. Sato, Y. Tada, S. Iyasu, N. Kobayashi and Y. Hayashi, “Partially Isolated Multiport Converter With Automatic Current Balancing Interleaved PWM Converter and Improved Transformer Utilization for EV Batteries,” *IEEE Transactions on Transportation Electrification,* vol. 9, no. 1, pp. 1273-1288, 2023.

[87] Y. Nie, Y. Zhang and Y. Hu, “Integrated Power/Signal Transmission in Triple Active Bridge Converters Based on Partial Power Processing for Energy Routers,” in *2022 IEEE Transportation Electrification Conference and Expo, Asia-Pacific (ITEC Asia-Pacific)*, Haining, China, 2022.

[88] Guan-Chyun Hsieh and J. C. Hung, “Phase-locked loop techniques. A survey,” *IEEE Transactions on Industrial Electronics,* vol. 43, no. 6, pp. 609-615, 1996 .

[89] Y. Kai, Y. Wang and B. Liu, “GreenRouter: Reducing Power by Innovating Router's Architecture,” *IEEE Computer Architecture Letters,* vol. 12, no. 2, pp. 51-54, 2013.

[90] A. Karbozov, M. G. Majumder, H. S. Krishnamoorthy and K. Rajashekara, “Triple Active Bridge Based Multiport Energy Router for Subsea – Renewable Interconnection,” *IEEE Transactions on Industry Applications,* vol. 59, no. 4, pp. 4528-4538, 2023.

[91] Y. Chen, P. Wang, Y. Elasser and M. Chen, “Multicell Reconfigurable Multi-Input Multi-Output Energy Router Architecture,” *IEEE Transactions on Power Electronics,* vol. 35, no. 12, pp. 13210-13224, 2020.

[92] H. Wen, J. Li, H. Shi, Y. Hu and Y. Yang, “Fault Diagnosis and Tolerant Control of Dual-Active-Bridge Converter With Triple-Phase Shift Control for Bidirectional EV Charging Systems,” *IEEE Transactions on Transportation Electrification,* vol. 7, no. 1, pp. 287-303, 2021.

[93] Z. Sun, Q. Wang, L. Xiao and Q. Wu, “A simple sensorless current sharing control for input-parallel output-parallel dual active bridge converters,” *IEEE Transactions on Industrial Electronics,* vol. 69, no. 11, pp. 10819-10833, 2021.

[94] G. Chen, Y. Deng, K. Wang, Y. Hu, L. Jiang, H. Wen and X. He, "Topology Derivation and Analysis of Integrated Multiple Output Isolated DC–DC Converters With Stacked Configuration for Low-Cost Applications," *IEEE Transactions on Circuits and Systems I: Regular Papers,* vol. 64, no. 8, pp. 2207-2218, 2017.

[95] G. Chen, Y. Deng, Y. Hu, L. Jiang, X. He and Y. Wang, "A Family of Zero-Voltage-Switching Magnetic Coupling Nonisolated Bidirectional DC–DC Converters," *IEEE Transactions on Industrial Electronics,* vol. 64, no. 8, pp. 6223-6233, 2017.

[96] Y. Liu, G. Chen, Y. Hu, L. Huang and X. Qing, "Magnetic Coupling Branch Based Dual-Input/Output DC–DC Converters With Improved Cross-Regulation and Soft-Switching Operation," *IEEE Transactions on Industrial Electronics,* vol. 67, no. 9, pp. 7167-7178, 2020.

[97] F. Krismer and J. W. Kolar, "Efficiency-optimized high-current dual active bridge converter for automotive applications," *IEEE Transactions on Industrial Electronics,* vol. 59, no. 7, pp. 2745-2760, 2011.

[98] Y. Yu, K. Masumoto, K. Wada and Y. Kado, "Power flow control of a triple active bridge DC-DC converter using GaN power devices for a low-voltage DC power distribution system," *2017 IEEE 3rd International Future Energy Electronics Conference and ECCE Asia (IFEEC 2017 - ECCE Asia),* pp. 772-777, 2017.

[99] B. Zhao, Q. Song and W. Liu, "A practical solution of high-frequency-link bidirectional solid-state transformer based on advanced components in hybrid microgrid," *IEEE Transactions on Industrial Electronics,* vol. 62, no. 7, pp. 4587-4597, 2014.

[100] H. Bai and C. Mi, "Eliminate Reactive Power and Increase System Efficiency of Isolated Bidirectional Dual-Active-Bridge DC–DC Converters Using Novel Dual-Phase-Shift Control," *IEEE Transactions on Power Electronics,* vol. 23, no. 6, pp. 2905-2914, 2008.

[101] W. Choi, K. -M. Rho and B. -H. Cho, “Fundamental Duty Modulation of Dual-Active-Bridge Converter for Wide-Range Operation,” *IEEE Transactions on Power Electronics,* vol. 31, no. 6, pp. 4048-4064, 2016.

[102] J. Lu, K. Bai, A. R. Taylor, G. Liu, A. Brown, P. M. Johnson and M. McAmmond, “A Modular-Designed Three-Phase High-Efficiency High-Power-Density EV Battery Charger Using Dual/Triple-Phase-Shift Control,” *IEEE Transactions on Power Electronics,* vol. 33, no. 9, pp. 8091-8100, 2018.

[103] T. Liu, X. Yang, W. Chen, Y. Li, Y. Xuan, L. Huang and X. Hao, “Design and Implementation of High Efficiency Control Scheme of Dual Active Bridge Based 10 kV/1 MW Solid State Transformer for PV Application,” *IEEE Transactions on Power Electronics,* 卷 34, 编号 5, pp. 4223-4238, 2019.

[104] S. Shao, H. Chen, X. Wu, J. Zhang and K. Sheng, “Circulating Current and ZVS-on of a Dual Active Bridge DC-DC Converter: A Review,” *IEEE Access,* vol. 7, pp. 50561-50572, 2019.

[105] Y. Nie, X. Zhang, M. Nasr Esfahani and M. S. Alkahtani, “Automatic Power Direction Control of DAB Converter in Emergency Energy Supply,” in *2024 IEEE 4th International Conference on Power, Electronics and Computer Applications (ICPECA)*, Shenyang, China, 2024.

[106] K. E. Lucas, D. J. Pagano and R. L. P. Medeiros, “Single Phase-Shift Control of DAB Converter using Robust Parametric Approach,” in *2019 IEEE 15th Brazilian Power Electronics Conference and 5th IEEE Southern Power Electronics Conference (COBEP/SPEC)*, Santos, Brazil, 2019.

[107] S. Shao, L. Chen, Z. Shan, F. Gao, H. Chen, D. Sha and T. Dragičević, “Modeling and advanced control of dual-active-bridge DC–DC converters: A review,” *IEEE Transactions on Power Electronics,* vol. 37, no. 2, pp. 1524-1547, 2021.

[108] R. Chattopadhyay, U. Raheja, G. Gohil, V. Nair and S. Bhattacharya, "Sensorless phase shift control for phase shifted DC-DC converters for eliminating DC transients from transformer winding currents," in *2018 IEEE Applied Power Electronics Conference and Exposition (APEC)*, San Antonio, TX, USA, 2018.

[109] K. Zhang, S. Troitzsch, S. Hanif and T. Hamacher, "Coordinated Market Design for Peer-to-Peer Energy Trade and Ancillary Services in Distribution Grids," *IEEE Transactions on Smart Grid,* vol. 11, no. 4, pp. 2929-2941, 2020.

[110] R. K. Prajapati, R. Kumar and R. Kumar, "Investigation on Photovoltaic Cells with Battery Integration," in *2023 International Conference on Computer, Electronics & Electrical Engineering & their Applications (IC2E3)*, Srinagar Garhwal, India, India.

[111] S. -H. Park, I. -D. Kim, S. -M. Song and J. Kim, "Design of Battery Charger and Discharger using Series-input and Parallel-output connected DAB Converter," in *2022 25th International Conference on Electrical Machines and Systems (ICEMS)*, Chiang Mai, Thailand, 2022.

[112] K. Wang, X. Hu, H. Li, P. Li, D. Zeng and S. Guo, "A Survey on Energy Internet Communications for Sustainability," *IEEE Transactions on Sustainable Computing,* vol. 2, no. 3, pp. 231-254, 2017.

[113] Y. Nie, Y. Zhang, Y. Hu, M. Alkahtani, M. Alquraish and H. Xu, "Energy Router for Peer-to-Peer Trading under Emergency with Energy Traceable Functionality," *IEEE Access,* 2023.

[114] W. Tushar, T. K. Saha, C. Yuen, D. Smith and H. V. Poor, "Peer-to-Peer Trading in Electricity Networks: An Overview," *IEEE Transactions on Smart Grid,* vol. 11, no. 4, pp. 3185-3200, 2020.

END